ELT M5 — The Lightweight Field Stabilisation Mirror
MAVIS on the VLT: A powerful, synergistic ELT complement in the visible
The Journey of Lithium
ESO Hypatia Colloquium Series

ESO

Contents

Front cover: This bright cluster of stars is 47 Tucanae (NGC 104), shown here in an image taken by ESO's VISTA (Visible and Infrared Survey Telescope for Astronomy) from the Paranal Observatory in Chile. This image was taken as part of the VISTA Magellanic Cloud survey, a project that is scanning the region of the Magellanic Clouds, two small galaxies that are very close to our Milky Way. Credit: ESO/M.-R. Cioni/VISTA Magellanic Cloud survey. Acknowledgement: Cambridge Astronomical Survey Unit

Back cover: This poster shows 42 of the largest objects in the Solar System's asteroid belt, located between Mars and Jupiter (orbits not to scale). The images in the outermost circle of this infographic have been captured with the Spectro-Polarimetric High-contrast Exoplanet REsearch (SPHERE) instrument on ESO's Very Large Telescope. The asteroid sample features 39 objects larger than 100 kilometres in diameter, including 20 larger than 200 kilometres. The poster highlights a few of the objects, including Ceres (the largest asteroid in the belt), Urania (the smallest one imaged), Kalliope (the densest imaged) and Lutetia, which was visited by the European Space Agency's Rosetta mission.

ELT M5 — The Lightweight Field Stabilisation Mirror

Elise Vernet [1]
Michele Cirasuolo [1]
Jean-François Pirard [1]
Marc Cayrel [1]
Roberto Tamai [1]
Pablo Zuluaga Ramírez [1]
Constanza Araujo Hauck [1]
Bertrand Koehler [1]
Fabio Bianca Marchet [1]
Juan-Carlos Gonzalez [1]
Mauro Tuti [1]
and the ELT team

[1] ESO

The Extremely Large Telescope (ELT) is at the core of ESO's vision to deliver the largest optical and infrared telescope in the world. Following on from our previous Messenger articles we continue with the description of the optical elements of the ELT. In this article we focus on the quintenary mirror (M5), the field stabilisation unit. In combination with the M4 mirror, M5 is vital to delivering the sharp diffraction limited images needed for science by correcting for the vibrations of the telescope, wind shaking and the atmosphere. We describe the main characteristics of the M5, as well as the challenges and complexity of this unique field stabilisation unit and its design and manufacturing status.

Figure 1. The ELT M5 mirror is a 2.7 × 2.2-metre ellipsoidal mirror made of silicon carbide, supported by the M5 cell (ESO renderings of SENER Aeroespacial and Safran Reosc design).

Background: how the ELT works

The optical design of ESO's Extremely Large Telescope (ELT) is based on a novel five-mirror scheme capable of collecting and focusing the light from astronomical sources and feeding state-of-the art instruments for the purposes of imaging and spectroscopy. The light is collected by the giant primary mirror, 39 metres in diameter, relayed via the M2 and M3 mirrors (each of which is around 4 metres in diameter) to the M4 and M5 mirrors that are the core of the telescope's adaptive optics; the light then reaches the instruments on one of the two Nasmyth platforms. This design provides an unvignetted field of view (FoV) of 10 arcminutes in diameter on the sky — an area of 80 square arcminutes (1/9 of the full Moon's area) — and thanks to the combination of M4 and M5 it is capable of correcting for both atmospheric turbulence and the vibration of the telescope structure itself induced by motion and wind. This adaptive capability is crucial in allowing the ELT to reach its diffraction limit, which is ~ 8 milliarcseconds in the J band (at $\lambda \sim 1.2~\mu m$) and ~ 14 milliarcseconds in the K band, thereby providing images 15 times sharper than those from the NASA/ESA Hubble Space Telescope and with much greater sensitivity. Translated into astrophysical terms this means opening up new discovery spaces, from exoplanets closer to their stars, to black holes, to the building blocks of galaxies both in the local Universe and billions of light-years away. For example, it will be possible to detect and characterise, with unprecedented sensitivity, extrasolar planets in the habitable zone around our closest star, Proxima b, or to resolve giant molecular clouds (the building blocks of star formation) down to ~ 50 parsecs in distant galaxies at $z \sim 2$ (and even smaller structures for sources that are gravitationally lensed by foreground clusters).

The quintenary mirror (M5)

M5 is the field stabilisation unit of the telescope. The term "field stabilisation" means that the mirror is moving in a rigid way (tip-tilting) to steer the image and correct for vibrations of the telescope structure induced by its motion and by the wind, as well as some of the atmospheric turbulence. This is achieved by the M5 cell which is composed of three piezo actuators. It supports and moves the M5 mirror up to 10 times per second. M5 is a flat, elliptical mirror with a diameter of 2.2 metres on the minor axis and 2.7 metres on the major axis (see Figure 1). The role of the M5 unit (mirror + cell) is to reduce the image movement down to a level where the M4 mirror can take over. The M5 mirror assembly needs to be very stiff and at the same time very light (less than 500 kilogrammes in total) to allow its cell to move it fast enough whilst remaining flat when moving.

Initial studies have demonstrated that to achieve this highly demanding level of performance only specialist materials can be used for the mirror, either silicon carbide (SiC) or ultra-low-expansion
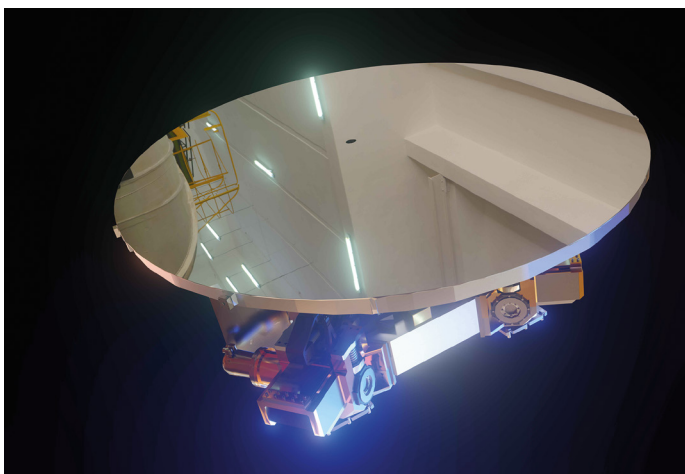
glass machined in a special way to make it extremely lightweight.

The French company Safran Reosc has been selected to manufacture the M5 mirror assembly while the Spanish company SENER Aeroespacial is responsible for the M5 cell.

Safran Reosc developed a design for the M5 mirror using Boostec® SiC. This material is well known for its high stiffness (stiffer than steel, carbon fibre or beryllium) and low density, properties that make the mirror very lightweight. SiC has been used for many space telescopes and the Herschel Space Observatory primary mirror is a good example of its technological feasibility, as well as acting as the reference body for the ELT's M4 mirror.

As in the case of the Herschel primary mirror, it is not possible to manufacture such a large mirror in a single piece, so M5 is made of six segments which must be brazed together. SiC is a very porous material and has micron-sized holes on the surface which would remain after the mirror is coated, so the segments first need to go through another very complex process called chemical vapour deposition (CVD), in which a layer of pure silicon about 900 nanometres thick is spread over each of the SiC segments.

The M5 unit is a lightweight structure including three different types of ribs following triangular patterns. The mirror is supported by three axial supports and one central lateral support (Vernet et al., 2020).

The design of the support is optimised to allow the tip-tilt movement and also provide the required stiffness laterally and in clocking. The three axial and the central lateral supports are mounted on a fast-motion tip-tilt stage with a stroke of ±0.5 milliradians inducing a displacement of more than ±0.5 millimetre. This is achieved using three piezo actuators (see Figure 2). The operation of the actuators is based on a design developed by CEDRAT TECHNOLOGIES for the M5 demonstrator more than ten years ago. Each actuator includes a system to preload the piezo stacks, an amplification frame based on patented amplified piezo
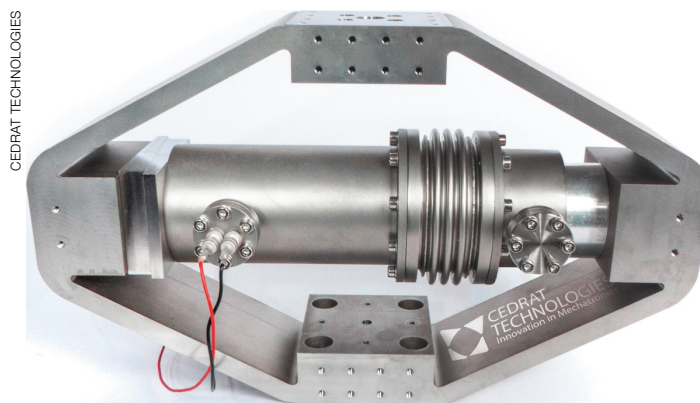

CEDRAT TECHNOLOGIES

Figure 2. Amplified piezo actuator.

actuators (APA®) and protection of the active material from the environment. The stainless steel amplification frame connects the M5 mirror and the alignment stage and magnifies the piezo stack deformation to provide the required stroke and stiffness. It also acts as one of the interfaces with the M5 mirror assembly. The cell also includes an active alignment system which allows the M5 mirror to piston by ±5 millimetres and tip-tilt by ±5 milliradians at a low rate. The alignment stage resolution is 0.025 millimetres for piston and 0.025 milliradians for tip-tilt and its repeatability is ±0.1 millimetres for piston and ±0.05 milliradians for tip-tilt.

Manufacturing the M5 mirror

Whilst the cell is at the preliminary design stage, the mirror assembly had its Final Design Review in May 2021 and the actual mirror blank has already been in manufacturing for more than a year. This is mostly because the manufacturing procedures for such a unique SiC mirror are complex and extremely challenging. The full production chain is shown in Figure 3 and consists of the following key steps:

1. The silicon powder is mixed with some additives and inserted into a mould which is pressed to become what is called a "green blank".
2. The green blank is machined into the required segment shape.
3. The segment is sintered, a special process by which the particles of the material are fused together by heat or pressure to become a solid mass, but without reaching the melting point.
4. The segment is ground and prepared for the CVD cladding.

5. Using a very challenging technique a thin layer of silicon is deposited using CVD.
6. At this point each segment is ground and prepared for the final assembly and brazing.
7. Once the six segments are ready, the final mirror blank is assembled and brazed.
8. A final grinding of the surface removes any small misalignment.

These are the eight key steps in the manufacturing of the mirror blank. After that, the blank will be transferred to Safran Reosc and the lateral and axial supports will be integrated before proceeding with the final grinding and polishing phases.

As described above, six segments are needed for the mirror blank but to reduce the risk of delay it was agreed that six spare segments ready for cladding would also be prepared. So far five segments have been successfully manufactured with CVD cladding, six additional segments are ready for CVD cladding and the last one has been sintered. Figure 4 shows three of the segments after CVD cladding at Boostec.

One of the critical aspects that the SiC manufacturer Mersen Boostec needs to verify before starting any grinding of the optical face is that the thin CVD layer reached the right thickness and adhered adequately to the segment. This has been achieved for five segments. Once the six segment blanks are ready, it will take approximately nine months to complete the grinding and preparation for brazing.

The final step in the mirror blank manufacturing is the brazing of the six petals.
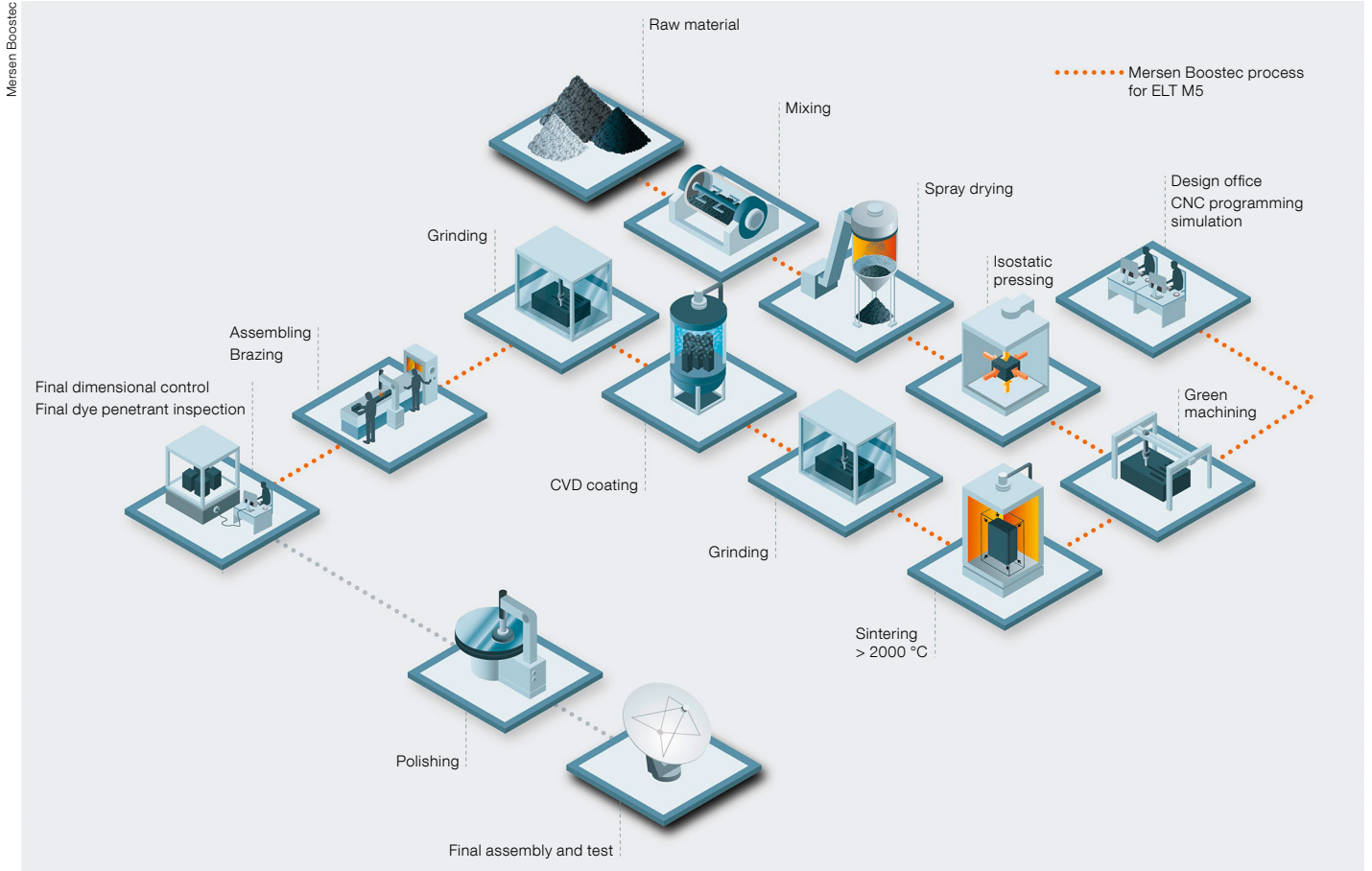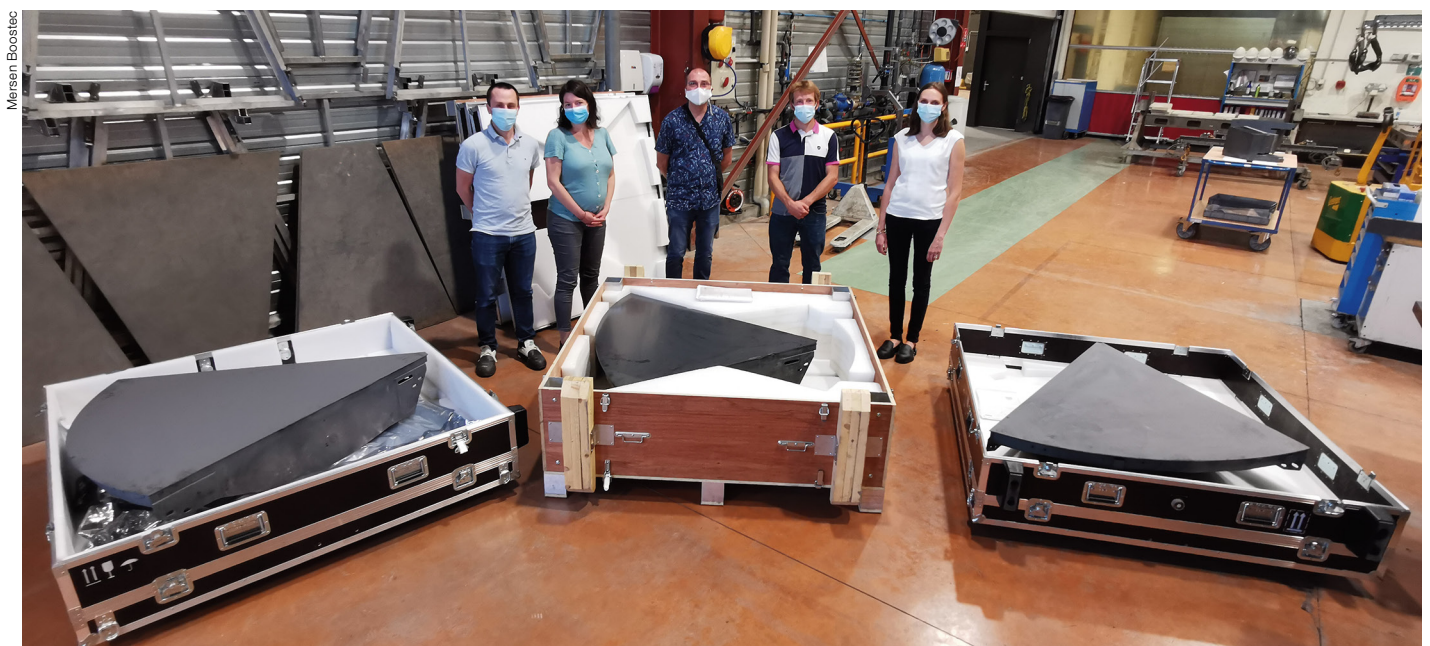
Figure 3. (Above) Full manufacturing process of the M5 mirror.

Figure 4. (Below) Early July 2021: three mirror segments with CVD cladding at Boostec.

Before brazing them together, the segments must be aligned in such way that the positions of the axial support interfaces are within the required tolerance and that the brazing joints meet the specified thickness. Once the six petals are well aligned, the unit is brazed. The CVD layer requirements reduce the tolerance one can accept in the segment positioning as any misalignment of the optical surface will reduce the final CVD layer available for polishing. After brazing, Mersen Boostec will perform a final grinding of the flat optical surface to make the blank ready for delivery to Safran Reosc.

The mirror blank will be delivered to Safran Reosc in the autumn of 2022 and once the axial and lateral supports are mounted, polishing will last for two and a half years. The mirror will be ready to be shipped to the observatory by the end of 2025.

M5 cell description

The M5 cell design is driven by the technological challenge of performing a fast-steering motion capable of rejecting perturbations at the scale of a few tens of milliarcseconds on the sky.

SENER Aeroespacial is the company developing the M5 cell re-using experience acquired with the development of a functional M5 field stabilisation unit demonstrator (Barriga et al., 2014), in collaboration with CEDRAT TECHNOLOGIES for the piezo actuators.

The design of the M5 cell has been driven by stricter requirements than those that applied to the demonstrator and this has forced the SENER Aeroespacial team to apply state-of-the art methods and procedures whilst analysing different alternatives and iterating them to obtain a robust result. Moreover, the addition of a new functionality — providing active alignment at low rate in piston and tip-tilt — has necessitated the division of the M5 cell into two stages, which has added a new twist to the design (see Figure 5).

The high relative accuracy and resolution requirements have driven the design of the tracking chain and have justified the selection of high-precision sensors and state-of-the-art acquisition electronics. The decision to reposition the M5 Cabi-net and the front-end electronics to the M5 cell has also improved the design of the M5 cell.

Another demanding requirement has been the new and higher minimum eigenfrequencies of the M5 cell, and this has had direct implications for the stiffness of the final model.

The technological challenge of both improving the stiffness and the stroke of the M5 tip-tilt actuators and developing a new compact actuator for the M5 alignment stage has been met with good results.

SENER Aeroespacial, together with CEDRAT TECHNOLOGIES (for the APA), is presently finishing the qualification campaign of the different mechanisms. The Final Design Review is expected to take place in the autumn of 2021, well in line with the schedule.

References

Barriga, P. et al. 2014, Proc. SPIE, 9145, 91451O
Vernet, E. et al. 2020, Proc. SPIE, 11445, 114453O

Figure 5. M5 cell alignment and tip-tilt stage.
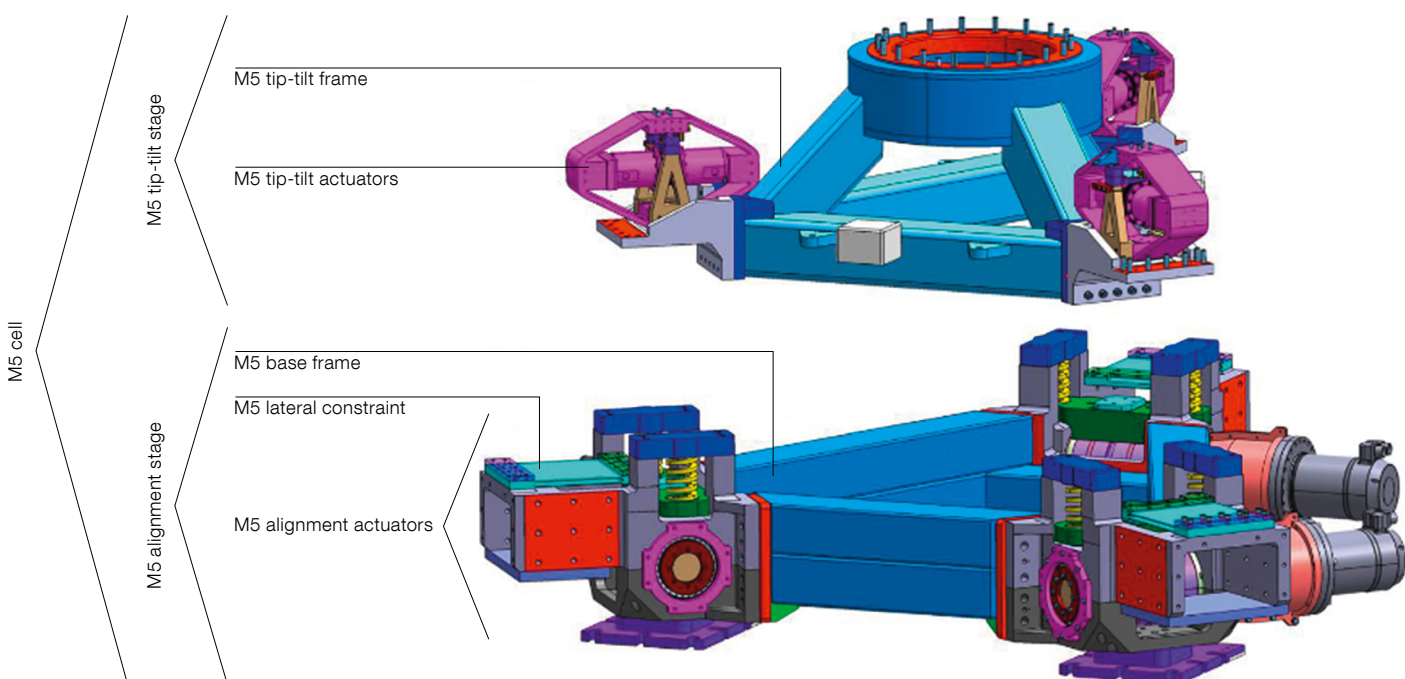
SENER Aeroespacial

MAVIS on the VLT: A Powerful, Synergistic ELT Complement in the Visible

François Rigaut[1]
Richard McDermid[2]
Giovanni Cresci[3]
Guido Agapito[3]
Matteo Aliverti[3]
Simone Antoniucci[3]
Andrea Balestra[3]
Andrea Baruffolo[3]
Olivier Beltramo-Martin[4]
Maria Bergomi[3]
Andrea Bianco[3]
Marco Bonaglia[3]
Giuseppe Bono[3,5]
Jean-Claude Bouret[4]
David Brodrick[1]
Lorenzo Busoni[3]
Giulio Capasso[3]
Elena Carolo[3]
Simonetta Chinellato[3]
Mirko Colapietro[3]
Robert Content[2]
Jesse Cranney[1]
Gayandhi de Silva[2]
Sergio D'Orsi[3]
Simon Ellis[2]
Daniela Fantinel[3]
Thierry Fusco[4,7]
Antony Galla[1]
Gaston Gausachs[1]
Damien Gratadour[1]
Davide Greggio[3]
Marco Gullieuszik[3]
Pierre Haguenauer[6]
Dionne Haynes[1]
Nick Herrald[1]
Anthony Horton[2]
Devika Kamath[2]
Laura Magrini[3]
Antonino Marasco[3]
Luca Marafatto[3]
Davide Massari[3]
Helen McGregor[2]
Trevor Mendel[1]
Stephanie Monty[1]
Benoit Neichel[4]
Enrico Pinna[3]
Cédric Plantet[3]
Elisa Portaluri[3]
David Robertson[2]
Bernardo Salasnich[3]
Salvatore Savarese[3]
Pietro Schipani[3]
Christian Schwab[2]
Scott Smedley[2]
Rosanna Sordo[3]
Stefan Ströbele[6]
Annino Vaccarella[1]
Daniele Vassallo[3]
Valentina Viotto[3]
Lew Waller[2]
Alessio Zanutta[3]
Hao Zhang[1]
Ulf Seemann[6]
Harald Kuntschner[6]
Robin Arsenault[6]

[1] Australian National University, Canberra, Australia
[2] Macquarie University, Sydney, Australia
[3] INAF, Italy
[4] Laboratoire d'Astrophysique de Marseille (LAM), France
[5] Tor Vergata University of Rome, Italy
[6] ESO
[7] Département d'Optique et Techniques Avancées (DOTA), Office National d'Etudes et de Recherches Aérospatial (ONERA), Paris, France

On 1 June 2021 ESO and a consortium of Australian, Italian and French institutions signed an agreement for the design and construction of the MCAO Assisted Visible Imager and Spectrograph (MAVIS). This Very Large Telescope (VLT) instrument will push the frontier of new astronomical instrument technologies to provide, for the first time, wide-field, diffraction-limited angular resolution at visible wavelengths. In combination with the VLT Adaptive Optics Facility, it will use multiconjugate adaptive optics (MCAO) to feed a 4k × 4k imager covering 30 × 30 arcseconds, as well as an Integral Field Spectrograph (IFS). Angular resolution down to 18 milliarcseconds will be achieved at a wavelength of 550 nm (*V* band). The IFS will provide four spectral modes, with spectral resolutions from 4000 to over 15 000 between 370 and 950 nm. This will enable a wide variety of science cases, spanning themes that include the emergence of the Hubble sequence, resolving the contents of nearby galaxies, star clusters over cosmic time and the birth, life, and death of stars and their planets. Delivering visible images and integral-field spectroscopy at an angular resolution two to three times better than that of the Hubble Space Telescope will make MAVIS a powerful complement at visible wavelengths to future facilities like the James Webb Space Telescope and the 30–40-metre-class ground-based telescopes currently under construction, which are all optimised for science at infrared wavelengths.

About MAVIS

Pushing adaptive optics (AO) technologies to the visible region has been the holy grail of high angular resolution observations since the inception of AO. It is indeed a very challenging proposition: enabling compensation at shorter wavelengths means deformable mirrors with more actuators (proportional to $\lambda^{-2.4}$), faster systems ($\lambda^{-1.2}$) and a correction valid over smaller isoplanatic patches ($\lambda^{-2.4}$). As a result the overall complexity grows as λ^{-6}. Having more actuators also means smaller subapertures in the wavefront sensors (WFSs), which requires more powerful lasers. It all becomes more complicated — and more expensive. Some extreme AO systems have been working in the visible, generally focused on high-contrast applications, but these systems generally have very low sky coverage, with access to only a few hundred targets and small fields of view (MagAO at the Magellan Telescopes, the First Light Adaptive Optics [FLAO] system at the Large Binocular Telescope, and the Spectro-Polarimetric High-contrast Exoplanet REsearch [SPHERE] instrument at ESO's Very Large Telescope [VLT]).

AO has matured over the last decades, and recently it has become possible to consider building a wide-field, high-sky-coverage facility instrument to serve a large number of science cases in the visible (Esposito et al., 2016). This was made possible by a number of key developments.

– The maturation of key technologies, including: (a) large, high-actuator-density deformable mirrors and deformable secondary mirrors; (b) high-power commercial lasers to create sodium guide stars like the ones used in the VLT Adaptive Optics Facility (AOF); and (c) high-throughput, low-latency real-time computers, and in particular the variant based on a graphics processing unit, which has

seen major performance and functionality improvements in the past decade.

– New control techniques. AO control got stuck with linear integrator controllers for a long time, but the past decade has seen the emergence of many promising techniques, such as Minimum Mean Square Error, Learn and Apply and the various incarnations of predictive controllers such as Linear Quadratic Gaussian control, together with the emergence of tricks like super-resolution.

– The success of on-sky demonstrators (for example, the Multi-conjugate Adaptive-optics Demonstrator [MAD] at ESO), or first-generation facility systems like GeMS, the MCAO system at the Gemini telescope, that could be considered as the precursor of MAVIS, with its five laser guide stars (LGSs) and three deformable mirrors. The consortium is also drawing from the experience of the AOF and more recently, the InfraRed Low Order Sensor (IRLOS) WFS upgrade for the Multi Unit Spectroscopic Explorer (MUSE).

MAVIS will go at the Nasmyth A focus of the VLT AOF (at Unit Telescope 4), opposite MUSE (see Figure 1). MAVIS is composed of four main modules (Rigaut et al., 2020): the AO module, that processes the light and compensates for most of the atmospheric-induced aberrations; a 4k × 4k imager equipped with a set of narrow- and broadband filters; an integral field spectrograph (IFS) with two modes, one with a field of view of 3.6 × 2.5 arcseconds and spaxels of 25 milliarcseconds, the other with a field of view of 7.2 × 5 arcseconds and spaxels of 50 milliarcseconds, and multiple spectral resolutions; and the calibration unit, which provides what is needed for the calibration of the AO module and the instruments. Both the imager and the spectrograph cover the wavelength range 370–950 nm in the baseline design, and have been informed by a comprehensive science case built in consultation with the ESO user community (McDermid et al., 2020).

The MAVIS consortium[1] is made up of ASTRALIS[2] (Australia, formerly the AAO Consortium), INAF (Italy), the Laboratoire d'Astrophysique de Marseille (LAM, France) and ESO. ASTRALIS (the AAO and ANU nodes) provides the Project
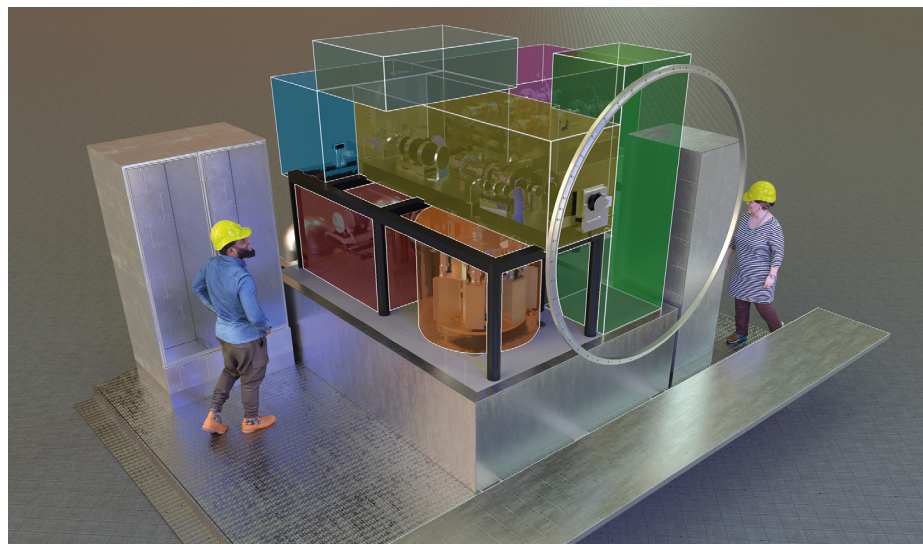

Figure 1. A rendering of MAVIS on the Nasmyth platform. The circle represents the rotator-adaptor interface (to which MAVIS is not attached). The various volumes are coloured as follows: yellow — adaptive optics module; orange — laser guide star wavefront sensor; red — natural guide star wavefront sensor; blue (behind) — imager; purple — spectrograph; green — calibration unit; grey — electronics cabinets. MAVIS will be fitted with a light-tight enclosure, but will rely on passive thermal management, with the possible exception of the spectrograph which might be actively temperature controlled (currently being studied).

Office, the imager and spectrograph, the LGS WFS, the Real-Time Controller, the detectors, and the calibration unit. INAF is responsible for the AO module, as well as the natural guide star (NGS) WFS, the performance simulations, and the Instrument Control System. LAM provides AO expertise and point spread function reconstruction. Finally, ESO is responsible for driving the deformable mirror development and procurement, the LGS Facility upgrade to split the four existing LGS beams into eight beacons, the interface with the VLT, and the commissioning. ESO will also provide nine smALl vIsible CamEra (ALICE) cameras and up to five Next Generation Controller II detector controllers. The COVID-19 pandemic posed a major challenge to the smooth operation of such a distributed consortium. In particular, the closure of Australia's borders (likely to stay in effect until sometime in 2022) has without a doubt impaired the efficiency of communication within the consortium.

Phase A of MAVIS began in February 2019 and the Phase A final review was passed with flying colours in May 2020. The ESO follow-up team organised the start of Phase B and coordinated the various approval steps (by the Scientific Technical Committee, the Finance Committee and Council) with the Paranal Instrumentation Programme. The agreement for Phases B to E was signed on 1 June 2021.

A period of slightly more than one year is planned for each of the preliminary design and final design. Preliminary Design Review is expected in July 2022 and Final Design Review in August 2023. The Preliminary Acceptance Europe milestone is scheduled for 2027 and could take place in Australia (to be decided). First light is currently scheduled for the second semester of 2027, in line with first light of ESO's Extremely Large Telescope (ELT).

Science drivers

By probing the frontiers of angular resolution and sensitivity across a large portion of the observable sky (~ 50% at the galactic pole) at visible wavelengths, MAVIS will enable progress on an array of scientific topics, from studies of the Solar System to planetary systems around other stars, and from the physics of star formation in the Milky Way to the first star clusters in the Universe.

The point-source imaging sensitivity of MAVIS will exceed that of the Hubble Space Telescope (HST), giving an order of magnitude greater depth, and with higher angular resolution. In 10 hours of integration, MAVIS will detect point sources and compact galaxies down to 30.4 *AB* in *I* band, about 1 magnitude deeper than the Hubble Ultra-Deep Field in *i775*, despite its integration time a factor of 10 longer (96 hrs). This will allow MAVIS to produce the deepest optical images ever obtained on a large field of view. This will open a new window onto the study of the structural properties of the first galaxies and of compact galaxies across cosmic time, as illustrated by Figure 2.

Spectroscopically, the combination of high spatial resolution, large wavelength coverage and high spectral resolution ($R > 5000$) will allow MAVIS to finally trace the evolution of the interstellar medium (ISM) during the critical galaxy transformation in the redshift range $0.2 < z < 0.8$, from the clumpy and turbulent discs observed at high redshift into the thin discs of local late-type galaxies, resolving the intrinsic velocity dispersion and the chemical and physical properties of the ISM.

The astrometric precision and magnitude limits of MAVIS will exceed those of

Figure 2. Example of a morphological study of a high-*z* galaxy as observed in the *I* band with the HST, the Multi-AO Imaging Camera for Deep Observations (MICADO) at ESO's ELT, NIRCam on the James Webb Space Telescope and MAVIS. Based on the $z = 5$ high-resolution simulated "Althaea" galaxy (Pallottini et al., 2017), shown in the first panel, the other panels show how the same target of 25 *AB* magnitude would appear in the *I* band if observed with different facilities for a fixed exposure time of 1 hour. In the VLT/MAVIS image, clumpy regions as faint as 29 *AB* magnitude are detected with a signal-to-noise ratio of five.

the HST and will extend the ultra-precise local framework from the Gaia mission into the densest and most crowded fields, out to the furthest reaches of the Milky Way and into the Local Group. MAVIS will provide proper motion accuracies of 5–10 km s^{-1} out to distances of ~ 100 kpc over five-year timescales, approaching the radial velocity accuracy from MAVIS spectroscopy. The combined spectral and imaging capabilities will provide full 6D phase-space information of individual stars, giving a new precision to studies of intermediate mass black holes in globular clusters (Monty et al., 2021), and unique dynamical information to constrain the dark matter properties of local group dwarf galaxies.

MAVIS will enable access to the new regimes of faint sources and complex crowded fields that will become commonplace at longer wavelengths in the era of ELTs, but with the diagnostic power of optical wavelengths. This will be particularly important in the low-redshift Universe ($z < 0.5$), where the best-calibrated and understood physical diagnostics are found at wavelengths below 1 µm. In this way, MAVIS will be a crucial complement to the capabilities of ESO's ELT, delivering angular resolution in the optical comparable to that delivered by ELTs in the infrared. A key example of this synergy is in studying resolved stellar populations beyond the Local Group. Whilst ELTs will be able to detect individual stars in galaxies beyond several Mpc with modest integration times, infrared wavelengths probe mainly the Rayleigh-Jeans tail of the stellar black body spectrum, making infrared colours largely degenerate to key stellar population parameters such as age and metallicity. By contrast, the shallower depths accessible on an 8-metre telescope are fully compensated by the increased diagnos-

tic power of optical colours, making MAVIS a crucial tool for capitalising on ELT science.

The unprecedented combination of sensitivity, angular resolution, blue coverage and moderately-high-resolution spectroscopy ($R > 12\,000$) afforded by MAVIS and the AOF will allow, for the first time, the characterisation of the cores of globular clusters. It will be possible to explore abundances anomalies, multiple stellar populations, and core binary fractions: the missing link to understanding the formation scenario and subsequent dynamical and chemical evolution of these systems.

Finally, MAVIS will be transformational for our understanding of the life and death of stars and their planets, by revealing uncharted details of their close environment, such as protoplanetary discs, jets and companions. This includes our own Solar System, where MAVIS will provide spectroscopy and high-contrast imaging of planetary atmospheres, cometary activity and Kuiper Belt Objects.

Given this broad range of foreseen scientific applications, combined with a robust and flexible operational model, MAVIS will represent the general purpose facility instrument that will fill the gap for high-spatial-resolution optical capabilities in the post-HST era. Moreover, MAVIS operations will closely overlap with the new generation of giant telescopes optimised for near-IR observations, providing their fundamental complement in the optical regime.

Instrument design concept

Informed by a number of trade-off studies of the most crucial elements, the MAVIS
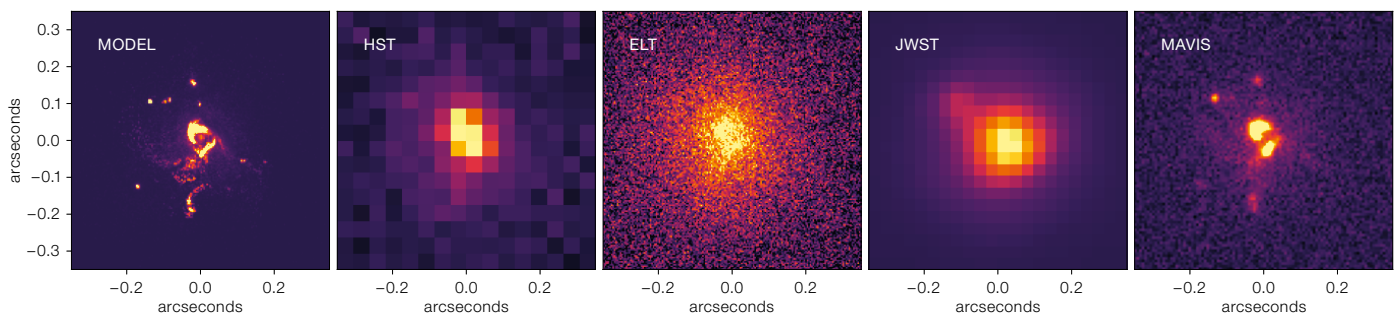
design went through several iterations during Phase A, to finally converge on the current baseline. The considerable expertise within the consortium in AO and post-focal instrumentation helped in converging on a healthy design, in particular the optical design, which maximises throughput and minimises optical aberrations and field distortion, whilst allowing easy alignment and modular integration (Viotto et al., 2020; Ellis et al., 2020).

The current MAVIS design can be summarised as follows:
– A largely transmissive design across the board (AO module, imager, spectrograph), using only on-axis optics. The intention is to minimise field distortions, as well as to make the optical alignment more tolerant.
– A gravity-invariant design, in which the science and NGS WFSs are commonly de-rotated optically and the LGS WFSs use mechanical de-rotation to track the LGS constellation.
– Three deformable mirrors: the AOF secondary (1170 actuators) and two post-focal deformable mirrors, optically conjugated to 6 and 13.5 kilometres, for a grand total of 5420 actuators.
– Eight laser guide stars created from splitting the four existing AOF lasers, feeding eight 40 × 40 Shack-Hartmann WFSs. The current concept makes use of diffraction gratings to split each laser and is minimally invasive to the LGS Facility, maintaining full compatibility with existing AOF operation modes.
– Three near-infrared NGS WFSs, providing tip-tilt and focus information (each has a selectable 1 × 1 or 2 × 2 lenslet array). These WFSs use SAPHIRA detectors over the J and H bands and NGCII controllers for maximum sensitivity, leading to a limiting magnitude of more than $V = 18.5$.
– An imager covering the 30 × 30 arcsecond field of view, better-than-Nyquist sampled in the V band (7.36 milliarcseconds pixel^{-1}, for images of 18 milliarcseconds full width at half maximum [FWHM] in good conditions). Note that for relatively obvious geometric reasons, the image quality performance is specified over the disc of radius 15 arcseconds, but we are looking for ways to also optimise the field corners.
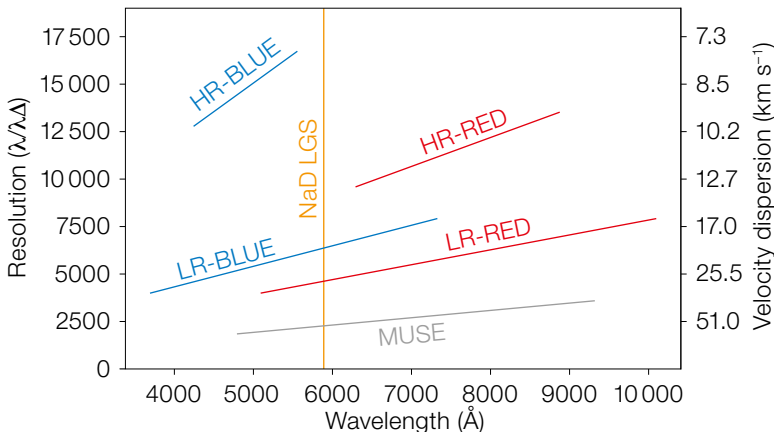– A very compact, high-throughput monolithic IFS, covering 370 to 950 nm

Figure 3. (Above) The four MAVIS IFS spectral resolution modes and corresponding dynamical scales, chosen to address key science areas. These include: the study of chemical abundances and radial velocities in crowded fields (HR-BLUE); exploring the evolution of ISM turbulence in galaxy discs and hunting intermediate-mass black holes (HR-RED); probing the extremes of mass and metallicity of young stars and untangling the complexity of ionised gas in galaxies (LR-BLUE); and resolving Lyman-alpha emitters at $z > 6.5$, and studying stellar dynamics in $z < 1$ galaxies (LR-RED). MUSE is shown in grey for comparison.

Figure 4. (Below) The MAVIS focal plane, with eight laser guide stars (orange) and three natural guide stars (red). The imager covers/defines the "science field" (green). The integral field spectrograph (IFS) field is in purple (coarse mode) and blue (fine mode). The exact shape and location of the IFS field of view are still being optimised. Having the IFS off-centred with respect to the technical field increases the capture range for natural guide stars, and thus the sky coverage.
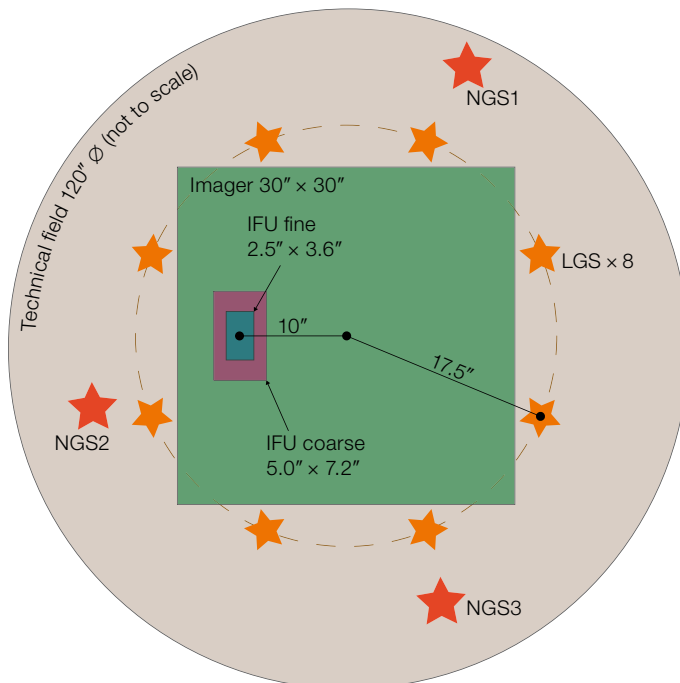
(possibly to 1000 nm), with four spectral modes, providing spectral resolutions from 4000 through over 15 000 (see Figure 3) and two spaxel scales (approximately 25 and 50 milliarcseconds spaxel^{-1}), corresponding to fields of view of 3.6 × 2.5 arcseconds and 7.2 × 5 arcseconds. The current design uses a field of view offset from the optical axis by about 8 arcseconds (see Figure 4), which slightly improves the probability of finding NGSs. We are looking into the option of using the imager and the spectrograph simulta-

neously, which will provide interesting opportunities to extract information from the IFS when in crowded fields.

Performance

The system performance requirements were specified for typical Paranal turbulence conditions, i.e., a seeing of 0.87 arcseconds at a zenith angle of 30 degrees. There has been a huge push during phase A and the start of phase B on numerical simulations (Agapito et al., 2020). These were instrumental in driving the instrument AO design: how many actuators were needed? how many deformable mirrors? how many laser guide stars and wavefront sensors? natural guide stars? All of these design parameters were optimised on the basis of the initial call for proposal requirements. Once the baseline design was settled, numerical simulations were then used to fine tune performance estimates. The consortium is still in this phase, and we have embarked on statistical performance estimates and sensitivity analyses, based on the recently released database of turbulence profiles for Paranal.

Because of the very tight wavefront error allowance — of the order of 110 nm — resulting from the fact that MAVIS targets correction at visible wavelengths, the MAVIS simulation and control group has had to make use of both proven (for example, Learn and Apply or Minimum Mean Square Error) and more novel control techniques. The latter include predictive control (Cranney et al., 2020) and "super-resolution", a technique to increase wavefront sensing diversity (or reduce redundancy) by shifting/rotating the WFSs with respect to each other.

Figure 5 presents the long-exposure Strehl ratio (well known to AO connoisseurs, the Strehl is a measure of how close the image is to the diffraction limit). These results include only atmospheric and AO error terms. The average Strehl over the disc of radius 15 arcseconds is 28.9%, which provides a very healthy margin over the specified 15% to accommodate other error sources such as optics, vibrations, etc. The absolute Strehl standard deviation over the same circular field is 1.3% (4.5% relative), indi-
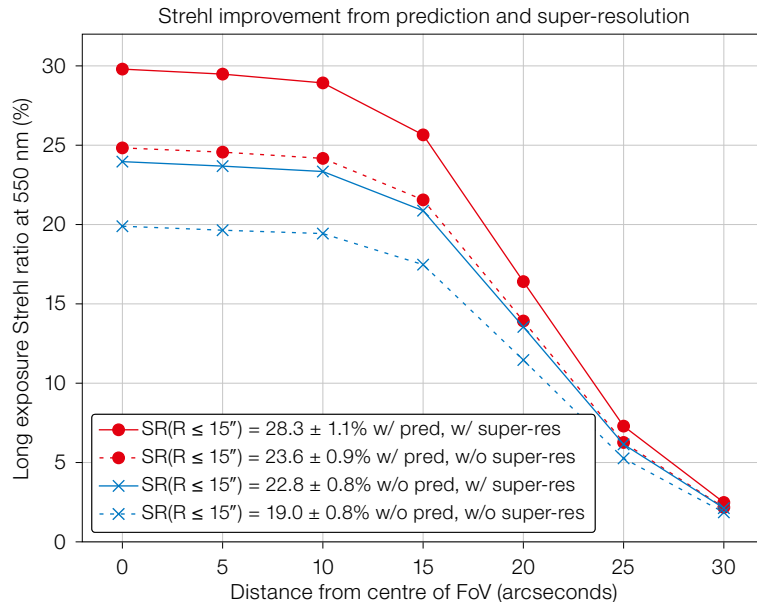

Figure 5. Strehl radial profile as a function of the off-axis distance, for various controllers (Minimum Mean Square Error or Learn and Apply, with or without predictive control and super-resolution). The Strehl performance specifications are defined over the disc of radius 15 arcseconds (not over the 30 × 30 arcsecond-square field). This set of simulations uses three bright natural guide stars on a triangle, at 20 arcsecond radius from the centre of the field.

cating a very uniform image quality — a trademark of multi-conjugate AO. At this level of Strehl, the images appear essentially diffraction-limited, i.e., close to λ/D in FWHM. When including vibrations, and various detector effects, we are expecting image sizes of 18 milliarcseconds.

The choice of near-infrared wavelengths for the NGS WFS provides a welcome boost to the sky coverage of MAVIS, where sources in the partially-corrected NGS patrol field are diffraction-limited at 1.6 µm, with moderate to high Strehl. Combined with the use of near-infrared avalanche photodiode arrays, this allows it to reach high sky coverage values; over 50% of the pointings at the galactic pole will provide images with better-than-HST angular resolution (< 50 milliarcseconds).

Finally, a preliminary exposure time calculator has been developed and is available on github[3]. MAVISIM[4], a tool to generate synthetic images, has also been developed. It employs a user-provided object model (currently only point sources) and a database of field-varying point spread functions from end-to-end numerical AO simulations. A future version will offer compatibility with extended objects. Both the exposure time calculator and

MAVISIM are under active development, with updated versions expected throughout phase B.

References

Agapito, G. et al. 2020, Proc. SPIE, 11448, 114483R
Cranney, J. et al. 2020, Proc. SPIE, 11448, 114482L
Ellis, S. et al. 2020, Proc. SPIE, 11447, 11447AO
Esposito, S. et al. 2016, Proc. SPIE, 9909, 99093U
McDermid, R. M. et al. 2020, arXiv: 2009.09242
Monty, S. et al. 2021, MNRAS, 507, 2192
Pallottini, A. et al. 2017, MNRAS, 471, 4128
Rigaut, F. et al. 2020, Proc. SPIE, 11447, 114471R
Viotto, V. et al. 2020, Proc. SPIE, 11448, 114480D

Links

[1] The MAVIS consortium: mavis-ao.org/consortium
[2] AUSTRALIS: https://astralis.org.au/
[3] MAVIS exposure time calculator: https://github.com/jtmendel/mavisetc
[4] MAVISIM image generation tool: https://github.com/smonty93/MAVISIM

The Carina Nebula, one of the largest and brightest nebulae in the night sky, has been imaged by ESO's VISTA telescope at the Paranal Observatory in Chile. By observing in infrared light, VISTA has peered through the hot gas and dark dust enshrouding the nebula to show us myriad stars, both newborn and in their death throes.

The LEGA-C Survey Completed: Stellar Populations and Stellar Kinematics of Galaxies 7 Gyr Ago

Arjen van der Wel [1]
Rachel Bezanson [2]
Francesco D'Eugenio [1]
Caroline Straatman [1]
Marijn Franx [3]
Josha van Houdt [4]
Michael V. Maseda [3]
Anna Gallazzi [5]
Po-Feng Wu [6]
Camilla Pacifici [7]
Ivana Barisic [4]
Gabriel B. Brammer [8]
Juan Carlos Munoz-Mateos [9]
Sarah Vervalcke [1]
Stefano Zibetti [5]
David Sobral [10]
Anna de Graaff [3]
Joao Calhau [11, 12]
Yasha Kaushal [2]
Adam Muzzin [13]
Eric F. Bell [14]
Pieter G. van Dokkum [15]

[1] Astronomical Observatory, University of Ghent, Belgium
[2] Department of Physics and Astronomy, University of Pittsburgh, USA
[3] Leiden Observatory, Leiden University, the Netherlands
[4] Max Planck Institute for Astronomy, Heidelberg, Germany
[5] INAF – Astronomical Observatory of Arcetri, Florence, Italy
[6] National Astronomical Observatory of Japan, Tokyo, Japan
[7] Space Telescope Science Institute, Baltimore, Maryland, USA
[8] Cosmic Dawn Center (DAWN) Niels Bohr Institute, University of Copenhagen, Denmark
[9] ESO
[10] Department of Physics, Lancaster University, UK
[11] Astrophysics Institute of the Canaries, La Laguna, Tenerife, Spain
[12] Department of Astrophysics, University of La Laguna, Spain
[13] Department of Physics and Astronomy, York University, Toronto, Canada
[14] Department of Astronomy, University of Michigan, USA
[15] Astronomy Department, Yale University, New Haven, USA

The Large Early Galaxy Astrophysics Census (LEGA-C) survey is the final Public Spectroscopic Survey to be completed with the now-retired VIsible Multi-Object Spectrograph (VIMOS) instrument at ESO's Very Large Telescope (VLT). Its aim is to characterise with high precision and for a very large sample the stellar population and kinematic properties of galaxies at redshifts $0.6 < z < 1$, providing a first assessment of the star formation histories, the absolute mass scale, and the stellar kinematic structure of galaxies at large lookback times (7 gigayears ago). This article coincides with the third and final data release but mostly focuses on the large variety of scientific results achieved so far.

LEGA-C

Before LEGA-C, most of our understanding of the stellar bodies of galaxies at large lookback times derived from photometric measurements. Tremendous progress had been achieved in that way, by quantifying the evolution of the number of stars as a function of cosmic time, their distribution over galaxies with different masses, their structural properties and their crude spectral properties in terms of colours. But these measurements are merely indirect proxies for the quantities that are the most relevant for constraining galaxy formation models: galaxy mass, angular momentum and star formation/ assembly history. Moreover, sample sizes are now very large, so we have run up against the limit of systematic uncertainties instead of sample variance. Spectroscopic observations of the stellar continuum provide a more direct way of estimating those quantities with less bias, but it took more than 1000 hours of VLT observing time to collect such expensive data for galaxies at large lookback times.

This article briefly summarises the properties and quality of the data that have now been published in full, along with value-added catalogues, and the broad range of scientific results published so far. In a narrow sense, the LEGA-C survey has now been completed: the data have been collected, processed and published. But in a broad sense, the final data release[1] marks only the beginning. Our hope is that, for many years to come, researchers will use these data for a wide variety of purposes: to find detailed properties of specific galaxies, to utilise the full dataset to shed new light on old problems, to support follow-up surveys at different wavelengths, and to test galaxy formation models.

The data

For full technical details we refer to the recently published Data Release 3 paper (van der Wel et al., 2021). Very briefly, LEGA-C consists of several thousand galaxies at redshifts $0.6 < z < 1$ selected only by their Ks-band magnitude (van der Wel et al., 2016), a proxy for stellar mass. As a result, the survey contains galaxies of all types and colours above an approximate stellar mass limit of $3 \times 10^{10}\, M_\odot$. Of course, the majority of galaxies in the Universe have lower masses than this, but this mass limit does account for most of the mass (and star formation) budget and therefore can be considered as representative. The simplicity of the survey design allows for a precise determination of sample selection effects and completeness, enabling accurate measurements of ensemble properties.

The observations were carried out from December 2014 to March 2018, with ~ 20-hour integrations for each of the 32 slit masks. At a spectral resolution of $R \sim 3500$ the typical spectrum has a signal-to-noise ratio of ~ 15–20 per Ångstrom. The data processing is described in detail by Straatman et al. (2018) and van der Wel et al. (2021), and the collated spectra are shown in Figure 1. Broadly speaking these spectra serve two purposes: measuring stellar kinematic signatures (Bezanson et al., 2018b) and stellar population characteristics (for example, Chauke et al., 2018; Wu et al., 2018a). The detailed characteristics of the spectrum and the basic modelling approach are illustrated for just one example in Figure 2. The LEGA-C survey represents a 30-fold increase in sample size of galaxies with measured stellar kinematics and stellar population properties compared to all previous work combined and, equally importantly, samples the full galaxy population rather than a specifically selected sub-sample of very massive galaxies with mostly early-type morphologies.
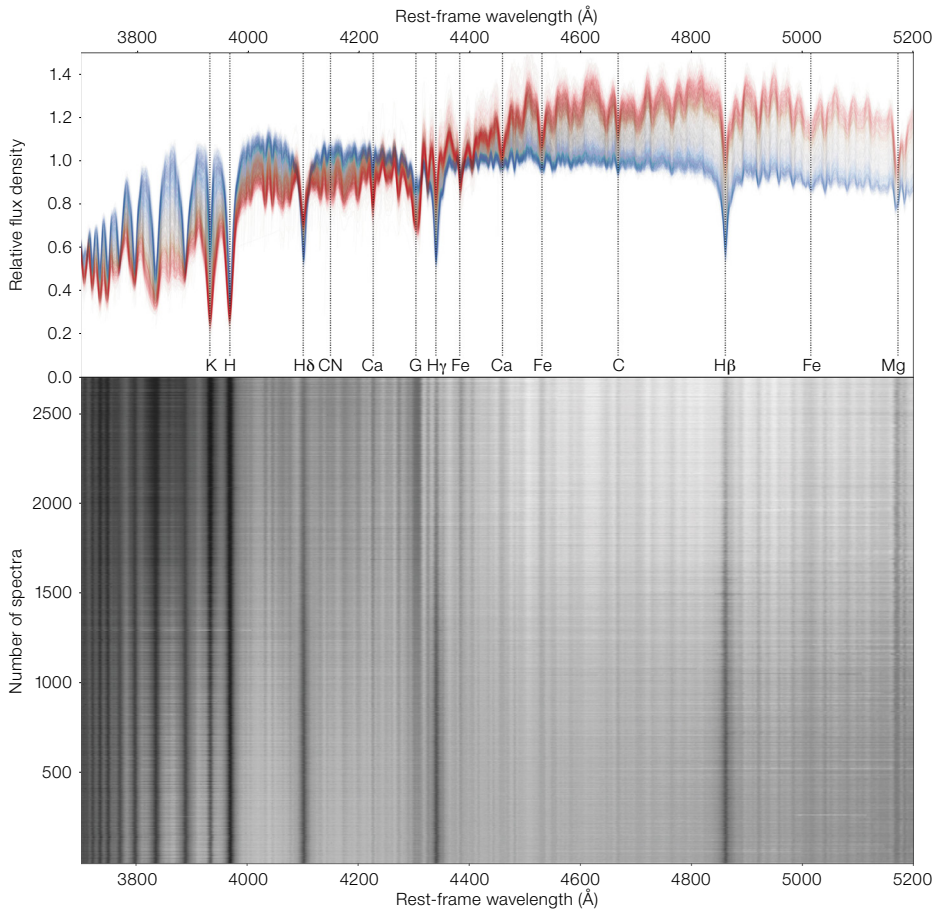
Figure 1. Compilation of 2707 normalised spectra with measured stellar velocity dispersions and Hγ indices. Top: The colour coding is based on the order of Hγ absorption (strongest/youngest: blue; weakest/oldest: red). Bottom: Horizontally aligned, vertically sorted by Hγ absorption. Emission lines are removed, and the rich structure in the spectra reflects the stellar population information content. The figure is adapted from van der Wel et al. (2021).

Figure 2. (Below) Example spectrum of a massive elliptical galaxy at redshift z = 0.66, illustrating the rich information content of each spectrum. In black we show the data, in red the model used to infer velocity dispersion and stellar population information. The figure is adapted from van der Wel et al. (2021).

Stellar populations

Galaxy age, as a concept, is somewhat ill-defined. Stars typically form over periods of many gigayears and the time since the formation of the first few stars is not the most relevant age parameter when it comes to characterising a galaxy's formation history (besides, it is impossible to measure from integrated spectra). A median or mass-weighted age is arguably the most informative single number, but this too is difficult to measure and highly sensitive to modelling assumptions. Light-weighted ages are close to the data, and are therefore easier to measure, but they are also less informative as they mostly tell us when the most recent period of high star formation activity occurred.

We start our exploration of the star formation history of galaxies in the most empirical manner possible. The Hδ absorption line strength is highly age-sensitive and its bimodal distribution
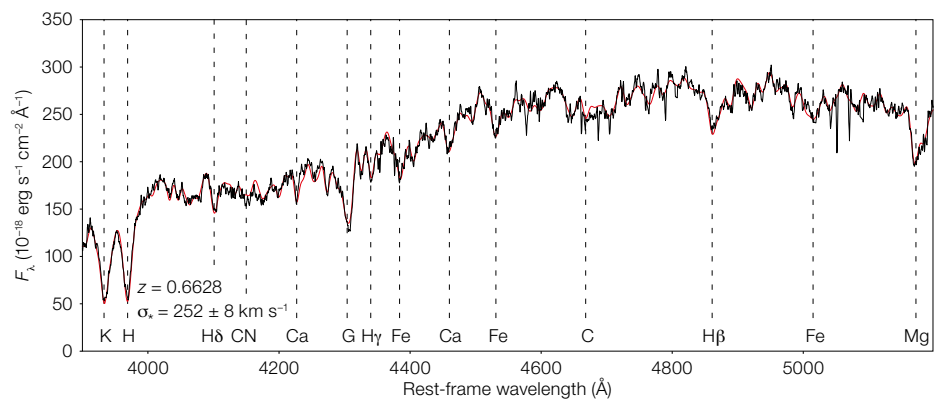
(Wu et al., 2018a) reflects and confirms what we already know about the bimodality of the galaxy population in terms of colour and star formation activity. The right-hand panel of Figure 3 shows the size–stellar mass distribution of galaxies, where more massive galaxies are generally older than less massive galaxies, and old galaxies are more compact than similarly massive young galaxies. These trends are even seen for galaxies that,

a priori, are selected as non-star-forming (Barone et al., 2021). This confirms that, even at early cosmic times, the separation of actively star-forming and quiescent galaxies must be relatively long lived: fast or frequent transitions from a highly star-forming state to a quiescent state would produce a blurred, unimodal distribution of an age indicator such as Hδ absorption (but see Chauke et al. [2019] for evidence of rejuvenation events that

move galaxies from a quiescent state back to an actively star-forming state for a brief period of time). We recently showed that galaxies from the state-of-the-art TNG cosmological simulation have similar ages — as judged by mock spectroscopic data — but with a less well defined bimodality (Wu et al., 2021); despite impressive progress in the ability of modern simulations to produce realistic galaxy populations, the processes that regulate the shutdown of star formation are not yet fully understood.

Individual spectral features such as Hδ absorption provide a qualitative sense of galaxy age, but to gain a quantitative understanding of age and, more generally, star formation history we need more. By modelling the full spectrum with modern stellar population synthesis models one can hope to retrieve dust attenuation properties (Barisic et al., 2020), as well as the full star formation and metal enrichment history of a galaxy. Whether this can in fact be achieved is very much an open question but with a number of simplifying assumptions we have already learned several important lessons. The main simplifying assumption we have made so far (Chauke et al., 2018) is that all stars have solar metallicity and solar abundance ratios, which is a useful starting point given the relatively high stellar masses of the galaxies in the sample: true metallicities are unlikely to differ by more than a factor of two. We find that the most massive galaxies have the oldest ages, typically 4 or 5 gigayears, putting their peak star formation redshift

at $z = 3$–5. Interestingly, Milky Way-mass disc galaxies at $z \sim 0.8$ are often still in the middle of their main formation phase, while at the present day, for the Milky Way itself and its siblings, star formation activity has been on the decline for many gigayears. This highlights the importance and power of applying the archaeological approach at large lookback times: we now witness the dynamical state and stellar population characteristics right in the middle of their main formation period, whereas for present-day galaxies this information remains mostly hidden in even the highest-quality datasets.

The next step is removing the assumption of constant, solar metallicity, starting with passive galaxies which have stronger absorption features, making them easier to model. Barone et al. (2021) show that the qualitative trends seen in Figure 3 hold: more compact galaxies are older than less compact galaxies. Meanwhile, dropping the assumption of solar abundance ratios, Beverage et al. (2021) find that the oldest galaxies have lower metallicities than younger passive galaxies. In the long term, extending these results to the general galaxy population will be one of the main outcomes of LEGA-C.

Stellar kinematics

The initial goal of LEGA-C as regards stellar kinematics was simply to measure the spatially integrated stellar velocity dispersion σ, allowing us to establish scaling relations and estimate dynamical

masses. The final sample includes more than 3500 galaxies with measured σ, presenting an unprecedented view of the Faber-Jackson relation (Bezanson et al., 2018b) and the Fundamental Plane (de Graaff et al., 2021; and see the left-hand panel of Figure 3). Despite important changes in the galaxy population since $z \sim 1$ — the number of stars roughly doubles, and the morphological mix of early- and late-type galaxies evolves significantly — these scaling relations are essentially unchanged, *modulo* the luminosity evolution expected from the ageing of stellar populations (de Graaff et al., 2020). As shown by de Graaff et al. (2021) it is of specific interest that old and young galaxies lie on the same Fundamental Plane, even though they occupy different regions in it, and with larger scatter for young galaxies. Despite vastly different evolutionary histories and different internal structures, all galaxies follow certain "rules" that force them to occupy a narrow region in the 3D parameter space of dynamical mass, stellar mass and size. Having determined this plane across half of cosmic time arguably puts the strongest constraints on galaxy formation models.

Stellar kinematic structure complements stellar population characteristics as a probe of assembly history: long-term, sustained star formation is usually associated with a disc-like structure, whereas an active merger history, especially during or after the main star formation epoch, leads to scrambled stellar orbits and a dynamically "hotter", more spheroi-
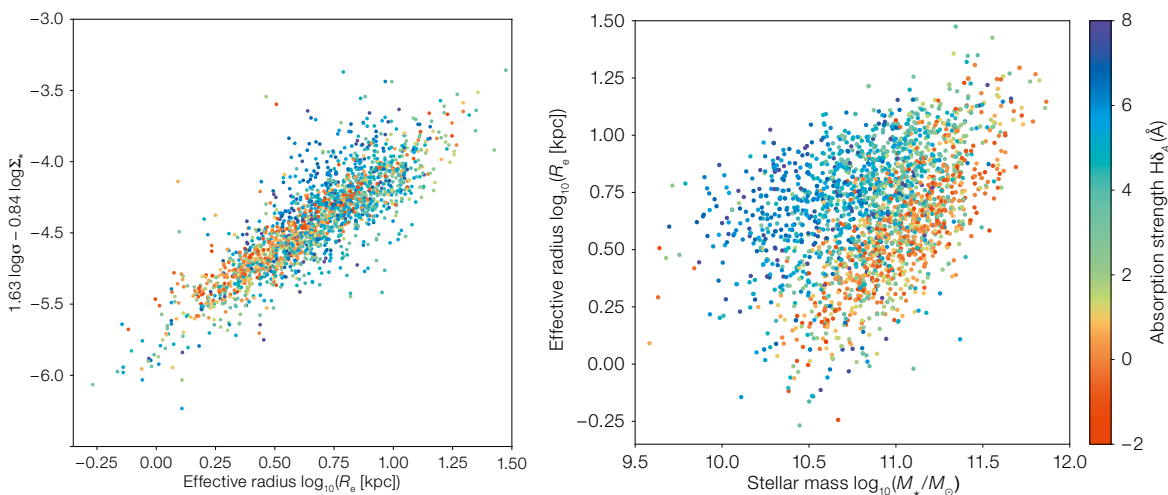

Figure 3. Left: Edge-on projection of the Fundamental Plane, with the effective radius on the x-axis, and a combination of the stellar velocity dispersion σ and the stellar surface mass density Σ on the y-axis. Right: Effective radius versus stellar mass. The colour coding denotes the Hδ absorption strength, which is a proxy for light-weighted stellar age.

dal system. But the integrated velocity dispersion does not tell us about the dynamical structure of a galaxy: a high σ may reflect a thin, fast-rotating disc or a rounder system with a high degree of quasi-random motion. One of the pleasant surprises of the LEGA-C data is that for nearly 800 galaxies we can measure stellar rotation curves along the slit (Bezanson, 2018a; van Houdt et al., 2021; see Figure 4), despite their large distances and the ground-based seeing (which is similar in angular extent to the galaxies themselves). As a first result, we showed that $z \sim 0.8$ quiescent galaxies are more rotationally supported ("discy") than their present-day counterparts (Bezanson et al., 2018a); such galaxies must gradually lose net angular momentum over time, presumably through merging.

To take full advantage of the spatially resolved kinematic information, we construct dynamical models (van Houdt et al., 2021; illustrated in Figure 4) to obtain the most accurate determination to date of the mass profiles of galaxies at large lookback times, as well as their kinematic structure, that is, the degree of rotational support. For the first time we have spatially resolved stellar dynamical information for both late- and early-type galaxies at large lookback times. We find that most star-forming galaxies are dominated by rotationally supported stellar discs, and that quiescent galaxies show a large variety. The fastest-rotating galaxies show little sign of star formation, but at the same time the most massive systems are often characterised by quasi-random motions, analogous to the slow rotators seen in the present-day Universe. These trends imply that galaxies do not (necessarily) undergo a change in dynamical structure when they transition from a star-forming to a quiescent state.

Synthesis

Galaxy structure and star formation history are closely linked; the true power of LEGA-C is therefore the availability of both stellar kinematics and stellar population information. We have only just begun to explore this direction, and for the general galaxy population we have so far only shown the global correlation between morphology, velocity dispersion and stellar population age (Figure 5). We see that young galaxies generally have late-type morphologies with disc-like structures, whereas old galaxies have early-type, bulge-dominated morphologies. At a fixed (integrated) velocity
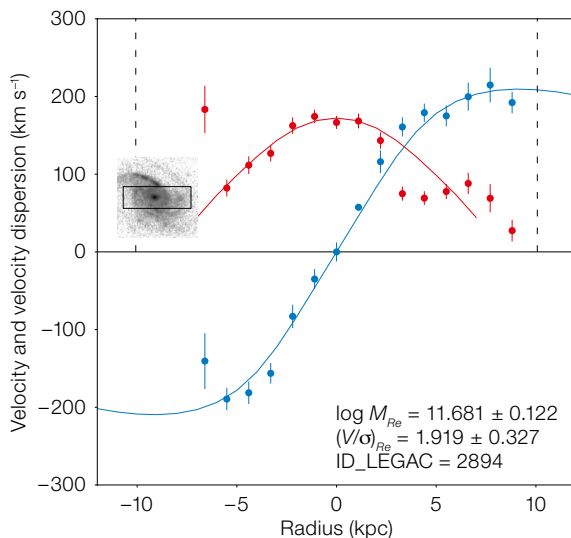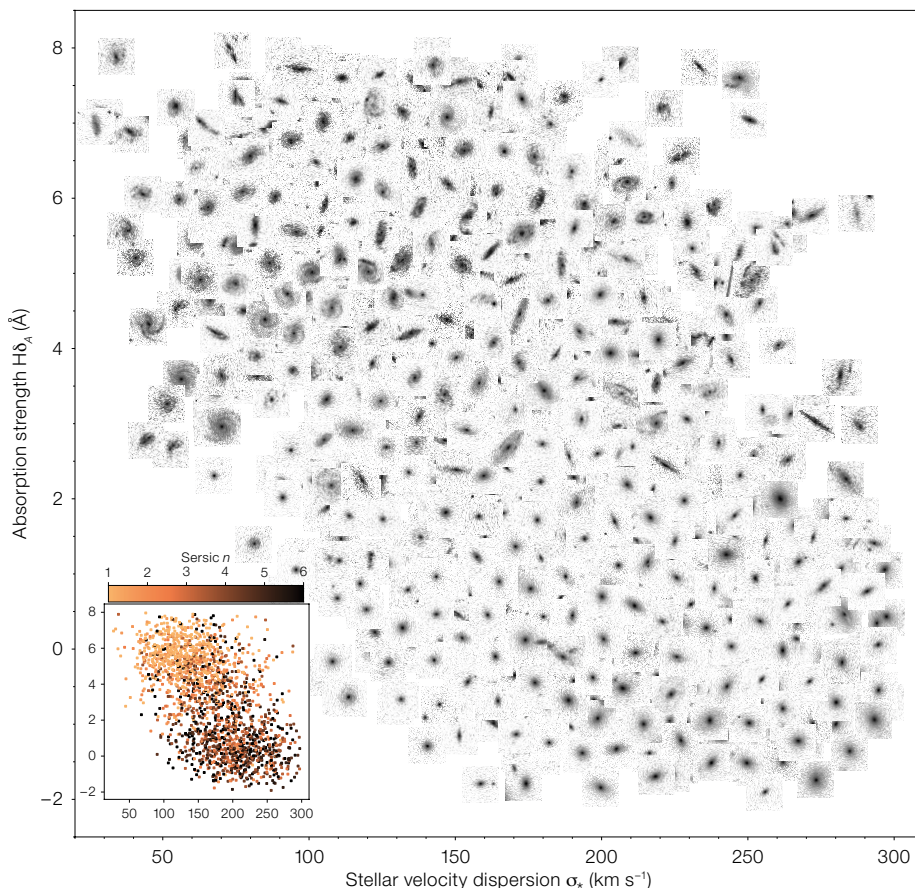

Figure 4. Spatially resolved stellar kinematic measurements with an axisymmetric model. The radial velocity is shown in blue and the velocity dispersion in red. These data constrain the dynamical mass (M) and the rotational structure (V/σ). The inset shows the Hubble Space Telescope image of this late-type galaxy, overlaid with the LEGA-C slit geometry as a rectangle. The kinematic information is extracted along the slit. The figure is adapted from van Houdt et al. (2021).

$\log M_{Re} = 11.681 \pm 0.122$
$(V/\sigma)_{Re} = 1.919 \pm 0.327$
ID_LEGAC = 2894

Figure 5. Hδ absorption strength — indicative of stellar population age — versus stellar velocity dispersion. Hubble Space Telescope images reflect the variation in morphology throughout this parameter space. The inset panel shows the Sérsic index (Sérsic, 1963), a structural property that distinguishes between disc- and bulge-dominated galaxies ($n = 1$ and $n = 4$, respectively). The figure is adapted from van der Wel et al. (2021).

dispersion, on the other hand, we see a large variety of morphologies, structures and ages.

Much more can be learned by reconstructing star formation histories and folding in the spatially resolved kinematics, and until now we have only examined in detail the connection between structure and stellar populations for a very specific type: post-starburst galaxies, defined as galaxies with high recent, but low current star formation activity, implying a sudden cessation of star formation or quenching 0.5–1 gigayear before the time of observation. These are the youngest quiescent galaxies, and we find that they are also among the most compact (Wu et al., 2018b): they stand out as young galaxies with very small sizes in Figure 3, breaking the general trend. This compactness is immediately linked to the recent starburst (Wu et al., 2020), as also evidenced by age gradients seen in the LEGA-C data: their centres are younger than their outer parts (D'Eugenio et al., 2020), which is the reverse of the gradients seen for the general population (old centres; young outskirts). We emphasise that this evolutionary trajectory is not rare at this cosmic epoch, but also that the majority of galaxies do not seem to follow it. Rather, for quiescent galaxies we see a positive correlation between age and size (at a fixed mass), and the younger quiescent population is rather similar in size and stellar kinematic structure to the star-forming population (Wu et al., 2020). This implies, as already mentioned above, that a (sudden) change in structure is not necessarily required to explain a declining star formation rate, but also that there are multiple pathways by which to evolve from actively star-forming to quiescent.

Looking ahead

In many ways we have just started the exploration of the rich LEGA-C dataset. In the near future we will present a consistent framework for estimating galaxy ages and metallicities, by comparing results from different models and fitting techniques. This provides the backbone for a full assessment of the star formation and chemical enrichment histories of the galaxy population at $z = 0.6–1$. Furthermore, supported by the absolute calibration of the galaxy mass scale and first determination of the angular momentum locked up in the stellar bodies of galaxies, we are in a great position to test the predictions of these fundamental quantities from the cosmological, hydrodynamical simulations.

On the observational side, the LEGA-C dataset will not be superseded in the foreseeable future. Large multiplex instruments on 8-metre-class telescopes (for example, the Multi-Object Optical and Near-infrared Spectrograph [MOONS] on the VLT) have the potential to extend the stellar population story to $z > 1$, but this will take a dedicated survey with ~ 100-hour integration times. Moreover, these fibre instruments do not provide spatially resolved information. Much of the value of LEGA-C is in the spatially resolved information enabled by the slit mask design, but no near-infrared multi-slit spectrographs are planned for the VLT. ESO's Extremely Large Telescope (ELT) will provide spectacular spatially resolved observations of high-redshift galaxies, but samples of hundreds, let alone thousands, of galaxies with high-signal-to-noise stellar spectroscopic data will likely remain out of reach.

References

Barisic, I. et al. 2020, ApJ, 903, 146
Barone, T. M. et al. 2021, MNRAS, in press, arXiv:2107.01054
Beverage, A. G. et al. 2021, ApJL, 917, L1
Bezanson, R. et al. 2018a, ApJ, 858, 60
Bezanson, R. et al. 2018b, ApJL, 868, L36
Chauke, P. et al. 2018, ApJ, 861, 13
Chauke, P. et al. 2019, ApJ, 877, 48
de Graaff, A. et al. 2020, ApJL, 903, L30
de Graaff, A. et al. 2021, ApJ, 913, 103
D'Eugenio, F. et al. 2020, MNRAS, 497, 389
Sérsic, J. L. 1963, Boletín de la Asociación Argentina de Astronomía, 6, 41
Straatman, C. M. S. et al. 2018, ApJS, 239, 27
van der Wel, A. et al. 2016, ApJS, 223, 29
van der Wel, A. et al. 2021, ApJS, in press, arXiv:2108.00744
van Houdt, J. et al. 2021, ApJ, in press, arXiv:2108.08142
Wu, P.-F. et al. 2018a, ApJ, 855, 85
Wu, P.-F. et al. 2018b, ApJ, 868, 37
Wu, P.-F. et al. 2020, ApJ, 888, 77
Wu, P.-F. et al. 2021, AJ, in press, arXiv:2108.10455

Links

[1] Lega-C: the final data release is accessed via the ESO Archive Science Portal: https://archive.eso.org/scienceportal/home?data_collection=LEGA-C

ESO/Vernazza et al./MISTRAL algorithm (ONERA/CNRS)
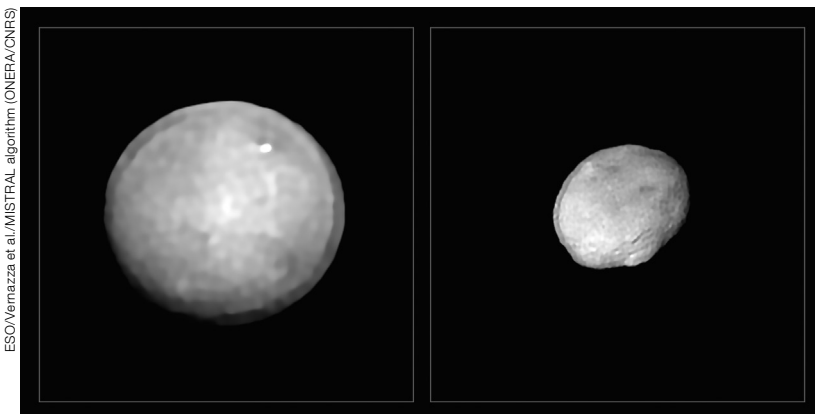
Ceres and Vesta are the two largest objects in the asteroid belt between Mars and Jupiter, approximately 940 and 520 kilometres in diameter. These images have been captured with the Spectro-Polarimetric High-contrast Exoplanet REsearch (SPHERE) instrument on ESO's Very Large Telescope as part of a programme that surveyed 42 of the largest asteroids in our Solar System. These two asteroids are also the two most massive in the sample.

The Journey of Lithium

Laura Magrini[1]
Rodolfo Smiljanic[2]
Nadège Lagarde[3, 4]
Elena Franciosini[1]
Luca Pasquini[5]
Donatella Romano[6]
Sofia Randich[1]
Gerry Gilmore[7]

[1] INAF – Astronomical Observatory of Arcetri, Florence, Italy
[2] Nicolaus Copernicus Astronomical Center, Polish Academy of Sciences, Warsaw, Poland
[3] UTINAM Institute, CNRS UMR 6213, University of Bourgogne Franche-Comté and Besançon Observatory, France
[4] LAB CNRS, University of Bordeaux, France
[5] ESO
[6] INAF – Astrophysics and Space Science Observatory of Bologna, Italy
[7] Institute of Astronomy, University of Cambridge, UK

Figure 1. The evolution of the lithium abundance A(Li) across the surface gravity–effective temperature (Kiel) diagram from the sixth Gaia–ESO internal data release.

After more than ten years and six data releases, the Gaia–ESO spectroscopic survey has come to an end. Gaia–ESO provides an extremely rich database of stellar parameters, radial velocities, and chemical abundances of more than 100 000 stars, amongst which the abundance of lithium can be considered one of the main products. Lithium is perhaps the most enigmatic of the elements, with several open issues regarding its nucleosynthesis and its evolution in stars and in the Galaxy. Gaia–ESO observations are allowing such issues to be addressed, by providing lithium abundances in stars from the pre-main sequence, through the main sequence, up to the red giant branch and the helium-burning red clump phase, over a wide range of masses. In the present work, we discuss the journey of lithium on the surface of evolved stars, using Gaia–ESO data for both field and cluster stars. We focus on the impact of extra mixing and possible lithium enrichment during the helium-burning phase. We briefly comment on the implications that these results may have for models of the chemical evolution of lithium in the Galaxy.
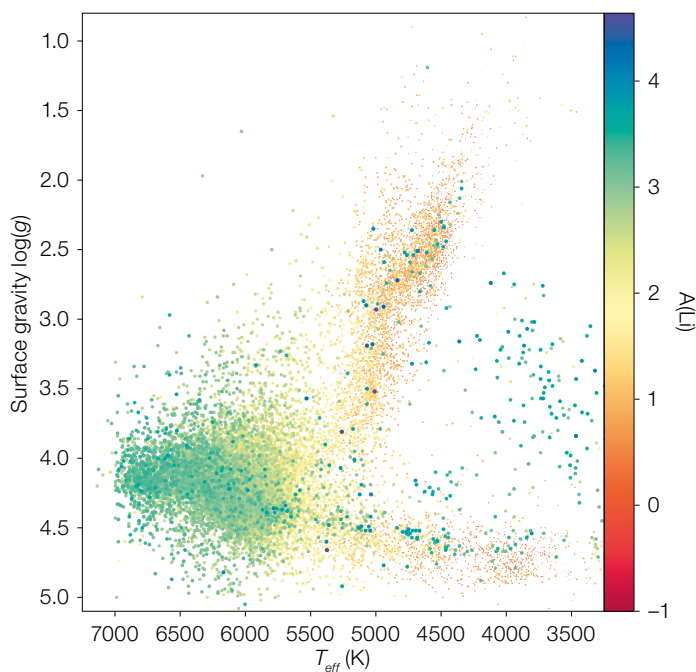
Introduction

Since the latest internal data release of the Gaia–ESO spectroscopic survey[1] in December 2020, many topics related to lithium (Li) abundances have been addressed by the Gaia–ESO collaboration. Recent publications include the serendipitous discovery of a rare Li-rich giant in the globular cluster NGC 1206 (Sanna et al., 2020), the study of the Galactic evolution of Li (Randich et al., 2020; Romano et al., 2021), the use of Li as an age tracer (Gutierrez Albarran et al., 2020; Binks et al., 2021), the exploitation of Li to put constraints on pre-main sequence evolutionary models and the effect of magnetic activity (Franciosini et al., submitted to *Astronomy and Astrophysics*), and the study of mixing processes in giant stars using Li as a tracer (Magrini et al., 2021a,b). We refer to Randich & Magrini (2021) for a description of the potential of the Gaia–ESO Survey data for Li studies. Figure 1 plots surface gravity against effective temperature (sometimes called a Kiel diagram) for all stars in the final data release of the Gaia–ESO Survey for which Li was measured. The figure highlights the data coverage in terms of evolutionary stages.

Of all the elements in the periodic table, Li, in the form of its main isotope ^{7}Li, has the most complex origin and evolution (see Romano et al., 2021). Li is one of the few elements, along with H and He, produced in the first instants of the Universe, by primordial nucleosynthesis after the Big Bang. However, the Li abundance we measure today is only in part the primordial one, because many destructive and constructive processes have occurred since (see, for example, Matteucci, D'Antona & Timmes, 1995; Romano et al., 2021; Randich & Magrini, 2021).

The production channels of Li include: stellar nucleosynthesis through the intermediate production of ^{7}Be, which is carried by convection to cooler stellar layers where it decays to ^{7}Li — the so-called Cameron-Fowler (CF) mechanism (Cameron & Fowler, 1971); thermonuclear runaways during classical nova explosions (Arai et al., 2021); Li production triggered by the flux of neutrinos emerging from the collapsing cores of exploding massive stars (Sieverding et al., 2018); and spallation of interstellar medium atoms by high-energy Galactic cosmic rays (Meneguzzi, Audouze & Reeves, 1971). However, as stated by Romano et al. (2021), *"it is a little disconcerting that none of the proposed ^{7}Li production channels have been firmly assessed yet"*. To shed light on the production of Li, all these mechanisms are considered by

Romano et al. (2021), who compare Gaia–ESO data with a model of chemical evolution. This comparison shows that most of the production of Li likely comes from nova outbursts, with the usual caution related to the non-uniqueness of the solution.

On the other hand, Li is easily destroyed in stellar interiors by proton capture at relatively low temperatures (~ 2.5 million K). Several transport mechanisms, such as convection, atomic diffusion, overshooting, rotation-induced mixing, mixing by internal gravity waves or magneto-hydrodynamic instabilities, might circulate material into these hotter layers, where Li is burned, and then up to the surface, resulting in the dilution of photospheric Li. The destruction of Li is particularly important after the main sequence (MS), when convection dominates the stellar envelopes and dilutes the Li abundance by a factor of 30 to 60 from the initial abundance (the so-called first dredge-up[a]; see Iben, 1967). Additional physical mechanisms, not included in standard evolutionary models, can cause further dilution of Li down to very low abundance values in the subsequent evolution of a star. These likely depend on the initial metallicity, mass and rotation of the star as well as other stellar properties, which still remain poorly understood if not uncomfortably unknown (see, for example, Anthony-Twarog et al., 2018; Charbonnel et al., 2021).

In this article, we will focus on the evolution of Li after the MS, where mostly destructive processes take place, but where some unexpected production can also happen. The results are described in detail in Magrini et al. (2021a,b).

The post-MS evolution of Li: catching the effect of extra mixing

In our investigation of the evolution of Li after the MS, we have used the homogeneously determined Li abundances for the combined Gaia–ESO sample of open cluster and field stars. Its large database of open clusters is indeed an important difference between Gaia–ESO and other surveys. For stars that are cluster members, metallicity, age and mass can be estimated more accurately than for field

stars. This allows a more thorough comparison between the observed Li abundances and the predictions of theoretical models. The Gaia–ESO data probe Li abundances in stars with a wide range of stellar masses and metallicities. In open clusters, the giant stars range from 1.1 to 4.5 $M_{\odot}$. With the complement of field stars, the mass range reaches even lower values.

We have tested two sets of models from Lagarde et al. (2012): the classical ones, which include convection as the main mixing mechanism, and models that include, in addition to convection, the effects of rotation during the MS and of mixing driven by thermohaline instability[b]. The comparison with the models confirms that convection alone cannot explain the observations, and that there is a strong contribution from rotation-induced mixing in the more massive stars in our sample. For the lower-mass giant stars in clusters and in the field, the comparison provides support to the hypothesis that a mixing process in the advanced phases of stellar evolution is required. This process might be thermohaline mixing.

These results are shown in Figure 2, in which the Li abundance A(Li) in open star clusters, divided into age bins, is shown as a function of effective temperature. Convection alone cannot explain the behaviour of Li after the first dredge-up and the observed further decrease in A(Li) can only be understood with the addition of some extra mixing processes. In Figure 2 we highlight a few special stars in which A(Li) is anomalously high, the so-called Li-rich giants. They are distributed around three main locations in the Hertzsprung-Russel (HR) diagram: the red giant branch (RGB) luminosity bump[c], the core-He-burning stages, and the early asymptotic giant branch. They are only a few percent of the total sample, but explaining their origin is quite challenging.

Are Li-rich giants the tip of the iceberg? Is there room for a general Li production after the RGB phase?

The existence of Li-rich giants has been known for many years (see, for example,

Brown et al., 1989; Charbonnel & Balachandran, 2000; Monaco et al., 2011; Kumar, Reddy & Lambert, 2011). However, their nature remains a mystery that has not yet been fully resolved. Usually, Li-rich giants are defined as those with A(Li) > 1.50, where this limit is the expected Li abundance after the first dredge-up. Many studies have shown that they amount to 1–2% of all red giant stars (see, for example, Casey et al., 2016; Smiljanic et al., 2018; Deepak & Reddy, 2019; Martell et al., 2020; Charbonnel et al., 2020). Recent results, based on a combination of spectroscopic and asteroseismic observations, have indicated the predominance of Li-rich giants in the core-helium-burning red clump (RC) phase (Silva Aguirre et al., 2014; Casey et al., 2019; Kumar & Reddy, 2020; Deepak & Lambert, 2021; Yan et al., 2021; Singh, Reddy & Kumar, 2019; Singh et al., 2021). Kumar et al. (2020) performed a large-scale investigation of the Li content in low-mass field stars in the RC phase. They suggest that the classical Li-rich RC giants (those with A(Li) > 1.50) are only the tip of the iceberg of a more general Li production in that phase. In their view, Li production in low-mass RC stars is actually ubiquitous. In our work, we explore this possibility from the point of view of open clusters.

Thanks to the high quality of the Gaia–ESO data, we can clearly separate RC stars from RGB stars in the HR diagram of open clusters. In Figure 3, we show the evolution of A(Li) after the MS. Following the prediction of the models (classical and with rotation and thermohaline mixing) from left to right in Figure 3 we begin with stars at the end of the MS, where A(Li) is between 2.5 and 3.4. Afterwards, the first dredge-up dilutes A(Li) at 1.3–1.5, almost independently of the stellar mass in classical models. In models with rotation and thermohaline mixing, the depletion of Li does not stop at the first dredge-up but continues: there is a further dilution at the RGB bump when the thermohaline instability is activated. After that, stars evolve towards the RGB tip and then drop in luminosity, reaching the RC. Further evolution during the RC can deplete Li down to −1 dex before the stellar luminosity increases again. The observations of stars in open clusters show that the typical A(Li) values of the
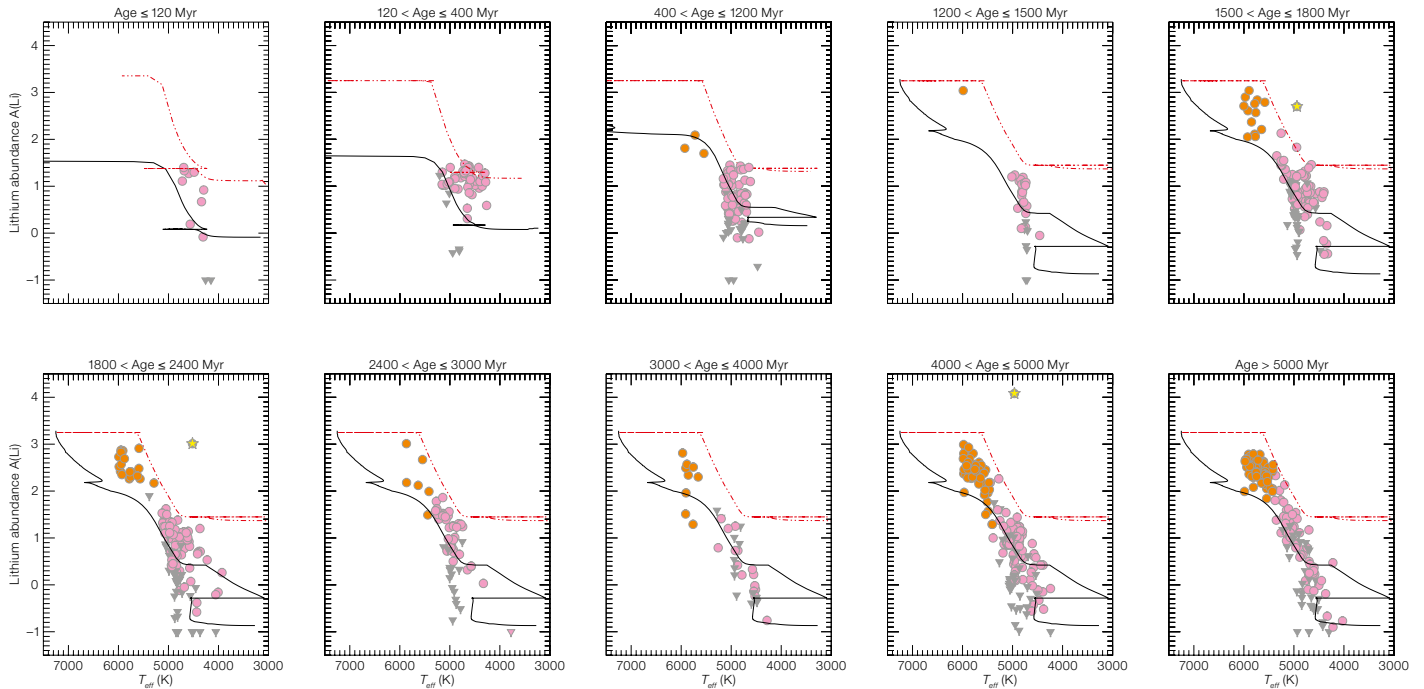
Figure 2. Lithium abundance A(Li) as a function of the effective temperature in open clusters in different age bins. The curves are the model predictions from Lagarde et al. (2012) for the closest stellar masses, with standard mixing (dashed lines) and including rotation-induced mixing (continuous lines), all for solar metallicity. The Li-rich giant stars are indicated with yellow stars.
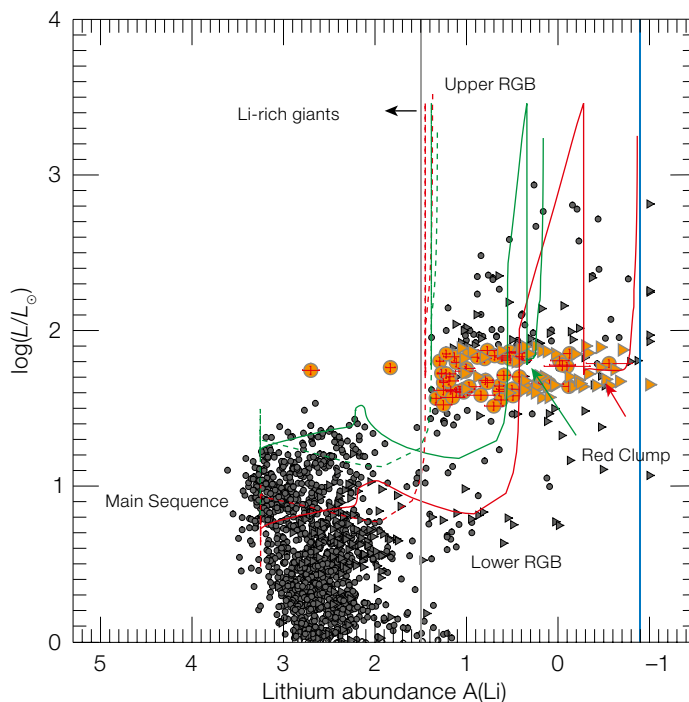
Figure 3. Luminosity versus A(Li) of member stars of open clusters with $1\,M_\odot < M < 1.8\,M_\odot$ and $-0.2 < [Fe/H] < 0.2$. Grey circles show the whole sample of member stars and coloured circles the stars at the RC. Triangles show the upper limits on A(Li). The continuous red and green curves are the models with rotation and thermohaline mixing at solar metallicity for $1.5\,M_\odot$ and $2\,M_\odot$, respectively, while the dotted red and green curves are the standard models for the same masses from Lagarde et al. (2012). The vertical black line indicates the limit for Li-rich giants with A(Li) > 1.5, while the vertical blue line at A(Li) > 0.9 shows the RC-RGB limit of Kumar et al. (2020). The locations of the RC in the models of Lagarde et al. (2012) that include rotation and thermohaline mixing are shown with green and red arrows.

RC stars are higher than expected from the models, while the same models fairly well reproduce A(Li) in the previous RGB phases.

What happens after the RGB, in the He-burning phase?

The data from open clusters in Figure 3 suggest that a further Li enrichment occurs just before or during the RC phase in a number of RC stars. The important thing is to evaluate the frequency at which this enrichment happens. In Figure 4 we show member stars in a representative cluster, Trumpler 5, separating them into the three evolutionary phases (RGB before and after the bump, and RC). The distribution of Li abundances in the RC stars shows values that are either similar to or even higher than those of
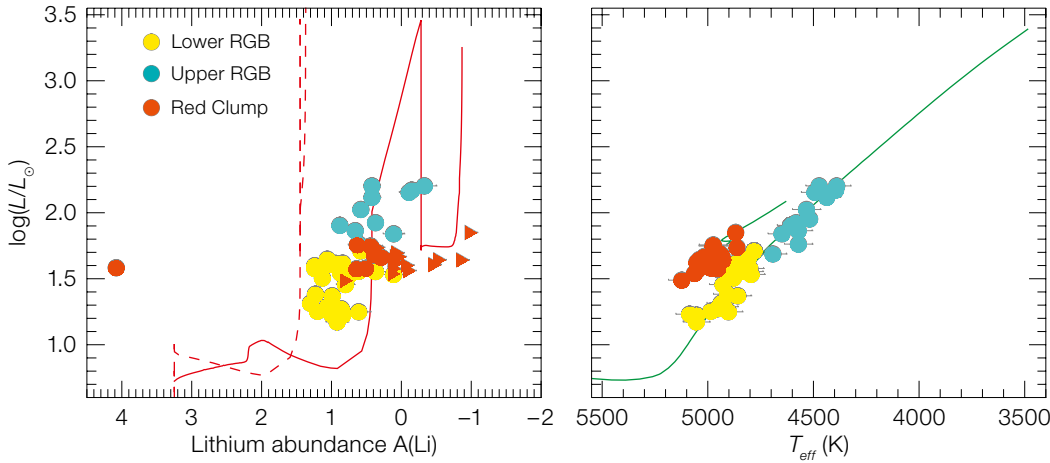
Figure 4. A(Li) and stellar parameters of member stars in the old cluster Trumpler 5. Left panels: Luminosity versus A(Li); yellow circles are lower RGB stars — prior to the RGB bump, cyan circles are upper RGB stars — after the bump, and red circles are RC stars. The continuous red curves are the models with rotation-induced mixing at solar metallicity for 1.5 $M_\odot$. The dotted red curves are the classical models with only convection from Lagarde et al. (2012). Right panels: HR diagrams with the Parsec isochrone (Bressan et al., 2012) at the age and metallicity of Trumpler 5.

the upper RGB stars. In practice, in Figure 4 we would expect RC stars to be located in the region where A(Li) reaches a plateau, with values between 0 and −1.

Considering only stars for which we provide measurements of A(Li), we find that from 35 to 50% of RC stars have A(Li) higher than stars in the previous phase, i.e., at the end of the RGB phase. Since the presence of several upper limits might hide much lower A(Li), we conclude that Li enrichment happens in a large percentage of RC stars, but that it might not be ubiquitous. The comparison with models that include additional mixing processes after the RGB phase, for instance He-flash mixing (Schwab, 2020) and neutrino momentum mixing (Mori et al., 2021), is very promising. Such models have the capacity to qualitatively explain the behaviour of the RC stars. Whilst they differ in terms of the description of the processes and their timescales, they do agree on the requirement for a mixing process during the He flash that is needed to activate the production of Li.

With the new data from Gaia–ESO, the journey of Li on the surface of evolved stars is seen to be complex. Even in evolutionary phases in which we might have expected only destructive processes, we find that Li can still be recreated. Since low-mass stars are the dominant population in the Galaxy that rules Li production at late times, this kind of production could have remarkable effects on our understanding of the whole evolutionary history of Li. In particular, we need to ascertain if Li production on the RC could

effectively compete with Li synthesis in thermonuclear nova outbursts, and this would push the quest for increasingly refined stellar and Galactic chemical evolution models.

References

Anthony-Twarog, B. J. et al. 2018, AJ, 155, 138
Arai, A. et al. 2021, ApJ, 916, 44
Binks, A. S. et al. 2021, MNRAS, 505, 1280
Bressan, A. et al. 2012, MNRAS, 427, 127
Brown, J. A. et al. 1989, ApJS, 71, 293
Cameron, A. G. W. & Fowler, W. A. 1971, ApJ, 164, 111
Casey, A. R. et al. 2016, MNRAS, 461, 3336
Casey, A. R. et al. 2019, ApJ, 880, 125
Charbonnel, C. & Balachandran, S. C. 2000, A&A, 359, 563
Charbonnel, C. et al. 2020, A&A, 633, A34
Charbonnel, C. et al. 2021, A&A, 649, L10
Deepak & Reddy, B. E. 2019, MNRAS, 484, 2000
Deepak & Lambert, D. L. 2021, MNRAS, 507, 205
Gutierrez Albarran, M. L. et al. 2020, A&A, 643, A71
Kumar, Y. B., Reddy, B. E. & Lambert, D. L. 2011, ApJL, 730, L12
Kumar, Y. B. & Reddy, B. E. 2020, Journal of Astrophysics and Astronomy, 41, 49
Kumar, Y. B. et al. 2020, Nature Astronomy, 4, 1059
Iben, I. 1967, ApJ, 147, 624

Lagarde, N. et al. 2012, A&A, 543, A108
Magrini, L. et al. 2021a, A&A, 651, A84
Magrini, L. et al. 2021b, arXiv:2108.11677
Martell, S. et al. 2020, arXiv:2006.02106
Matteucci, F., D'Antona, F. & Timmes, F. X. 1995, A&A, 303, 460
Meneguzzi, M., Audouze, J. & Reeves, H. 1971, A&A, 15, 337
Monaco, L. et al. 2011, A&A, 529, A90
Mori, K. et al. 2021, MNRAS, 503, 2746
Randich, S. & Magrini, L. 2021, Frontiers in Astronomy and Space Sciences, 8, 6
Randich, S. et al. 2020, A&A, 640, L1
Romano, D. et al. 2021, A&A, 653, A72
Sanna, N. et al. 2020, A&A, 639, L2
Schwab, J. 2020, ApJL, 901, L18
Sieverding, A. 2018, ApJ, 865, 143
Silva Aguirre, V. et al. 2014, ApJL, 784, L16
Singh, R., Reddy, B. E. & Kumar, Y. B. 2019, MNRAS, 482, 3822
Singh, R. et al. 2021, ApJL, 913, L4
Smiljanic, R. et al. 2018, A&A, 617, A4
Yan, H.-L. et al. 2021, Nature Astronomy, 5, 86

Links

[1] The Gaia–ESO spectroscopic survey: https://www.gaia-eso.eu/

Notes

[a] The first dredge-up is the first episode of mixing occurring when a star enters the RGB, and corresponding in Figure 2 to the point in the classical models at which we have no further decrease of A(Li).

[b] Thermohaline instability arises when an unstable gradient in composition is stabilised by a gradient in temperature — it also happens on Earth, in oceanic regions where evaporation produces a warm layer of saltier water above a layer of less salty, cooler water. The two layers can exchange heat though "salt fingers", which allow the mixing.

[c] The RGB bump is the evolutionary phase in which the shell reaches the discontinuity left by the envelope causing a momentary drop in the stellar luminosity.

This image captures both the northern and southern hemispheres at once — the whole night sky in one mind-bending image — something that would be impossible to see in real life. To create this image, photographers Petr Horálek and Juan Carlos Casado took two pictures at observatories located at the same latitudes in the northern and southern hemispheres. The top half is a photo taken at the Instituto de Astrofísica de Canarias's Roque de los Muchachos Observatory in La Palma in the Canary Islands, 29 degrees north of the equator, whilst the bottom half was taken at ESO's La Silla Observatory in Chile's Atacama Desert, 29 degrees south of the equator. When digitally stitched together, they create a continuous sweeping view of the night sky.

P. Horálek & J. C. Casado/ESO

The Hypatia Colloquium: Early Career Astronomer Series at ESO

Giacomo Beccari[1]
Henri M. J. Boffin[1]

[1] ESO

At a time when most planned international conferences, science events and seminars had been postponed or cancelled because of the COVID-19 pandemic, ESO decided to organise a new series of talks aimed at fostering the visibility of, and promoting the work of, astronomers at an early stage of their career: the Hypatia Colloquium.

The COVID-19 pandemic is a dramatic challenge that has affected the entire world. Almost two years of restrictions and social distancing have changed the way we live, work and interact with each other. Despite the closure of schools and universities, the adoption of distance learning measures has allowed the education system to be maintained in most countries. But there have been significant consequences for the overall educational experience of younger generations. Similarly, early-career astronomers at all levels (PhD and post-doc) have been forced to adapt to a new working scenario that presented numerous challenges. The "classical" approaches to building a solid and gratifying professional profile, creating a network of collaborations, and communicating the scientific results went through a complete revision which required (and still requires) creativity, strong commitment and support from senior astronomers, supervisors and mentors. We at ESO felt a responsibility to invest our energy and creativity into putting in place a channel that would allow excellent young researchers to show the results of their scientific work.

Thanks to the positive experience of the ESO Cosmic Duologues series (Beccari & Boffin, 2020), we have now learned to what extent online seminars can be an efficient way to engage the astronomical community, even under the severe restrictions imposed by the pandemic. As part of the ESO science activities, the Garching Office for Science in the Directorate for Science therefore organised a new series of seminars, called the

Hypatia Colloquium, dedicated to early-career scientists. Hypatia (ca. 350–415) was a Greek philosopher, mathematician and astronomer, the first female mathematician whose life is reasonably well recorded. Figure 1 shows the logo of the new series.

The call for abstracts

At the beginning of November 2020 ESO released a call for abstracts inviting PhD students and early postdocs (a maximum of three years from their PhD) working in any field of theoretical and observational astronomy and astrophysics, with no restriction on nationality or host country, to apply to be nominated as a speaker at a Hypatia Colloquium. Each event in the new series would host two seminars, making a total of 42 slots available for the talks. The deadline for applications was 30 November 2020 and in less than a month ESO received 334 valid applications from young astronomers around the world.

This extremely positive response from young astronomers was already witness to a strong desire to break down the walls within which the pandemic has confined our scientific life and to explore new ways to express their talent and creativity. The selection of the top speakers was made by an ad-hoc committee composed of ESO staff and Fellows from both Garching and Vitacura, and was based on the scientific quality of the submitted abstracts only. The 42 selected speakers were contacted towards mid-December and the full programme was released before Christmas 2020.

The complete programme of the talks can be found on the dedicated web page[1]. The programme page reports the name and a photo of each speaker, together with the title of the talk and the date and time of each event. By clicking on the title of the talk it is also possible to download the full abstract of the talk and a Curriculum Vitae of the speaker. We show in Figure 2 the distribution of gender and year of PhD of the speakers selected for the Hypatia Colloquium 2021. It is worth noting that the call was released in November 2020 and the programme published at the end of the
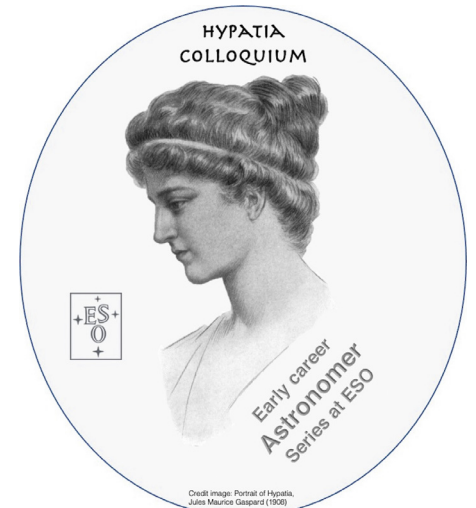

Figure 1. Logo of the ESO Hypatia Colloquium series.

same year. Hence, at the time of giving their talk, half of the speakers had not yet completed their PhD, an impressive fact when considering the scientific quality of the talks!

The new series

The talks were scheduled on Tuesdays at 15:00 CET from 2 February to 27 July 2021 (except once per month, when there was an ESO Cosmic Duologue). The format of the series foresees a 20-minute talk followed by questions and discussion. Most of the seminars were co-chaired by an ESO student and an ESO Fellow.

The seminars were hosted entirely online using the video conferencing tool Zoom and live-streamed on the Hypatia Colloquium YouTube channel[2]. Attendees could register for the series using a web form. Registered participants were able to attend the seminars and interact with the speakers via the Zoom meeting. Alternatively, the community was invited to attend the live events on the dedicated YouTube channel. All YouTube attendees could ask questions during the live event using the Live Chat on YouTube (or using a web form or by email if they preferred). All the video recordings of the live events, including the content of the live chat, are available on YouTube. The link to each seminar is available on the web page of
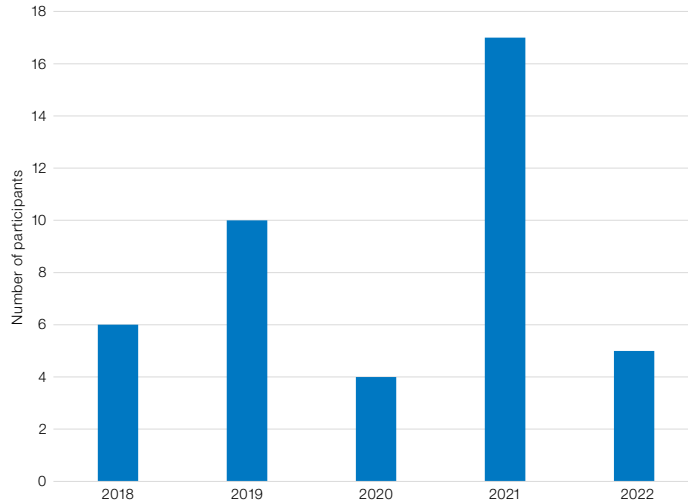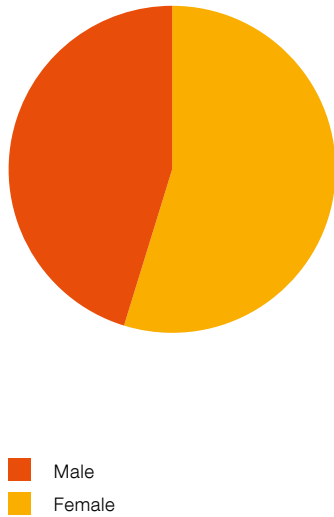
Figure 2. Distribution of gender (left) and year of PhD (right) of the speakers in the Hypatia Colloquium series. The call was released in November 2020 meaning that all speakers who were expected to complete their PhD in 2021 or 2022 were still PhD students at the time of giving their talk.

the programme[1]. We show in Figure 3 a screenshot of the front page of the Hypatia Colloquium YouTube channel.

The channel analytics clearly attest to the success of the series. Whilst each event was followed live by a total of 40 to 60 participants spread equally between Zoom and YouTube, the videos record (at the time of writing) a total of 4400 views.

Whilst the numbers are already quite impressive, it is when watching the seminars that the real quality and impact of the series can be fully appreciated. With the Hypatia Colloquium, ESO allowed the young generation of astronomers to paint a remarkable and unique picture of the excellence of the science being done by early career astronomers. The videos available online represent an

Figure 3. Screenshot of the YouTube channel of the Hypatia Colloquium. All the talks in the 2021 series are available on the dedicated playlist.
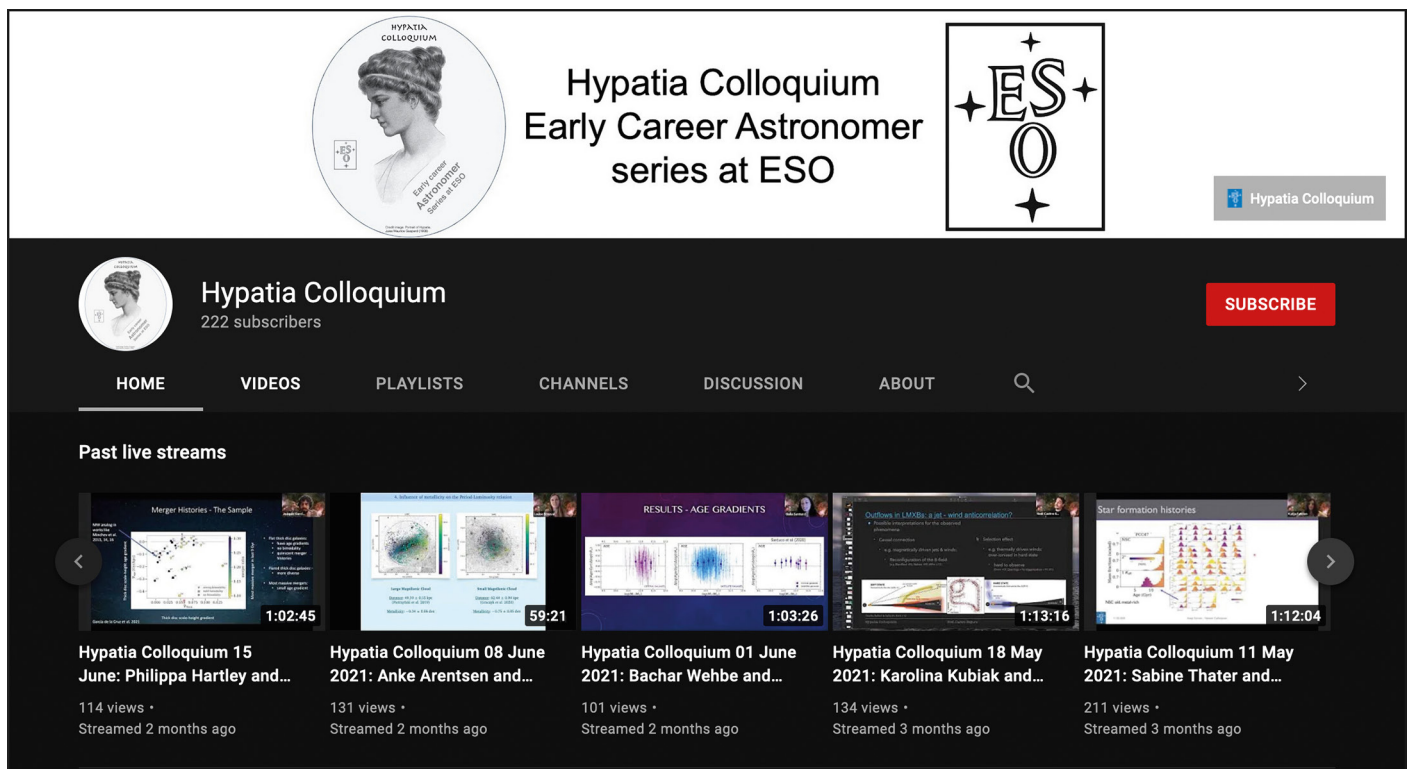
extraordinary and exploitable treasure and resource of talent.

The future of the series

Given the success of the series and the enthusiastic reaction of the community, ESO will continue the series and released a new call for applications in October 2021. The new series will likely be scheduled for the period January to June 2022, so that it concludes around the time of the annual meeting of the European Astronomical Society (EAS).

To provide the community with a complete collection of scientific topics presented in this first series of talks, the "Hypatia Colloquium 2021" proceedings collect two-page contributions from each speaker. These are available for download on the ESO website[3] and on Zenodo.

Finally, we would like to acknowledge the struggles that young astronomers are experiencing during these challenging times. It is not easy to maintain focus and motivation when such a dramatic event like the COVID-19 pandemic is putting our (and our loved ones') health, life and safety in great danger. Science is a wonderful endeavour which requires dedication and sacrifice but always pays back through astonishing discoveries that reveal the hidden beauty of our Universe. Universities, research institutes, senior astronomers and mentors at all levels now have a responsibility to build the infrastructures and to redesign evaluation and hiring processes, in order to face the new reality with a modern attitude, appropriate to the times and able to create the space in which the creativity of the youngest generations can bloom and grow. At the same time, we must all help each other to remember that gratitude, humility, passion and professionality are key to translating our efforts into knowledge for future generations.

References

Beccari, G. & Boffin, H. M. J. 2020, The Messenger, 181, 34

Links

[1] Hypatia colloquium programme: https://www.eso.org/sci/meetings/garching/hypatia-colloquium/program.html
[2] YouTube channel of the Hypatia Colloquium: https://www.youtube.com/c/HypatiaColloquium/featured
[3] Hypatia Colloquium 2021 proceedings: https://www.eso.org/sci/activities/garching/Hypatia/2021/ESOHypatia2021.pdf

P. Horálek/ESO

This photograph shows some of the antennas comprising the Atacama Large Millimeter/submillimeter Array (ALMA) against the backdrop of a panoramic view of the Milky Way. There is far more to ALMA than shown here; the array can span distances of up to 16 kilometres and is formed of 66 individual antennas. Some features visible in the sky include the constellation Crux (The Southern Cross) just above and to the right of the nearest antenna, and the Carina Nebula slightly further to the right.

Report on the ESO/ESA Workshop

Detector Modelling Workshop 2021

held online, 14–16 June 2021

Elizabeth George [1]
Benoît Serra [1]
Thibaut Prod'homme [2]
Matej Arko [2]
Frédéric Lemmel [2]
Bradley Kelman [3]

[1] ESO
[2] European Space Agency, ESTEC, Noordwijk, the Netherlands
[3] Open University, Milton Keynes, UK

The Detector Modelling (DeMo) workshops aim to bring together a community of scientists and engineers who are interested in modelling detector effects and simulating detectors for astronomy. The first such workshop was held online over three afternoons from 14 to 16 June 2021. The three afternoons were organised around blocks of contributed talks from the community covering a wide range of detector topics such as detector effects like persistence and radiation damage, instruments covering a wide range of astronomical wavelengths from X-ray to the optical and infrared, and detectors used in other fields like particle physics. In addition to the scientific programme, the workshop featured a tutorial series on how to use the Pyxel detector simulation framework and how to contribute to Pyxel.

Introduction

As astronomical observations move ever further into the realm of precision astronomy, systematic effects in instruments, especially detectors, are beginning to dominate instrument error budgets. Understanding, modelling, and correcting for detector effects are now necessary to achieve science goals ranging from characterising exoplanet atmospheres, to measuring chemical abundances in high-redshift galaxies, to performing precision astrometry of stellar fields.

Engineers working on detectors at ESO and the European Space Agency (ESA) have been collaborating for several years, under the umbrella of the ESA–ESO collaboration, on a detector simulation tool named Pyxel[1]. The goal of Pyxel is to create an open-source simulation tool that allows astronomical instrument builders to simulate their detectors at the design and engineering stage as well as helping astronomers develop calibration or analysis strategies to address detector effects that may impact their science. The DeMo workshop was envisioned both as a way to share Pyxel with the community through hands-on tutorial sessions, and as a forum for the exchange of ideas around detector modelling for astronomy via a programme of contributed talks. Figure 1 is the workshop poster.

Scientific programme

The scientific programme was based on the contributions of the participants and consisted of 22 talks in seven thematic blocks. These were:
– optical and infrared instrument simulators (two blocks);
– detector measurements and models (three blocks);
– X-ray instrument simulators;
– particles and radiation modelling.

One of the most popular themes of the conference was instrument simulators. Speakers presented ScopeSIM (the simulator for the Multi-AO Imaging Camera for Deep Observations [MICADO] at ESO's Extremely Large Telescope), PLATOsim, the Euclid suite of instrument simulators, SIXTE (a generic X-ray instrument simulation) toolkit, xifusim (the Athena X-IFU instrument simulator), and PhoSim for Vera C. Rubin Observatory. These complete instrument simulators often include modules for generating astronomical scenes and transmission through the instrument optics, a simulation of detector effects, and in some cases also an analysis pipeline for the resulting data. The goal of these simulation tools is complete end-to-end modelling of an instrument, or even a complete simulation of a specific instrument science case including the analysis of synthetic data.

Following the full instrument simulators, detector-specific simulations were presented in several sessions covering simulation work for the China Space Station Telescope (CSST), the European Synchrotron Radiation Facility's X-DECIMO (a Python package for X-ray detector modelling), CERN's Allpix Squared (silicon detector Monte Carlo simulations for particle physics), and electron avalanche photodiode (e-APD) saphira modelling. In these sessions we had several presentations from fields outside astronomy (particle physics, for example) which provided a different perspective on detector characteristics and modelling.

The largest number of talks covered measurements, models, and/or simulations of individual detector effects. These tended to be very detailed models of single detector effects that astronomers and engineers had worked hard to understand in order to enable a specific science case. These included C3TM (radiation damage in CCDs), CosmiX (charged particles in detectors), and various models covering interference, non-linearity, inter-pixel capacitance effects, persistence, and luminescence effects in mercury cadmium telluride (MCT) hybridised arrays, as used in many ESO instruments. Some of the detector models presented are already integrated into Pyxel, and others will be added by the speakers in the coming months as the flexible nature of Pyxel allows users to add their own favourite models to the simulation framework. A highlight of these talks was the many cases where precision laboratory data were combined with physical knowledge of the detectors to create a model of detector behaviour.

The final theme covered by the scientific programme was the impact of detector effects on science instruments and the use of detector simulations in instrument design and systems engineering. Speakers presented Pandeia (the James Webb Space Telescope exposure time calculator), persistence correction in ESO's instruments, mitigation of tearing in the Vera C. Rubin Observatory CCDs, and NASA's Spectro-Photometer for the History of the Universe, Epoch of Reionization and Ices Explorer (SPHEREx) mission. These talks provided valuable context for why detector modelling is so important for precision astronomical instruments, as the impacts of the effects are clearly seen in the (synthetic) data.

Whilst the models and simulations presented at DeMo were all different, some

of the challenges associated with simulating detectors and instruments are common, and all workshop participants were exposed to a huge range of instrument and detector simulation tools already in existence. We are confident that participants looking to simulate detector effects now have a buffet of options to choose from when getting started with their own modelling project.

Pyxel tutorials

This dense programme of scientific talks was complemented by two sessions dedicated to Pyxel, comprising close to four hours of live interactive tutorial. The goal of these tutorial sessions was to introduce Pyxel to the community and allow participants hands-on practice using the simulation tool. The tutorials were organised as a walkthrough using jupyter notebooks with the participants being able to follow, either by running the notebooks without any prior installation using binder in their web browser, or by installing Pyxel beforehand on their own computers. Installation instructions and support were provided in a dedicated channel under the workshop Discord server before, during and after the workshop.

The first tutorial session was dedicated to (i) introducing all the necessary information needed to start working with the tool, (ii) a simple demonstration of Pyxel focusing on single image mode, an explanation of the configuration file, and how to interact with Pyxel's outputs, and (iii) a guide on how to add new detector models to the framework. The second Pyxel tutorial session took a deeper look into the three advanced modes: (i) parametric mode, to run the pipeline multiple times looping over a range of parameters, (ii) dynamic mode, to simulate time-dependent effects, and (iii) calibration mode, to optimise models or detector parameters to fit target datasets. The tutorial notebooks are available online for anyone who would like to try them out[2].

Demographics

The Science Organising Committee was a small group made up of the Pyxel developers at ESO and ESA. It was decided early on that the workshop should be free, 100% online, and open to anyone to submit an abstract so as to ensure the broadest participation possible. All abstracts submitted to DeMo were excellent, so all submissions were scheduled in one of the scientific blocks, ensuring talks from a range of career levels from students onwards. We did not collect demographic data at workshop registration; however, we held a post-workshop survey that approximately one third of the 270 workshop participants completed.

The profiles of the participants who took part in the post-workshop survey were:
– 50% early career and 50% mid-late career;
– 77% male, 14% female, and 2% diverse (7% no response);
– 47% university and 44% research/government organisation, < 8% from industry.

Additionally, based on the affiliations given at registration, there were participants from five continents, with speakers from North America, Europe and Asia. The online format of the workshop allowed a much broader geographic participation than is usually seen at in-person detector conferences, with peak participation of 150 simultaneous talk viewers and 100 simultaneous instances of the Pyxel tutorial notebooks running. Three of the 22 talks were given by women, matching the participant demographics. Figure 2 is a conference "photo" of some attendees at one of the virtual talks.

We also collected data on the professional activities of the participants and found that around 80% are involved in detector simulation activities or detector characterisation, and the majority are involved in instrument development, with many detector engineers. The full list of participants with names and affiliations and all presentations are now openly available online on the event website[3].

Conclusions and way forward

Overall the DeMo2021 workshop was a success in terms of the number of participants, the quality of the presentations, and the engagement of the participants, but above all because it accomplished its main goal of building a community of scientists and engineers who are interested in modelling detector effects and simulating instruments for astronomy and beyond. At the end of the workshop, everyone (including the organisers!) had learned about a huge number of detector models and simulation tools that might be useful for their own work.

During the workshop we had good interaction between participants on the workshop Discord server, but the post-workshop survey indicated that only 67% of participants felt engaged with the other participants. Future versions of this workshop, whether online, hybrid, or in-person, will have more interactive sessions so that workshop participants can get to know each other outside of the strict format of plenary talks.

The vast majority (98%) of those who responded to the survey felt welcome at the workshop and are interested in participating in a future version of this workshop. The survey brought some interesting information which will guide the organisation of the next iteration of this workshop: for example, 66% would like an event every year and 33% every two years, 55% are interested in a hackathon component, and 89% would like tutorials for some of the other simulations tools presented at DeMo.

Links

[1] Pyxel website: https://esa.gitlab.io/pyxel/
[2] Pyxel tutorials: https://gitlab.com/esa/pyxel-data
[3] DeMo workshop website: https://indico.cern.ch/event/1026001/

The 10th VLTI School of Interferometry: Premiering a Fully Online Format

Florentin Millour[1]
Anthony Meilland[1]
Alexis Matter[1]
Guillaume Mella[2]
Laurent Bourgès[2]
Claudia Paladini[3]
Isabelle Tallon-Bosc[4]
Michel Tallon[4]
Ferreol Soulez[4]
David Buscher[5]
Antoine Mérand[3]
Myriam Benisty[12]
Roy van Boekel[6]
Pierre Cruzalèbes[1]
Denis Defrère[7]
Armando Domiciano de Souza[1]
Mercedes Filho[8]
Paulo Garcia[8]
Sebastian F. Hönig[9]
Roxanne Ligi[1]
Camille Maccotta[1]
John McKean[10, 11]
Fabien Patru[1]
Karine Perraut[12]
Jörg-Uwe Pott[6]
Alain Spang[1]
Sophie Rousset[1]

[1] University of Côte d'Azur, Côte d'Azur Observatory, CNRS, Lagrange Laboratory, France
[2] University of Grenoble Alpes, CNRS, IRD, INRAE, Météo-France, OSUG, France
[3] ESO
[4] University of Lyon, ENS de Lyon, CNRS, Lyon Centre for Astrophysical Research, France
[5] Cavendish Laboratory, University of Cambridge, UK
[6] Max Planck Institute for Astronomy, Heidelberg, Germany
[7] Institute of Astronomy, KU Leuven, Belgium
[8] CENTRA/SIM, Department of Physics Engineering, University of Porto, Portugal
[9] School of Physics & Astronomy, University of Southampton, UK
[10] Kapteyn Astronomical Institute, University of Groningen, the Netherlands
[11] ASTRON, Institute for Radio Astronomy, Dwingeloo, the Netherlands
[12] University of Grenoble Alpes, CNRS, IPAG, France

Very Large Telescope Inerferometer (VLTI) schools have nearly a 20-year history and have trained a significant fraction of today's optical interferometrists who use high-angular-resolution techniques on a regular basis. Very early in the development of the VLTI, training was identified by the community as a necessary tool, as the expertise in optical long-baseline interferometry was limited to a few groups in France and Germany (in those early years the UK was not an ESO member state). The first VLTI school took place in Les Houches, France, in 2002 and since then VLTI schools have been organised in several locations (France, Germany, Hungary, Poland, Portugal) roughly every two years, the previous one being held in 2018 in Lisbon. The VLTI schools are funded and coordinated through the European Interferometry Initiative (Eii).

Very Large Telescope Interferometer (VLTI) schools[1] (Garcia, 2009) have been held every two years since 2002, the 9th being in 2018 in Lisbon (Garcia et al., 2018). Here we report on the 10th VLTI school[2], which was organised by the J.-L. Lagrange laboratory in Nice, and had its focus on the latest VLTI instrument: the Multi-AperTure mid-Infrared SpectroScopic Experiment (MATISSE; Lopez et al., 2021). MATISSE is a four-beam combiner operating in the mid-infrared, from 2.8 to 13 microns, with an emphasis on interferometry for planetology. The GRAVITY instrument and other instruments from the Center for High Angular Resolution Astronomy (CHARA) observatory were also presented. It was aimed at graduate and PhD students, as well as postdocs, who wish to learn the theory and practicalities of optical and infrared interferometry. It was originally intended to hold the school in June 2020, in the technology park named Sophia Antipolis, near Nice in France, a beautiful location in a pine forest, just 10 minutes from sandy beaches. However, the COVID-19 pandemic situation forced us to shift the date, first to September 2020 and finally to June 2021. Given the unfavourable evolution of the global pandemic situation in early 2021, we finally decided to switch to a 100% online format with lectures and tutorials.

To adapt to the new situation we had to swiftly reorganise the school schedule, with the expertise and support of the technical group of the Jean-Marie Mariotti Center (JMMC), and we accepted the challenge of hosting 100% online practice sessions with students scattered all over the world. All the school's teachers accepted the added complication of giving their lectures either prerecorded or live (with recorded videos[3]). Finally, to allow students from most countries to attend the school at decent hours, we extended its duration to 2 weeks and limited the mandatory online presence to 4 hours a day.

The school took place online in a specially tailored Gather (gather.town) space for direct interactions (chat, voice and video) and practice sessions, combined with Zoom sessions for the lectures, and the Nuclino live wiki-like environment for the exchange of information and files (see Figure 1). On the technical side, the most challenging part was the setup of 21 virtual machines for the students to run all the practice sessions, the students being typically in groups of three. It was possible thanks to the strong involvement of the JMMC technical group and the resources of the Grenoble Alpes Research Scientific Computing and Data Infrastructure (GRICAD) service.

There were 63 registered students (participating in both the lectures and the practice sessions) plus 59 free listeners (following the lectures only), 45 of whom were MSc or PhD students, including 35 female participants. The registered students originated from 23 different countries (see Figure 2): nine from France, six each from Chile, Poland and the USA, five from Germany, four each from Italy and Switzerland, three from Belgium, two each from Egypt, Great Britain, India, the Netherlands and Turkey, and one each from Brazil, China, Greece, Ireland, Iran, Iraq, Malta, Peru, Spain and Sweden. That balance changes a bit when account is taken of the free listeners, as there was a massive participation from Chile and China at the lectures. The interferometric expertise of the students was diverse, allowing students to learn from each other too. The number of connections to the lectures was around 60 on average with peaks up to 86.
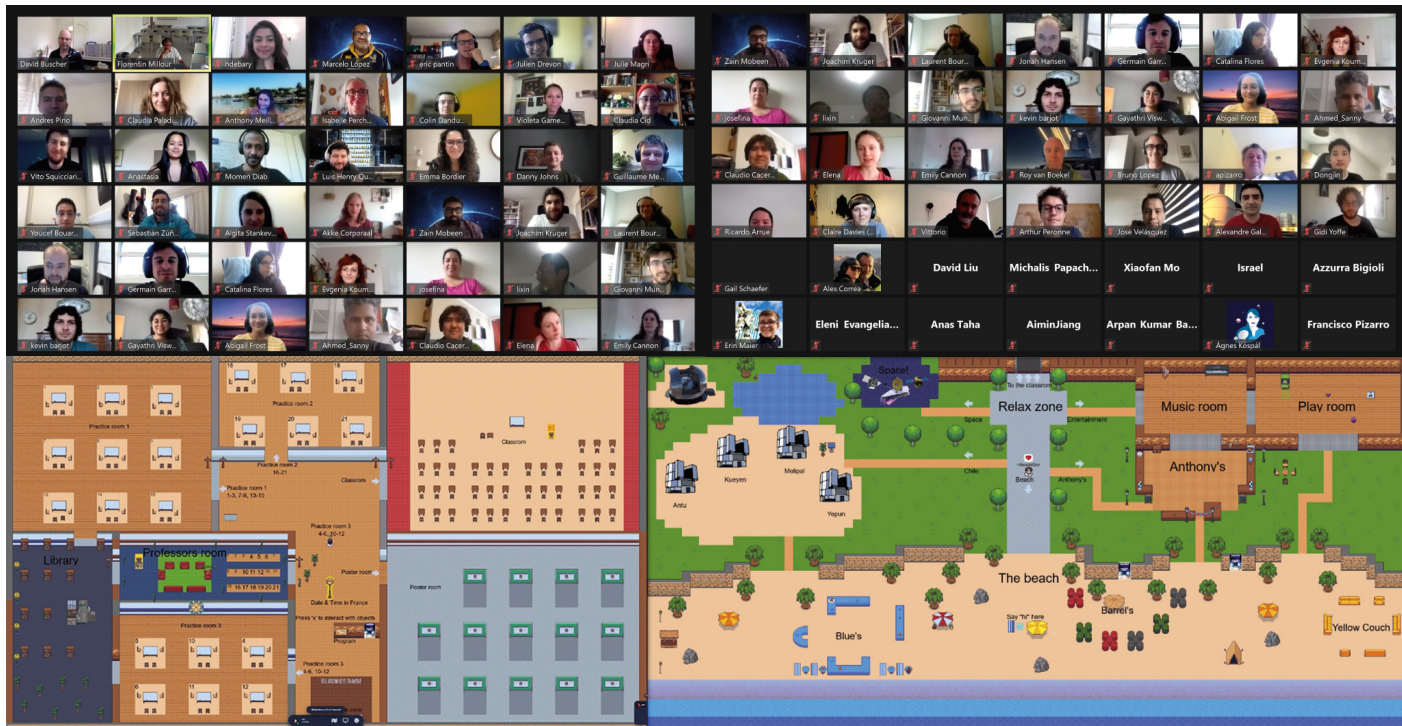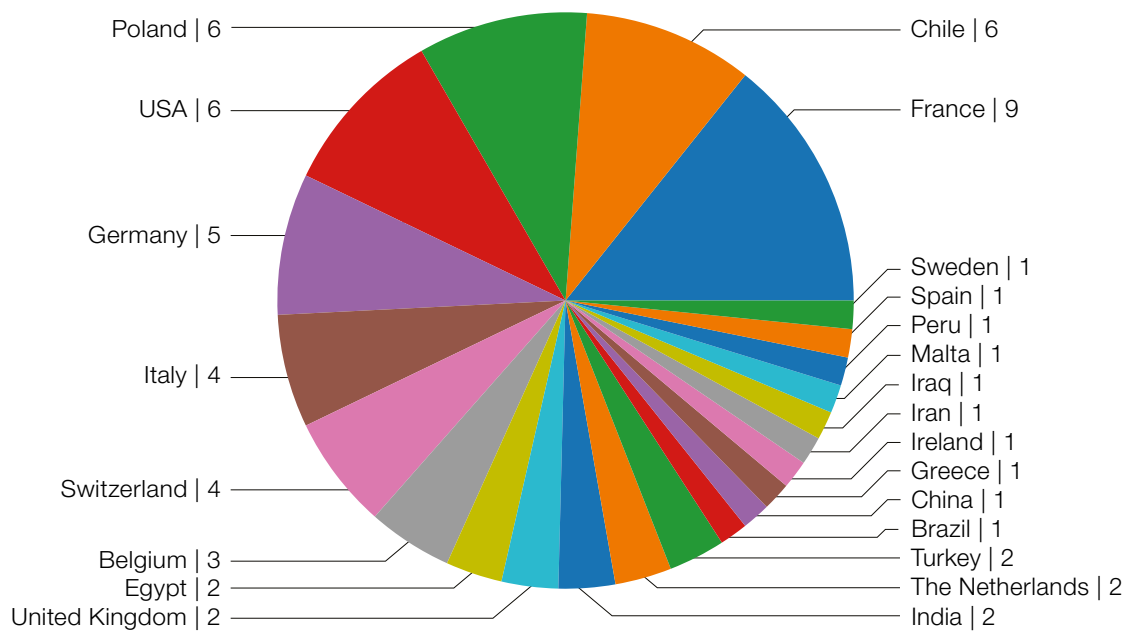
Figure 1. (Above) Top row: The Zoom school picture (featuring 67 of the participants). Bottom row: The Gather school places: on the left are the workspace with a classroom, rooms for the practice sessions with shared whiteboards, a library (collection of links to useful resources), and a poster room; on the right is the relax zone with many split rooms used for informal or group discussions.

Figure 2. (Below) Registered participants' countries. We note the presence of students and free listeners from developing countries (Peru, Iraq, Iran, Egypt etc.), who were able to access the school thanks to its 100% online nature. Finally, we note a newcomer to the field of optical interferometry, China, that may be a sign of exciting new developments!

Poland | 6
Chile | 6
USA | 6
France | 9
Germany | 5
Sweden | 1
Spain | 1
Peru | 1
Malta | 1
Iraq | 1
Iran | 1
Ireland | 1
Italy | 4
Greece | 1
China | 1
Brazil | 1
Switzerland | 4
Turkey | 2
Belgium | 3
The Netherlands | 2
Egypt | 2
India | 2
United Kingdom | 2

All the lectures and scientific presentations are now available to anyone who wants to follow them at their pace[2].

The school was designed to be very practical, introducing the students to many tools commonly used in VLTI observation preparation and data reduction. The Gather space was central as it was used to connect to the lectures of the school through Zoom sessions. Moreover, it was also used to allow interactions between the students and the teachers during the practice sessions on the virtual machines, as well as for the "coffee breaks" and informal discussions.

The lectures were exhaustive and varied, with a thorough introduction to long-baseline interferometry, presentations of facilities (the VLTI and CHARA), of instruments (MATISSE, GRAVITY, Stellar Parameters and Images with a Cophased Array [SPICA], the Michigan InfraRed Combiner-eXeter [MIRCX] and the Michigan Young STar Imager at CHARA [MYSTIC]), introductions to data reduction, model fitting, image reconstruction, and radiative transfer for astrophysical modelling, and also several science courses on young stellar objects, exoplanets and asteroids. These courses were backed up by practice sessions on the basics of interferometry and observation preparation, a MATISSE data reduction session, model fitting and image reconstruction sessions, and for the first time a practice session on radiative transfer. Finally there was a proposal preparation homework that lasted throughout the school, starting with a presentation of the principles of telescope time application, and ending with the students' proposal presentations in front of a mock observing programme committee.

When polled after the school, the students were very satisfied with the quality of the lectures and the practice sessions. Of course, the 100% online format of the school complicated the organisation and the interactions. Fortunately, however, the Gather platform, with its persistent space including video chatting, helped a lot to allow frequent interactions between students and teachers during the practice sessions and outside the opening hours. The lecturers and teachers were very impressed by the professionalism of the students, especially during the proposal preparation session.

In conclusion, we hope that the 10th VLTI school will have provided the participants with all the skills and knowledge they need to make successful proposals and to publish, in the near future, astonishing scientific results using optical interferometry.

School environmental impact

The environmental impact of astronomical meetings is an increasing concern (Burtscher et al., 2020). To compare the impact of a VLTI school held online and one held in person, we compared the impact of this school with the impact of the 2018 school in Lisbon. A relevant metric is the equivalent tonnage of CO_2 produced by an activity; we can use the numbers provided by Burtscher et al. (2020). The VLTI schools have a similar attendance composition to the European Astronomical Society Annual Meetings (EAS, formerly known as EWASS). Such an in-person meeting produces 1.5 t CO_2e per capita, essentially from travel (1855 t CO_2e for 1240 participants in the 2019 meeting), whilst an online meeting produces 328 g CO_2e per capita (582 kg for 1777 participants at EAS 2020). Translated into VLTI schools, the 2018 Lisbon school (52 participants in person) produced an equivalent of 75 t of CO_2, mainly the result of transportation (by plane or train). On the other hand, the 2021 online school produced an equivalent of 48 kg of CO_2, mainly from the activity of the computer servers dedicated to the school. In addition, we mailed goodies to the students that account for ~ 950 kg CO_2e, including manufacturing (300 kg CO_2e, the manufacturer being in France) and mailing (650 kg CO_2e), raising the total impact of the 2021 school to roughly 1 t CO_2e. This therefore confirms that conducting such a school in a 100% online format, even with goodies sent to the students at home, reduces by a tremendous amount the environmental impact compared to a normal in-person school.

References

Burtscher, L. et al. 2020, Nature Astronomy, 4, 823
Garcia, P. 2009, The Messenger, 135, 50
Garcia, P. J. V. et al. 2018, The Messenger, 173, 49
Lopez, B. et al. 2021, accepted for publication
    in A&A

Links

[1] List of all the previous VLTI schools:
   http://www.jmmc.fr/english/training
[2] 10th VLTI school website: https://vltischool2021.
   sciencesconf.org
[3] Course videos: https://pod.univ-cotedazur.fr/vlti-
   school-2021
[4] European Interferometry Initiative: https://
   european-interferometry.eu

Report on the EAS 2021 Symposium

Exploring the High-Redshift Universe with ALMA

held online, 28–29 June 2021

Evanthia Hatziminaoglou[1]
Gergö Popping[1]
Martin Zwaan[1]

[1] ESO

The properties of the interstellar medium (ISM) of the highest-redshift galaxies and quasars provide important indications of the complex interplay between the accretion of baryons onto galaxies, the physics that drives the build-up of stars out of this gas, the subsequent chemical evolution and feedback processes and the reionisation of the Universe. The Atacama Large Millimeter/submillimeter Array (ALMA) continues to play a pivotal role in the characterisation of the ISM of high-redshift galaxies. Observations of the dust continuum emission, atomic fine-structure and molecular lines arising from high-redshift galaxies are now carried out routinely, providing ever more constraints on the theoretical models of galaxy formation and evolution in the early Universe. The European Astronomical Society's EAS 2021 symposium dedicated to the exploration of the high-redshift Universe with ALMA provided a forum for the observational and theoretical high-redshift ALMA communities to exchange their views and recent results in this rapidly evolving field.

The EAS 2021 symposium talks addressed five intertwined themes spread over six sessions: ALMA's unmatched potential to study high-redshift galaxies, its contribution to our understanding of the properties of dust in the early Universe, the properties of the ISM, the feeding and feedback processes at high redshift and the synergies with current and future facilities. Figure 1 shows a schematic representation of some examples of science with ALMA. Highlights from each theme are summarised below, underlining the power of ALMA and its remarkable contribution to groundbreaking discoveries.

## High-redshift galaxies as observed by ALMA

Observations of "old" galaxies at $z > 8$, an epoch at which the peak of dust emission falls in ALMA's bands 7 and 8, can provide information about the time at which these very first galaxies were born. Indeed, ALMA observations of galaxies at $z \sim 9$ confirmed a formation redshift beyond ~ 11 (Hashimoto et al., 2018; Laporte et al., 2021a), providing an indirect probe into the cosmic dawn.

According to Mahsa Kohandel, simulations predict that early galaxies could form their discs as early as during the epoch of reionisation (EoR) but Sander Schouws showed that the majority of galaxies ($\sim 70\%$) at the EoR are dispersion-dominated, with stellar mass only accounting for up to 10% of their dynamical mass. Ana Carolina Posses

Nascimento, on the other hand, presented a galaxy at $z = 6.8$ that is rotationally supported, as derived from [CII] observations. At $z \sim 4$ at least some galaxies have regular rotating discs (as explained by Francesca Rizzo); however, Fernanda Roman de Oliveira showed that there is a diversity in V/σ, leading to the well established dominance of rotation by $z \sim 2$.

Other than targeted observations of high-z galaxies, several ALMA extragalactic Large Programs[1] have demonstrated ALMA's capability to be used as a survey instrument, despite its small field of view. Indeed, many of the results presented in the symposium come from such projects. Hanae Inami focused her invited talk on the Reionization Era Bright Emission Lines Survey (REBELS; Bouwens et al., submitted to ApJ), a [CII] and [OIII] survey of 40 Lyman-break galaxies (LBGs) at $6.5 < z < 9.5$ and reported dust continuum detections for about half of the sources. The [CII] and dust emissions are spatially extended and diverse (Inami, in preparation; also reported by Rebecca Bowler in her talk). Serendipitous detections of dust-obscured galaxies, discussed by Pascal Oesch, imply that normal star-forming galaxies existed in the EoR but were essentially missed until now, setting constraints on the obscured star formation out to the EoR.

In a talk introducing the ALMA Large Programme to INvestigatE (ALPINE; Le Fèvre et al., 2020), which carried out [CII] observations of 122 main-sequence

Figure 1. ALMA's windows on the Epoch of Reionization (EoR) — from Joris Witstok's talk.
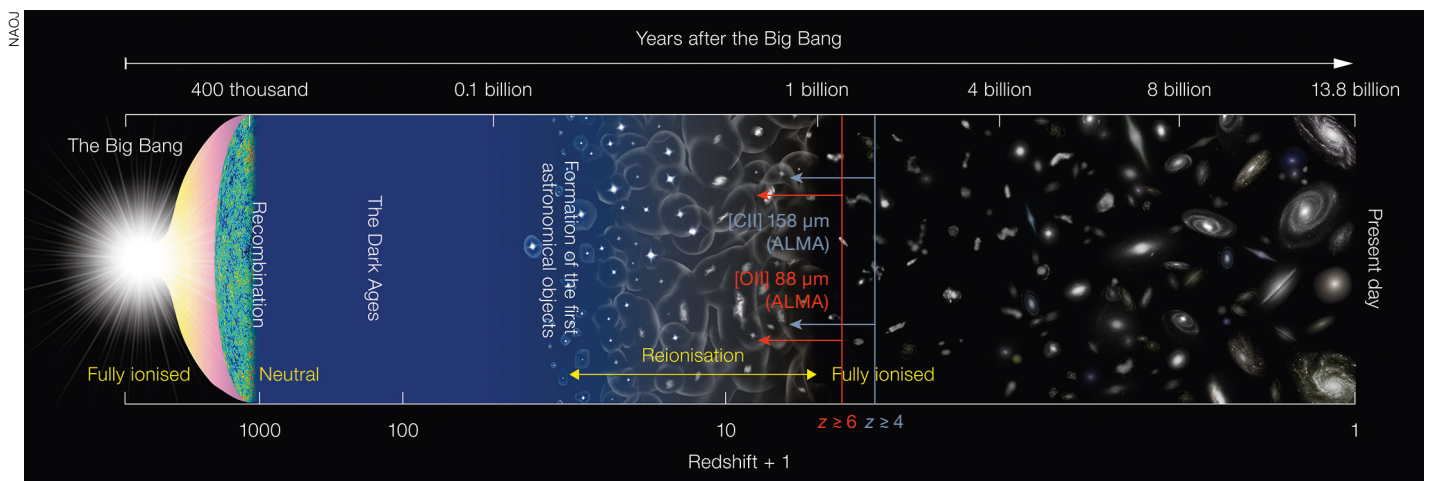
star-forming galaxies at $z \sim 5$, Matthieu Bethermin reported on the large morpho-kinematic diversity amongst $z \sim 5$ main-sequence galaxies. ALPINE demonstrated the presence of large gas reservoirs at $z \sim 6$ and a marginal decrease with redshift of the gas consumption timescale from $z \sim 6$ to the present day (Dessauges-Zavadsky et al., 2020). The same study showed that the progenitors of Milky Way-like galaxies and massive present-day galaxies evolve differently across cosmic time. Finally, ALPINE suggests that the star formation rate density remains almost constant from $z \sim 2$ to $z \sim 6$ and is five to eight times higher than the optical/UV estimates (Gruppioni et al., 2020; Figure 2).

ALMA has resolved more than half of the sources contributing to the cosmic infrared background; however, the study of the sub-milliJansky population is still difficult, even with ALMA's capabilities. Kotaro Kohno presented results from the ALMA Cluster Survey (Caputi et al., 2021; Fujimoto et al., 2021; Laporte et al., 2021b), a Band 6 survey of 33 clusters from the Hubble Space Telescope (HST) Treasury programme that explores the faint-end regime of the 1-millimetre ALMA sky and that has yielded 133 unique > 5σ continuum detections at 1 millimetre and about 60 line detections. The power of lensing in the study of high-z galaxies with ALMA was also demonstrated by Francesca Rizzo, who reported on the presence of bulges already at these redshifts (Rizzo et al., 2021).

Dust in the early Universe

Dust plays a crucial role in galaxy assembly despite contributing only 1% of the total baryonic mass. ALMA is now called upon to constrain dust temperature and dust production mechanisms at redshifts beyond four. The Calzetti law (Calzetti, Kinney & Storchi-Bergmann, 1994) has traditionally been used to correct for dust attenuation in galaxies across cosmic time. ALMA, however, showed a rapid evolution of the properties of dust at higher redshifts, where galaxies agree more with a Small Magellanic Cloud attenuation curve, representative of lower-metallicity environments.
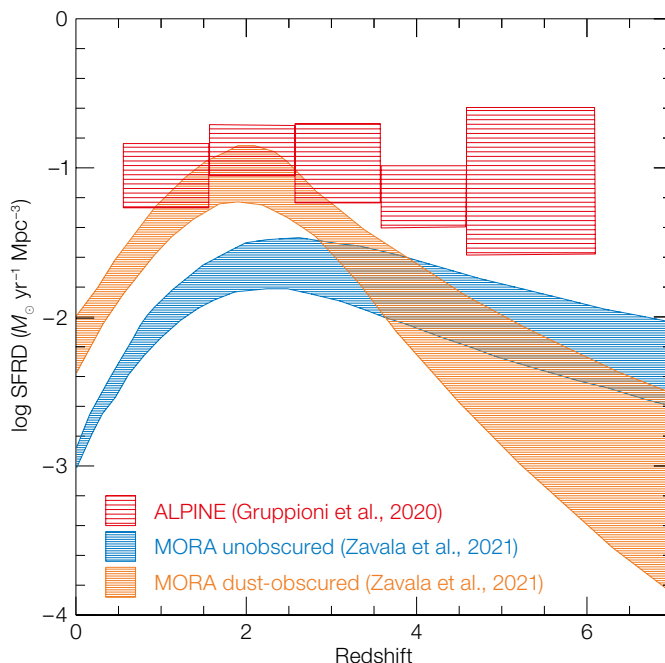

Figure 2. Star formation history of the Universe: obscured, derived from infrared/submillimetre observations (orange) and unobscured, derived from UV surveys (blue) and the ALPINE Large Programme (red).

Although theoretical work supports hotter dust (> 60 K and as high as 90 K) at higher redshifts, ALMA multi-band observations of four $z \sim 6$ LBGs lead to temperature estimates of T = 30–43 K (Faisst et al., 2020), despite degeneracies in the dust emissivity index (the exponent of the power-law fit) and large uncertainties. This is in very good agreement with the latest REBELS results of 39–52 K (Sommovigo et al., in preparation). Joris Witstok also reported the flattening of the T–z relation up to $z \sim 7$.

At the highest redshifts ($z \sim 8$) the ALMA detections of very dust-rich galaxies (for example, Laporte et al., 2017; Tamura et al., 2019) challenge the models of dust production. Such large dust masses could be the result of high supernova rates or efficient grain growth in the ISM, more efficient in massive, more metal-rich galaxies, as reported by Elisabete da Cunha (see also the review by Hodge & da Cunha, 2020). Additionally, a more top-heavy IMF, as suggested by Zhi-Yu Zhang based on ALMA studies of CO isotopologues in $z \sim 3$ galaxies, could also lead to the efficient production of dust. All the above indicate the clear need for multiband, high-frequency ALMA observations to measure temperature, luminosity and dust mass in galaxies (da Cunha et al., 2021) and quasars (outlined in Roberta Tripodi's talk) at the EoR.

The ISM in the early Universe

ALMA observations of rest-frame far-infrared fine-structure lines such as [CII] 158 μm and [OIII] 88 μm can provide direct measurements of the molecular gas content, metallicity, star formation rate (SFR) and gas density of high-z galaxies. Figure 3 is a schematic representation of the various ISM components from which the fine structure and molecular line emission originate.

[CII] 158 μm, the brightest line in most star-forming galaxies, is used to trace star formation across cosmic time. $L_{[CII]}$–SFR$_{UV+IR}$ at $z > 6$ is consistent with that in the local Universe, but the dispersion is larger (Carniani et al., 2020). Yuexing Li reported on the theoretical luminosity functions derived by combining Adaptive Refinement Tree (ART2) and the TNG100 and 300 cosmological simulations, that reproduce the $L_{[CII]}$–SFR$_{UV+IR}$ relation all the way to $z \sim 10$, suggesting that [CII] is indeed a good tracer of star formation but pointing out that the correlation is not linear at these high redshifts.

Joint [CII]-[OIII] line detections are powerful diagnostics of the conditions in the ISM at the EoR, with L[OIII]/L[CII] larger than in the local Universe (Carniani et al., 2020). The deviation from the local relation might be due to the more extended
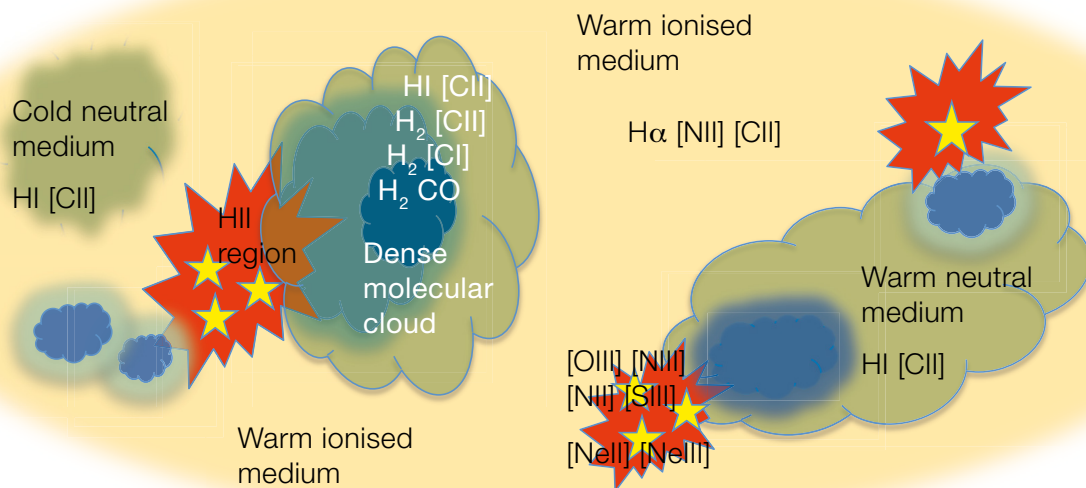
Figure 3. Origin of fine structure and molecular line emission from the various ISM components. Reproduced from van der Tak et al. (2018) with the author's permission.

[CII] emission with respect to that of [OIII]/UV (Ginolfi et al., 2020a; Herrera-Camus et al., 2021). With the help of zoom-in cosmological simulations and ISM modelling, the above can be put in a wider context, indicating ISM conditions pointing towards an efficient conversion of gas into stars. The high metallicity and gas density are indicative of a dense ISM where bursts of star formation rapidly enrich the gas (Vallini et al., 2021). Simulations by Ramos Padilla et al. (2021), combining EAGLE cosmological simulations with CLOUDY cooling tables, showed that at $z \sim 6$ [CII], [OIII] and other lines in fact trace different phases of the ISM depending on metallicity and SFR.

Extended [CII] emission observed in galaxies beyond redshift ~ 6 (although not seen in a deep stack by Jean-Baptiste Jolly) can be produced by cooling outflows with mass loading factors larger than three (for example, Pizzati et al., 2020). The presence of outflows is supported by larger values of L[OIII]/L[CII] compared to those in the local Universe (large values also reported by Joris Witstok) seen in galaxies at $z > 6$. However, the loading factors are observed

to be below or around one, indicating that the gas in the outflow might be in a warm ionised phase, or that the surface brightness of the outflows is low (Carniani et al., in preparation).

Feeding and feedback at high redshift

The circumgalactic medium (CGM) is a place where physical processes such as mixing, cooling and heating happen, modifying the properties of the gas that is moving in or out of the galaxies. One of the main challenges currently is to explain the coexistence of the cold gas ($T < 10^4$ K) in a medium filled with hot gas. "*The lack of cold gas in CGM simulations is a bias rather than a prediction*," to quote Claudia Cicone. Higher-resolution simulations lead to larger fractions of cold gas, but simulations are still not converging.

Owing to the lack of sensitivity of the current facilities, molecular gas is not detected in the CGM at $z \sim 0$. ALMA, however, can observe the CGM at high redshift. Claudia Cicone reported on observations of a halo extending out to a radius of 200 kpc around a $z = 2.2$ X-ray-selected quasar (Cicone et al., 2021). There is no evidence of an overdensity around it, making the interpretation of this CO halo challenging.

Overdensities around $z \sim 6$ quasars turn out to be low-z (~ 1–2) objects (Meyer, in preparation), in agreement with [CII] incidence rates of companion overdensities reported in the literature.

The recent literature on the stacking of [CII] observations in high-z active galactic nuclei (AGN) in search of evidence for outflows reports contradictory results. Even though the different spatial resolutions might explain the tension if outflows extend out to several kiloparsecs, Roberto Maiolino postulated that the estimated high-z cold outflows are not powerful enough to quench star formation via ejection, indicating either the importance of ionised outflows or a weaker coupling with the ISM.

At the same time, ALPINE found signatures of star formation-driven outflows (i.e., broad wings) in the stacked profiles of [CII] in galaxies with SFRs > 25 $M_\odot$ yr^{-1} (the median SFR of the ALPINE sample), but no evidence for outflows amongst galaxies with lower SFR (Ginolfi et al., 2020a). The outflowing gas in the highest-SFR galaxies moves at a maximum velocity ($v_{out} \sim 500$ km s^{-1}) below the escape velocities (400–800 km s^{-1}) and it will be trapped in the CGM of these galaxies (Ginolfi et al., 2020b). Hydrogen fluoride was reported by Maximilien Franco to be another excellent probe of

outflowing molecular gas, as well as a good tracer of H_2 in galaxies. Finally, ALMA observations of a $z \sim 5.5$ main-sequence galaxy showed ISM properties similar to those of local starburst galaxies, with extended [CII] emission, evidence for an outflow and a regular rotating disc (Herrera-Camus et al., 2021).

Synergies with current and future facilities

ALMA has undoubtedly revolutionised our knowledge of the physics of the early Universe. Synergies with existing and future facilities help push ALMA's potential to its limits. From the discovery of the very first galaxies to galaxy kinematics at redshifts close to the EoR to metallicities at redshifts of six and beyond, the possibilities for further groundbreaking discoveries are almost endless.

One of ALMA's challenges is to resolve the gas properties of galaxies with well resolved dynamics at high redshift and to decompose galaxies into their constituents (for example, Lelli et al., 2021). An obvious synergy, brought out by Mark Swinbank in his invited talk, is to improve dynamical constraints of galaxies at high redshifts by combining their ALMA CO and [CII] maps with stellar mass maps measured by the James Webb Space Telescope (JWST) and kiloparsec-scale dynamics measured by instruments like the Enhanced Resolution Imager and Spectrograph (ERIS) on ESO's Very Large Telescope and, in the future, the High Angular Resolution Monolithic Optical and Near-infrared Integral field spectrograph (HARMONI) on ESO's Extremely Large Telescope.

The JWST is going to observe optical rest-frame spectra of $z > 6$ galaxies for the first time. Combined observations of strong optical lines ([OII], [OIII], [SII] doublet) with the JWST and [OIII] 88 μm with ALMA will give direct estimates of metallicities at $z > 6$ (Jones et al., 2020).

ALMA [OIII] 88 μm observations impose strong constraints on the spectral energy distribution fit of Spitzer/IRAC-selected $z \sim 7$–9 galaxy candidates (Roberts-Borsani, Ellis & Laporte, 2020), especially prior to the arrival of the JWST, breaking

the degeneracies between nebular emission and Balmer break. Further ALMA-Spitzer synergies are illustrated by the Spitzer Matching survey of the Ultra-VISTA deep Stripes (SMUVS) project (using the Infrared Array Camera channels 1 & 2 to observe the Ultra-VISTA deep stripes) presented by Tomoko Suzuki, that studies the submillimetre properties of high-redshift galaxies in the $A^3COSMOS$ catalogue (Liu et al., 2019). Galaxies with ALMA counterparts are found to be systematically massive ($M_\star > 10^{10} M_\odot$) and tend to have larger dust extinction and higher star formation activity. Additionally, ALMA, Multi Unit Spectroscopic Explorer (MUSE) and HST observations of luminous galaxies at $z > 6$ presented by Jorryt Matthee indicate that high-redshift luminous galaxies likely reside in early ionised bubbles (Matthee et al., 2020).

Meanwhile, it remains unclear how the supermassive black holes (with masses often above $10^9 M_\odot$) residing in the centres of more than 200 known quasars at $z > 6$ have reached these sizes. Current theories predict a massive gas reservoir and ALMA-supported studies of these objects point towards rapidly star-forming high molecular gas and dust content hosts. These are often accompanied by submillimetre companions but simulations presented by Fabio Di Mascia indicate that such systems might be, instead, quasar merging systems. Alyssa Drake reported on MUSE Ly-α halo observations and complementing ALMA cold gas and gas continuum observations to find decoupled kinematics between halo gas and the ISM in high-z quasars (Drake et al., 2020). Follow-up observations of ALMA-detected high-redshift galaxies with the JWST or the Origins Space Telescope might reveal dust-obscured or faint AGN residing in them.

Conclusions

In its first decade of operation, ALMA has revolutionised our understanding of the high-redshift Universe. It has demonstrated the presence of massive dusty systems that contain large gas reservoirs fuelling vigorous star formation and accretion processes. ALMA has also exposed the presence of cold and metal-

enriched gas in the haloes surrounding galaxies at $z > 4$, indicative of CGM pollution by outflows. ALMA has furthermore opened entire new windows onto the chemistry and ISM physics of galaxies during the EoR, contributing to key questions pertaining to the build-up and reionisation of the early Universe. This symposium was a brilliant demonstration of these groundbreaking results and served as an inspiration to continue to push the envelope to deliver more exciting ALMA high-redshift results in the decade to come.

References

Calzetti, D., Kinney, A. L. & Storchi-Bergmann, T. 1994, ApJ, 429, 582
Caputi, K. I. et al. 2021, ApJ, 908, 146
Carniani, S. et al. 2020, MNRAS, 499, 5136
Cicone, C. et al. 2021, A&A, 654, L8
da Cunha, E. et al. 2021, ApJ, 919, 30
Dessauges-Zavadsky, M. et al. 2020, A&A, 643, A5
Drake, A. B. et al. 2020, ApJ, 902, 37
Faisst, A. L. et al. 2020, MNRAS, 498, 4192
Fujimoto, S. et al. 2021, ApJ, 911, 99
Ginolfi, M. et al. 2020a, A&A, 633, A90
Ginolfi, M. et al. 2020b, A&A, 643, A7
Gruppioni, C. et al. 2020, A&A, 643, A8
Hashimoto, T. et al. 2018, Nature, 557, 392
Herrera-Camus, R. et al. 2021, A&A, 649, A31
Hodge, J. A. & da Cunha, E. 2020, RSOS, 7, 200556
Jones, T. et al. 2020, ApJ, 903, 150
Laporte, N. et al. 2017, ApJL, 837, L21
Laporte, N. et al. 2021a, MNRAS, 505, 3336
Laporte, N. et al. 2021b, MNRAS, 505, 4838
Le Fèvre, O. et al. 2020, A&A, 643, A1
Lelli, F. et al. 2021, Science, 371, 713
Liu, D. et al. 2019, ApJ, 887, 235
Matthee, J. et al. 2020, MNRAS, 492, 1778
Pizzati, E. et al. 2020, MNRAS, 495, 160
Ramos Padilla, A. F. et al. 2021, A&A, 645, A133
Rizzo, F. et al. 2021, MNRAS, in press
Roberts-Borsani, G. W., Ellis, R. S. & Laporte, N. 2020, MNRAS, 497, 3440
Tamura, Y. et al. 2019, ApJ, 874, 27
Vallini, L. et al. 2021, MNRAS, 505, 5543
van der Tak, F. F. S. et al. 2018, PASA, 35, 2
Zavala, J. A. 2021, ApJ, 909, 165

Links

[1] ALMA Large Programmes: https://almascience.org/alma-data/lp

Report on the ESO Workshop

Galspec21: Extragalactic Spectroscopic Surveys: Past, Present and Future of Galaxy Evolution

held online, 12–16 April 2021

Boris Häußler[1]
Emanuela Pompei[1]
Yara Jaffé[2]

[1] ESO
[2] Instituto de Física y Astronomía,
   Universidad de Valparaíso, Chile

In April 2021 more than 200 participants gathered on Zoom for a meeting to discuss what we have learned about galaxy evolution using spectroscopic surveys, and to pay a special tribute to the Visible Multi-Object Spectrograph (VIMOS), which carried out some of the largest spectroscopic galaxy surveys to date and helped to pave the way for ongoing and future facilities. Despite being delayed twice and having to be adapted to an online format, the meeting was well received and many high-impact results were presented by a diverse body of participants. We present the organisation, lessons learned, and legacy of this workshop.

Motivation

Our understanding of galaxy evolution has changed dramatically in the last decade. One of the main advances has undoubtedly been the emergence of both large-scale and and/or deep surveys with multi-object spectrographs (MOS) and integral field units (IFU). These vast datasets have brought into focus the complex interplay between the ages, metallicities and kinematics of galaxies, as well as their masses, sizes, structures, nuclear activity and environments. Still, many open questions remain.

At the end of March 2018 the Visible Multi-Object Spectrograph (VIMOS), one of ESO's workhorses in Paranal observatory, was decommissioned from Unit Telescope 3 after nearly 15 years of service. During this time, VIMOS had amassed over 9700 hours of science data, mostly devoted to spectroscopic surveys of galaxies across cosmic time. To commemorate this milestone, we thought it appropriate to celebrate the achievements of this amazing instrument with a five-day workshop. The goal of this ESO workshop was also to bring together the low- and high-redshift extragalactic communities to review where we stand and prepare for the challenges ahead.

Run-up

We settled on a date in late 2019, to give the largest and latest VIMOS surveys (the Large Early Galaxy Astrophysics Census [LEGA-C] and VANDELS) enough time to produce some early scientific results using their final datasets and to present to the broader extragalactic community the vast set of raw and enhanced data that both surveys had publicly released. The date also coincided excellently with the planned arrival at ESO of new MOS facilities, such as the Multi-Object Optical and Near-infrared Spectrograph (MOONS) in 2021 and the 4-metre Multi-Object Spectroscopic Telescope (4MOST) in 2022, and elsewhere, such as the Multi-Espectrógrafo en GTC de Alta Resolución para Astronomía (MEGARA) at the Gran Telescopio Canarias and the WHT Enhanced Area Velocity Explorer (WEAVE) at the William Herschel Telescope. Further MOS and IFU instruments for future 30–40-metre-class telescopes are also appearing on the horizon, such as the Multi-Object Spectrograph for Astrophysics, Intergalactic medium studies and Cosmology (MOSAIC) and the High Angular Resolution Monolithic Optical and Near-infrared Integral field spectrograph (HARMONI) at ESO's Exremely Large Telescope, the Wide-Field Optical Spectrometer (WFOS) and the InfraRed Imaging Spectrograph (IRIS) at the Thirty Meter Telescope and the GMT Multi-object Astronomical and Cosmological Spectrograph (GMACS) and GMT Consortium Large Earth Finder (G-CLEF) at the Giant Magellan Telescope.

In June 2018 ESO approved financial support for our proposed workshop entitled Extragalactic Spectroscopic Surveys: Past, Present and Future of Galaxy Evolution (GalSpec19), to be hosted at the ESO offices in Vitacura, Santiago, Chile in November 2019.

We received well over 100 excellent abstracts, and the scientific organising committee (SOC) put together a well rounded programme. By mid-October 2019 everything was set for a successful workshop, bringing together experts from all over the globe to discuss the latest and most exciting results.

However, around this time a wave of social unrest in Chile began. The associated protests worried many workshop participants, so to avoid cancellations it was decided to postpone the meeting until a later date, aiming for March/April 2020, hoping that the unrest would have subsided by then. After checking with the registered participants, we decided to keep the same programme and the same participants, so Galspec19 became Galspec20, and we decided to hold it in October 2020 to avoid direct competition or overlap with other meetings.

We updated websites and started advertising the new dates. We had of course heard in the news that there was a new virus spreading, but like everybody else we did not make much of it at first, so we started replanning the workshop. Before we had even sent out anything concrete, however, the COVID-19 pandemic had reached Chile in full swing and by mid-March it was getting less and less likely that we could confidently plan a (in-person) meeting for October, with the observatory and much of the country going into lockdown, and no possibility of making a decision in May or June. Instead, we decided to postpone the workshop once again and within a few months decided to aim for April 2021 for one last try at hosting this workshop, ideally in person but with the possibility of holding it online or elsewhere (Garching, for example) if the pandemic would not allow a meeting in Santiago. And so Galspec20 became Galspec21.

By then the original workshop had been delayed by more than 18 months. As that would mean that the programme and talks would be quite outdated, we decided to start from scratch with a new abstract deadline in December 2020 and a final decision on whether the workshop would be held in person or virtually at around the same time. As the pandemic rolled on, we decided in November to hold the meeting online, with a reduced, half-day schedule. However, to allow additional talks we decided to try a
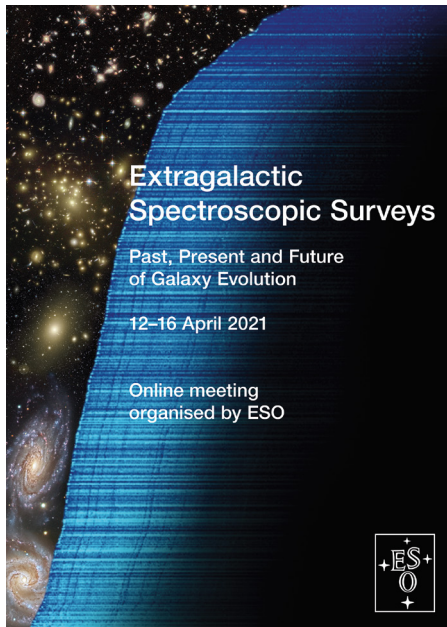
Figure 1. The Galspec21 workshop poster.

mixed scheme in which each session additionally featured several pre-recorded talks that participants could watch at their leisure, with discussion on these talks on Slack, along with long (~ 45 minutes) poster sessions on the video chat platform Gather, to allow as much personal interaction between participants as possible. The advantage of this setup was that the financial support provided by ESO more than covered the costs of the entire workshop, so registration was free for all participants. As travel costs also did not have to be covered, we received more than 140 abstracts for ~ 50 talk and ~ 50 poster slots and more than 250 registrations. We even had to close registration to avoid the workshop's becoming too big to handle, as we wanted the in-person contact to be an important element of the meeting, including discussion and Q&A sessions and person-to-person interaction during our poster sessions. Figure 1 shows the workshop poster.

Workshop and Legacy

Finally, in the second week of April 2021 and after 3 years of planning, up to 250 participants logged into our Zoom sessions, our Slack channels, and Gather for our poster sessions in a meeting that covered a wide range of topics:
– Stellar Populations and Star Formation History
– Stellar and Gas Kinematics
– Environment and Intergalactic Medium
– Star Formation and Interstellar Medium
– Upcoming Instrumentation

All contributions to the workshop were excellent; picking out one or two highlights would not do the other contributions justice and would present a very biased view. However, all talks (except for the discussion sessions) have been recorded and are available on YouTube[1], posters and talk slides have all been uploaded to Zenodo[2], and additional information is available on our website[3].

The talks given and the posters presented highlighted well that not only did VIMOS work efficiently as a redshift machine (see VIPERS, z-COSMOS, VVDS, VUDS, VANDELS, and other surveys), but was also extremely successful as an instrument used to derive properties of galaxies (see, for example, Sessions 1, Stellar Populations and Star Formation History, and 2, Stellar and Gas Kinematics) and to study the influence of environment on galaxy properties and active galactic nuclei (see, for example, Sessions 3, Environment and Intergalactic Medium, and 4, Star Formation and Interstellar Medium). VIMOS has left behind a vast dataset on the ESO archive, which will allow further studies to be carried out for years to come.

However, as well as VIMOS data, results using other instruments were also discussed during all the sessions. The Multi Unit Spectroscopic Explorer (MUSE) featured prominently as an instrument well suited for galaxy surveys, and results from the Atacama Large Millimeter/submillimeter Array (ALMA), the K-band Multi Object Spectrograph (KMOS) and other instruments were also discussed. These, and other upcoming instruments (see Session 5, Upcoming Instrumentation) will help us to answer outstanding questions in galaxy evolution. Important advances on future key issues were already presented during the workshop:
– How do gas and stellar kinematics evolve with redshift?
– How do gas accretion and outflows shape galaxy properties?
– Are rotation curves flat or declining at z > 1?
– How does environment impact the formation and evolution of galaxies?
– What is the redshift evolution of galaxy properties and scaling relations?
– How are metals distributed in galaxies and how are they modulated by accretion of gas, outflows, feedback and star formation?

The workshop was an excellent example of why we need these workhorse instruments on large telescopes to carry out large surveys of statistically significant samples over a large range of redshifts. Luckily, the next generation of such instruments, for example 4MOST, MOONS and the blue-optimised integral-field spectrograph BlueMUSE in the case of ESO instrumentation, and the next generation of dedicated survey telescopes (for example the Simonyi Survey Telescope at Vera C. Rubin Observatory, the EUCLID space telescope and others) are already well advanced or in development. They will be starting to take data in the coming years, opening yet another window onto the distant Universe, with even larger statistical samples and more interesting science to be done.

Demographics

Although it is hard to tell who actually participated in which sessions during an online meeting, the 251 registered participants signed up from 26 different countries from all continents (48% Europe, 21% South America, 13% North America, 10% Asia, 7% Australia, and two participants from Africa; see Figure 2). Of the 142 abstracts received, 64 (45%) were submitted by women, 78 (55%) by men, 40 (28%) by students, 50 (35%) by postdocs/fellows, and 52 (37%) by senior astronomers. Thanks to our amazing SOC, these fractions are nearly exactly represented in the 96 poster and talk contributions to the workshop (see Figures 3 & 4): 44 (46%) by women, 52 (54%) by men, 28 (29%) by students, 39 (41%) by postdocs/fellows, 29 (30%) by senior astronomers. Four out of the eight invited talks were given by women.
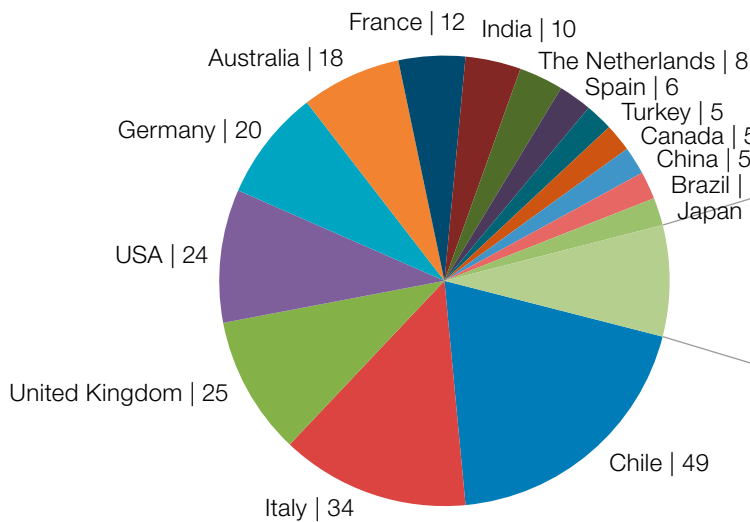
Figure 2. (Above) These pie charts show the countries hosting the workshop participants.
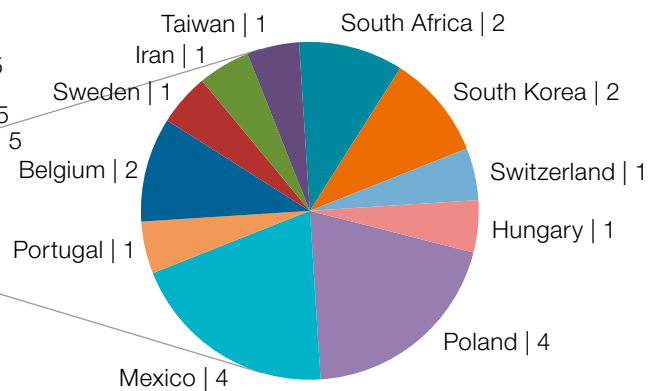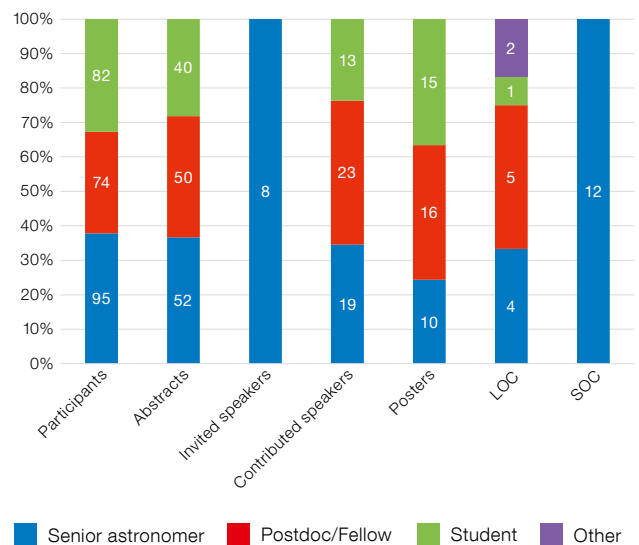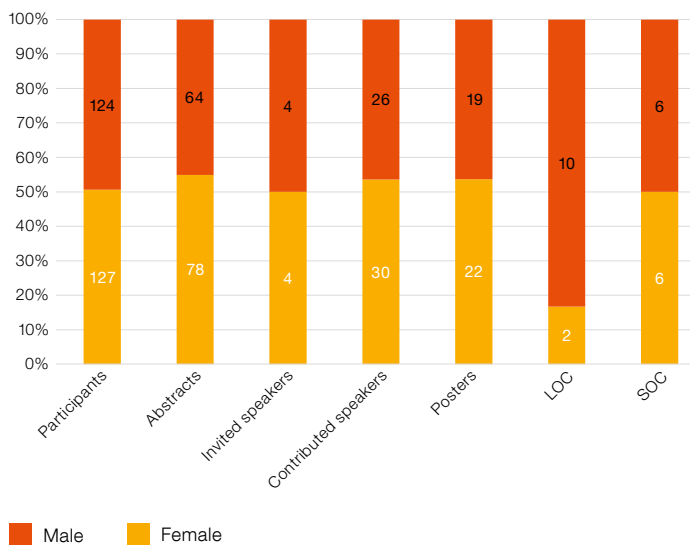
Figure 3. (Below left) Gender balance of presenters (talks and posters), which very closely resembles the gender distribution in the abstracts submitted.

Figure 4. (Below right) Distribution of seniority of presenters (talks and posters), which very closely resembles the distribution in the submitted abstracts.

Main conclusions & ways forward

Overall, we found that the online setup of the workshop worked surprisingly well, and we can recommend a similar combination of tools for other workshops that are held online in the future. We found, however, that it was critical to have very long poster sessions on Gather (see Figure 5) despite the half-day schedule of the meeting, in order to foster in-person contact and trigger discussion. This seemed to work very well, although it certainly required some getting used to. We had also outsourced the video editing for YouTube, which could in principle have been done by one of us but would have been a full-time job. The company we used was superb and got all talks online within a few hours, despite its being the end of the day at their location, so people around the world could watch them before we even met for the following day.
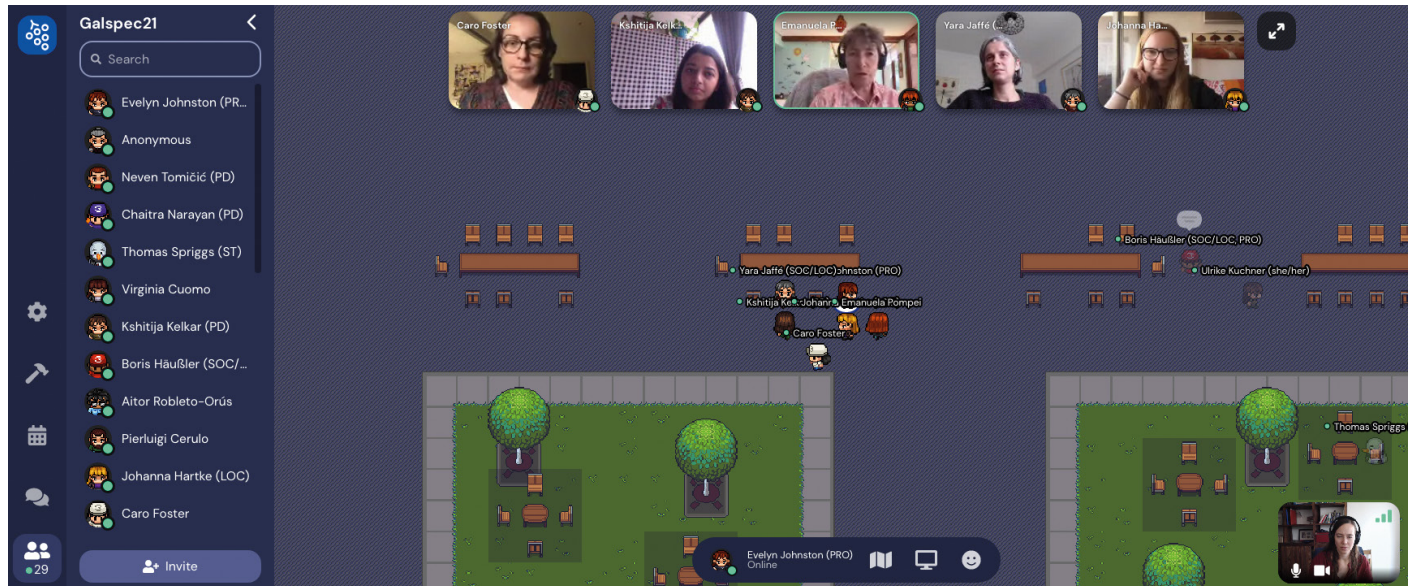
Figure 5. This picture shows a small screenshot from our space on Gather which was used for poster sessions, including two separate discussion groups.

(ESO's Director for Science) were very supportive of all our decisions and gave us the background and information that we needed to make them. Our thanks go to everybody who supported this workshop throughout, not least the amazing speakers and participants, and who made this workshop a success.
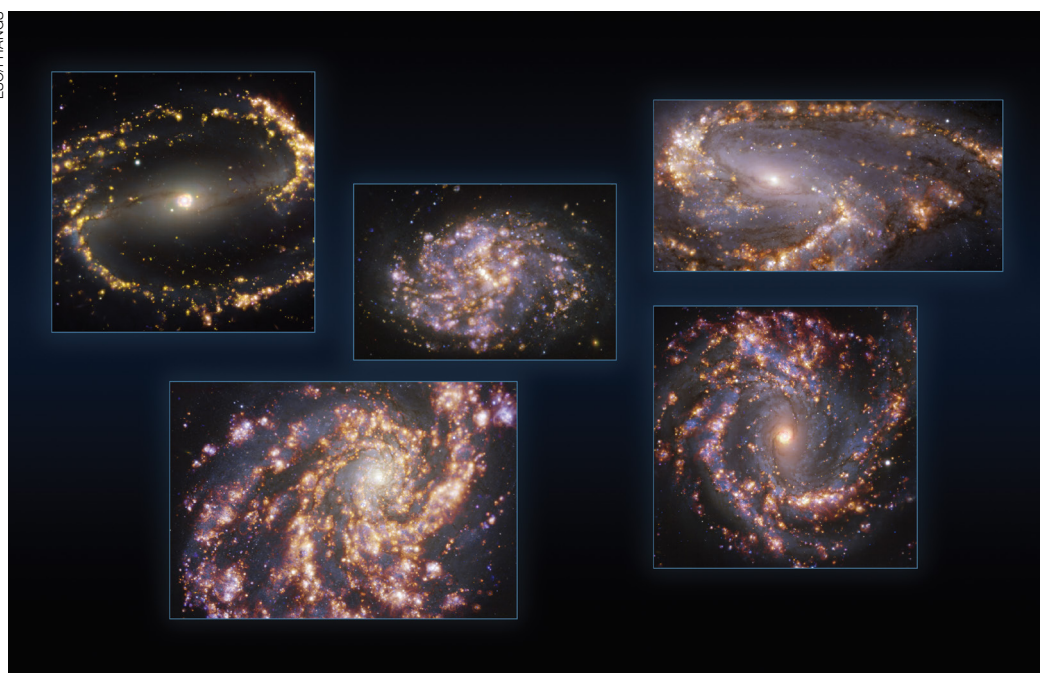
No scientific workshop can be successful without interesting science and the people behind it. We wish to remember the principal investigator of VIMOS, Olivier Le Fèvre, who died in 2020 after a serious illness. The extragalactic community and his family and friends were deeply saddened by this loss, but the news also hit those of us who met Olivier personally during the many VIMOS commissioning or first science runs and had the opportunity to know and appreciate his passion for his work and his dedication. We were truly sorry that he was not with us to discuss both the excellent results obtained with his instrument and also the interesting challenges for the future. A big thank you goes to

Olivier and to all the supporting staff for making a dream instrument come true!

Links

[1] Galspec21 YouTube channel: https://www.youtube.com/channel/UC7tsM_Uwa48BJEYICjYumvA/playlists
[2] Zenodo for posters and slides: https://zenodo.org/communities/galspec2021
[3] Workshop website: https://www.eso.org/sci/meetings/2021/galspec2021.html

ESO/PHANGS

The Physics at High Angular resolution in Nearby GalaxieS (PHANGS) project is making high-resolution observations of nearby galaxies with telescopes operating across the electromagnetic spectrum. Here five of its targets are shown: NGC 1300, NGC 1087, NGC 3627 (top, from left to right), NGC 4254 and NGC 4303 (bottom, from left to right). the images were taken with the Multi-Unit Spectroscopic Explorer (MUSE) on ESO's Very Large Telescope (VLT). Each individual image is a combination of observations conducted at different wavelengths of light to map stellar populations and warm gas. The golden glows mainly correspond to clouds of ionised hydrogen, oxygen and sulphur gas, marking the presence of newly born stars, while the bluish regions in the background reveal the distribution of slightly older stars. Read more in press release: eso2110.

Report on the ESO/Center for Astrophysics | Harvard & Smithsonian Workshop

Galaxy Cluster Formation II (GCF2021)

held online, 14–18 June 2021

Tony Mroczkowski[1]
Andra Stroe[2]
Stella-Maria Chasiotis-Klingner[1]

[1] ESO
[2] Center for Astrophysics | Harvard & Smithsonian, Cambridge, Massachusetts, USA

Galaxy clusters are both important cosmological probes and the large-scale environments influencing galaxy evolution. Processes such as ram pressure stripping, active galactic nucleus feedback and mergers, both on smaller galaxy-galaxy scales and larger cluster-cluster or cluster-subcluster scales play a major role in temporarily boosting and eventually throttling star formation in massive galaxies. The early assembly of galaxy clusters in particular remains a crucial phase for investigation. But it is a difficult one to probe, owing to their redshifts and the messy astrophysical processes involved in so-called "protoclusters", defined as as-yet unvirialised massive assemblies of galaxies, gas, and large dark matter overdensities that will one day form into bona fide galaxy clusters. This second workshop in the Galaxy Cluster Formation series, GCF2021, followed many advances in the field of study covering merging clusters, high-z protoclusters, and cluster assembly since the first workshop, held in 2017, GCF2017.

Galaxy clusters are the most massive objects to have formed by the present epoch and are likely the most massive that will ever form, given the accelerating expansion of the Universe. In the hierarchical picture of structure formation, the formation and assembly of these massive objects began 1–3 billion years after the Big Bang, and thus the past 10 gigayears have seen the rise and fall of galaxy cluster assembly. A protocluster found in the simulations of Bassini et al. (2020) and presented by Alex Saro at the workshop is shown in Figure 1.

An introduction to the motivations for the Galaxy Cluster Formation (GCF) workshop series is provided in Mroczkowski et al. (2017). Much has happened in the four
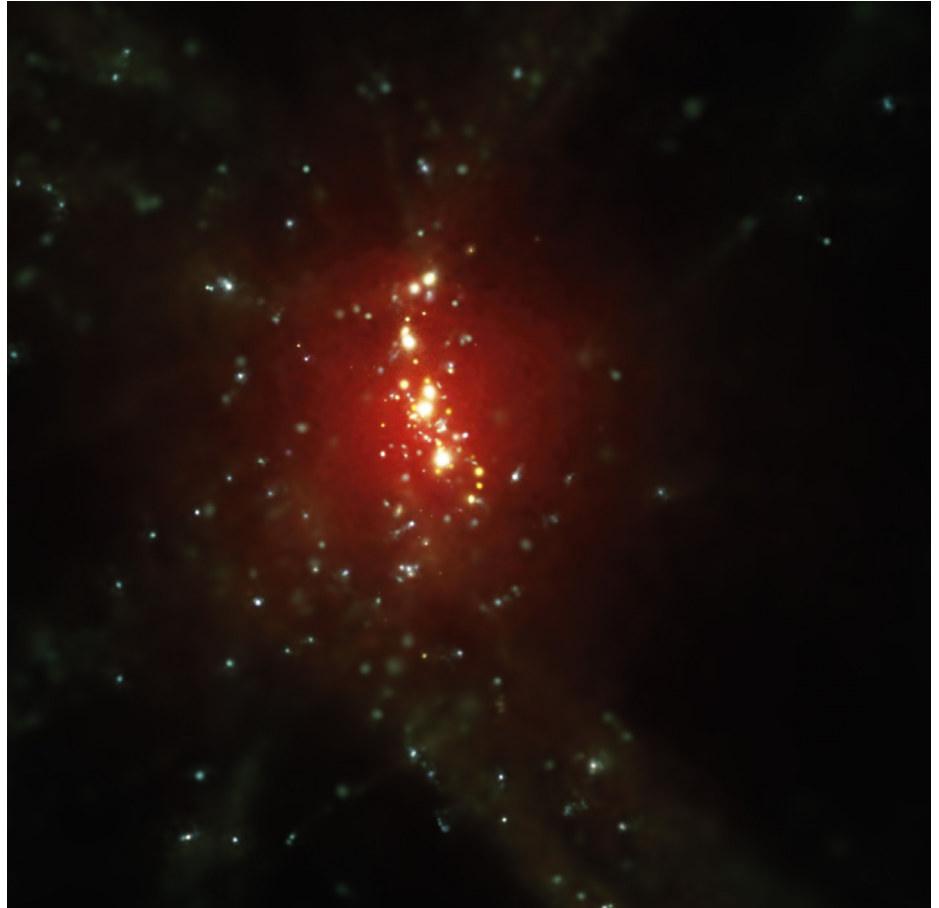

Figure 1. Simulation of a proto-cluster at $z \sim 2.5$ found in DIAGONA (Bassini et al., 2020). The image was produced by Alex Saro using the Splotch code (Dolag et al., 2008).

years since the first workshop, GCF2017[1], was held, though the best work towards fully understanding these systems lies ahead, using upcoming and planned new facilities such as the Square Kilometre Array (SKA), the Atacama Large Aperture Submillimeter Telescope (AtLAST), ESO's Extremely Large Telescope (ELT), the Nancy Grace Roman Space Telescope, the James Webb Space Telescope (JWST), the Advanced Telescope for High-ENergy Astrophysics (Athena), and the Lynx X-ray observatory.

The second workshop in the GCF series, GCF2021[2], covered a wide range of topics, including simulations, pioneering work on protocluster and cluster searches, studies of the evolution from protoclusters into clusters, processes that both promote and quell star formation, and how to estimate their mass.

A recurring theme in the workshop series is the identification and characterisation of protoclusters, which motivates observations across the electromagnetic spectrum. In particular, it remains a challenge to determine protocluster masses and assembly stages, and to estimate how massive they will grow to be. One of the main conclusions of the workshop is that protoclusters and clusters are not in fact a dichotomy, but rather are situated on a relatively continuous spectrum.

The workshop addressed a wide range of science topics. For instance, the session focusing on lower-redshift galaxy and black hole evolution, as seen from the perspective of the larger cluster/protocluster environment, revealed the need for deeper investigations into preprocessing (for example, interactions of galaxies, filaments and subgroups with other galaxies and the large scale environment) and cluster-wide processes (for example, group accretion and merger-driven shocks), both of which serve as

important but understudied pathways for the transformation of the member galaxies. Jellyfish galaxies were discussed in detail, addressing open questions as to how these disrupted galaxies are shaped by their environments. Not only is galaxy evolution heavily impacted in low-*z* clusters, but results showed that all types of active galactic nucleus activity can be promoted in such overdense environments. The workshop revealed opportunities for knowledge exchange between the lower- and higher-redshift cluster communities, with the possibility of unveiling and studying extended protocluster-like structures and mergers at lower redshift still undetected by current instruments. The participants agreed that new instruments such as Athena, the 4-metre Multi-Object Spectroscopic Telescope (4MOST), and Euclid will be transformational in unveiling these hidden populations.

It was originally intended that GCF2021 would be held in person in 2020, but it was delayed because of the COVID-19 pandemic. A considerable effort was made to adapt the workshop to a successful online format, with many sugges-

tions coming from within ESO and the wider community as represented by the workshop scientific organising committee (SOC). The meeting itself was hosted on the popular online meeting platform Zoom, and streamed live on YouTube for those who could not participate directly. Despite the distribution of participants across the globe, the number of active attendees during the live Zoom sessions was very high, fluctuating between 120 and 160 live Zoom participants throughout the five days of the workshop. In order to accommodate more time zones around the world, we recorded all but two of the presentations (subject to permissions) and posted them online on YouTube[3] after editing by an external professional video editing service. The videos garnered significant views from participants during the workshop and reached a broad audience during and after the conference. As of 25 August 2021, the workshop YouTube channel has 115 subscribers, over 3300 views and a total watchtime of almost 280 hours.

Interactions mainly took place in two ways. First, the questions and discussion

during the workshop were primarily through the Slack chat platform, which we organised in the following way. Each day was assigned its own Slack channel, while general announcements, personal introductions, job postings, SOC discussions, helpdesk issues, and random conversations each had their own channels. Each session of the workshop had a main chair to moderate the talks, and a Slack chair to monitor for relevant questions during the talk. During the discussion session, the Slack chairs constructed polls related to the main themes they identified for the session. These polls were disseminated using Mentimeter. The result of using Slack and Mentimeter was generally successful, and may have encouraged more active participation by early-career scientists.

The second component to the online interactions was through Gather, an online conference tool that participants

Figure 2. Conference photo montage produced by David Sobral using screenshots from Zoom and Gather.
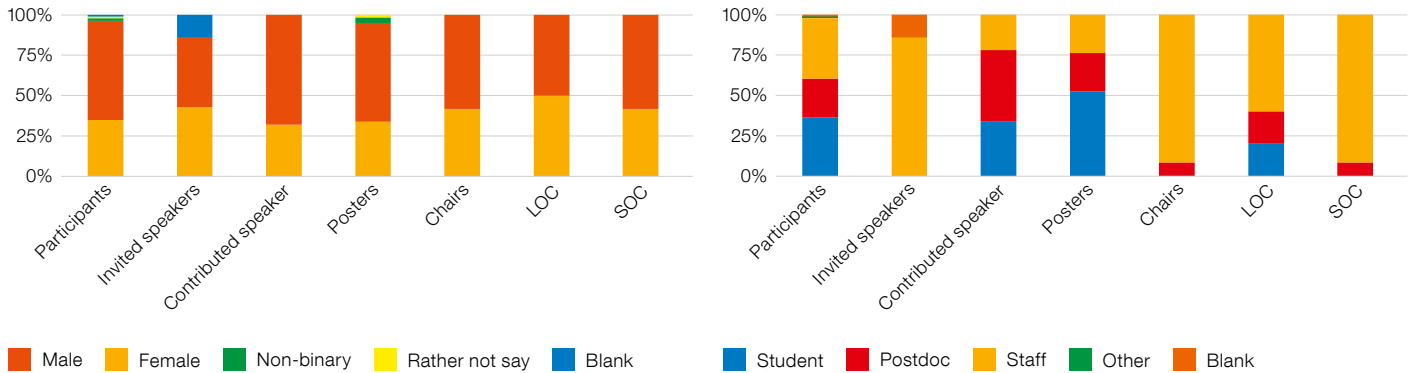
Figure 3. Charts depicting the distributions of gender (left) and career stage (right) of the participants in the workshop, where we note the categories shown may not accurately reflect the complex reality.

use to interact with a virtual space via an avatar cartoon, allowing one to visit poster sessions and meeting rooms, meet colleagues, and generally wander around as if in a real conference venue. Mixed feedback indicates it was generally successful, though a number of users reported delays and that disproportionately heavy CPU resources were required for both the software and web-based interfaces to the platform. A montage snapshot of the participants in Zoom and their avatars in Gather is shown in Figure 2.

Similarly to GCF2017, the majority of the presentations were collected on a voluntary basis, and are now available on the Zenodo platform[4], which provides Digital Object Identifier (DOI) links and is indexed by the SAO/NASA Astrophysics Data System (ADS).

Using Mentimeter, we conducted an exit poll after the workshop to gauge participants' perspectives on it. The consensus from the 45 respondents was that the workshop was extremely well received, with particular praise for the use of recordings that made the workshop more accessible, for the use of Slack to continue discussions after the live sessions and for the interactions in Gather. Whilst the consensus was that the conference was a great success as an online event, the vast majority of respondents hoped that the next GCF workshop will take place in person.

Demographics

As was the case for GCF2017 and many other ESO science workshops, we sought to ensure that the presenters were a fair representation of the community. Whilst we expected fewer than 150 participants, in the end we had 192 registered participants, of whom 67 were female, 118 were male, 3 were non-binary, and 4 did not identify. This was a dramatic increase over the 100 participants at GCF2017, and based on feedback from the participants was likely facilitated by hosting the workshop online and not having a registration fee. We note that only 72 of the participants were senior scientists, whilst the majority were early career scientists (graduate students and postdocs). In order to ensure active participation, we contacted those who did not submit an abstract for a talk or poster to verify that they were legitimately interested astronomers. We note that only 18 registered participants did not connect to the workshop.

Of the seven invited review talks selected by the SOC, three were by female scientists, three were by male scientists, and one speaker did not self-identify. Of the 50 accepted contributed talks, 16 were by female speakers and 34 by male speakers, whilst for the 59 poster presenters, 20 identified as female, 36 as male and two as non-binary, and one did not self-identify. The SOC itself comprised five female and seven male scientists, with one female and one male co-chair. These simple demographics are depicted in Figure 3.

Following a similar methodology to that successfully applied for talk selection in GCF2017, one SOC member removed names and identifying information from the abstract submissions and abstained from voting in the talk selection process. The result was that the allocated talks and posters reflect the gender distribution of those submitted. This also represented fairly the overall distribution of the participants, as the majority of participants had either a talk or poster presentation.

References

Bassini, L. et al. 2020, A&A, 642, A37
Dolag, K. et al. 2008, New Journal of Physics, 10, 125006
Mroczkowski, T. et al. 2017, The Messenger, 170, 63

Links

[1] GCF2017: https://www.eso.org/sci/meetings/2017/GCF2017.html
[2] GCF2021 workshop programme: https://www.eso.org/sci/meetings/2021/GCF2021.html
[3] Workshop YouTube channel: https://www.youtube.com/channel/UCntCTDx2OHfUbnpm4gUHtWg
[4] Online proceedings: https://zenodo.org/communities/gcf2021

Fellows at ESO

Marianne Heida

The most amazing thing about observing is, I find, the silence. Daytime is of course very different, but at night, when there's nothing to be heard except the wind and the movements of the telescope, it always feels a bit magical.

I didn't always want to be an astronomer. I didn't have a telescope as a child (and there wouldn't have been many stars visible anyway from our backyard in the western part of the Netherlands, one of the most densely packed pieces of land in Europe). I was always interested in science in general and wanted to be a doctor for a while, but I ended up studying physics because I liked the people and the fact that they had a particle accelerator in the basement. In the course of my BSc I abandoned my initial plan to focus on theoretical physics because it turned out to be a bit too theoretical for my liking, and I instead turned to astronomy. I very much enjoyed the courses but got absolutely hooked when I got to go to La Palma to observe on the William Herschel Telescope in the course of my BSc thesis work. I would return there many times during my MSc and PhD.

After finishing my BSc and MSc in astrophysics at Utrecht University (which sadly shut down the 370 year old astronomy department shortly afterwards) I continued as a PhD student at SRON, the Netherlands Institute for Space Research which at the time was also based in Utrecht, and the Radboud University Nijmegen. My thesis, under the supervision of Peter Jonker and Gijs Nelemans, was focused on near-infrared observations of ultraluminous X-ray sources (ULXs). These are pretty rare (~ 1 per Milky Way-sized galaxy), very luminous X-ray sources that are found outside galactic nuclei. They are not supermassive black holes, but exceed the Eddington limit of a normal stellar-mass black hole. When they were first discovered they were generally thought to be strong candidates for hosting intermediate-mass black holes (IMBHs). At the time I started my PhD, a consensus was forming that most of them were probably super-Eddington stellar-mass black holes instead, although some might still contain IMBHs. The only way to prove that is

Marianne Heida

through dynamical mass measurements of their donor stars, but these were very difficult to detect in the optical because all ULXs are extragalactic and because their accretion discs can hide the donor star emission. So we decided to look for red supergiant donors in the near-infrared, where the accretion discs are not as dominant. We managed to find several, but as the expected orbital periods for such systems are on the order of years, we're still observing them to look for radial velocity changes. In the meantime, X-ray pulsations have been detected from several ULXs, showing that the accretors in those systems are not black holes at all but neutron stars! So now, instead of hoping to find IMBHs, the question has become whether any ULXs actually contain black holes at all.

After finishing my PhD I moved to Caltech where I spent almost four years as a postdoc in the NuSTAR group of Fiona Harrison. I had a great time there and learned a lot about X-ray observations (and hopefully taught the X-ray astronomers a bit about optical/infrared observing). During my time in California I got to observe quite often at Palomar and Keck. Palomar observatory in particular is an amazing place, with such a rich history. One of my best memories is the special deluxe tour I got from the observing assistants on a particularly cloudy night, when we got to climb into the support structure of the Hale telescope and

peek out of one of the holes in the "horseshoe", ten metres above the floor.

In October 2019 I returned to Europe to start an ESO fellowship in Garching. I'm still observing ULXs, trying to figure out where these enigmatic sources fit in our picture of massive binary star evolution. For my functional duties I'm assisting Harald Kuntschner in the final development stage and (hopefully) commissioning of the Enhanced Resolution Imager and Spectrograph (ERIS). I've used data from ESO telescopes throughout my career, and seeing up close how the observatory works and how new instruments are developed has been an amazing experience. The wide variety of interests and expertise of the scientific community at ESO make for a great atmosphere. Of course the pandemic has made the last year and a half, well, very interesting. I'm very much looking forward to returning to normal, whatever that will look like, and hope to visit Paranal before the end of my fellowship to see ERIS in action!

Peter Scicluna

I was introduced to science fiction as a young child, and the fantastical stories and vistas quickly captured my imagination. This grew into an interest in all things related to space, and I set to devouring books about everything from space exploration to the lives and deaths of

stars and the birth of the Universe. Around the same time, two events occurred in relatively quick succession which made astronomy big news in the UK: the impact of comet Shoemaker-Levy 9 on Jupiter and the appearance of comet Hale-Bopp.

Before too long I had set my sights on becoming an astronaut, like many other children. I soon realised that, alas, this was not to be, so I was drawn to the next best thing: astronomy, although I didn't entirely realise this was the destination at the end. Growing up in Cambridge, I proceeded to drag my parents along to visit the Royal Observatory (now sadly closed) and any other observatory within reach, soaking up the scientific history of the town at every opportunity.

As I approached the end of secondary school, I knew I was going to study one of the sciences. In spite of my less-than-stellar mathematical ability and clear ease with chemistry, I opted to pursue physics at Manchester — perhaps my childhood self refusing to be turned from the path it had set out on. I struggled, partly because I was not prepared for study that required genuine effort, and partly because my mental health suffered in the first few years. As a result, I only ever managed to do just well enough to continue. Fortunately, I made it to the 4th year, where I got to do a research project tangentially related to radio astronomy, and I flourished. Immediately, I knew that research was the thing for me, and set about looking for opportunities to continue in astronomy.

This occurred at the worst possible time — as I was looking for a PhD, funding for research in the UK was facing an unprecedented squeeze. Funding for new PhDs was cut by 50% in one year, without warning. Unable to find a position, I took the only route I could see to extend my stay, doing a second Masters' degree in astrophysics at UCL. One year later, I had some new skills and had enjoyed another year of research, but the funding situation in the UK was no better.

As a result, I cast a wide net for opportunities, and was lucky enough to find a collaborative project between ESO and Kiel University in Germany. This meant
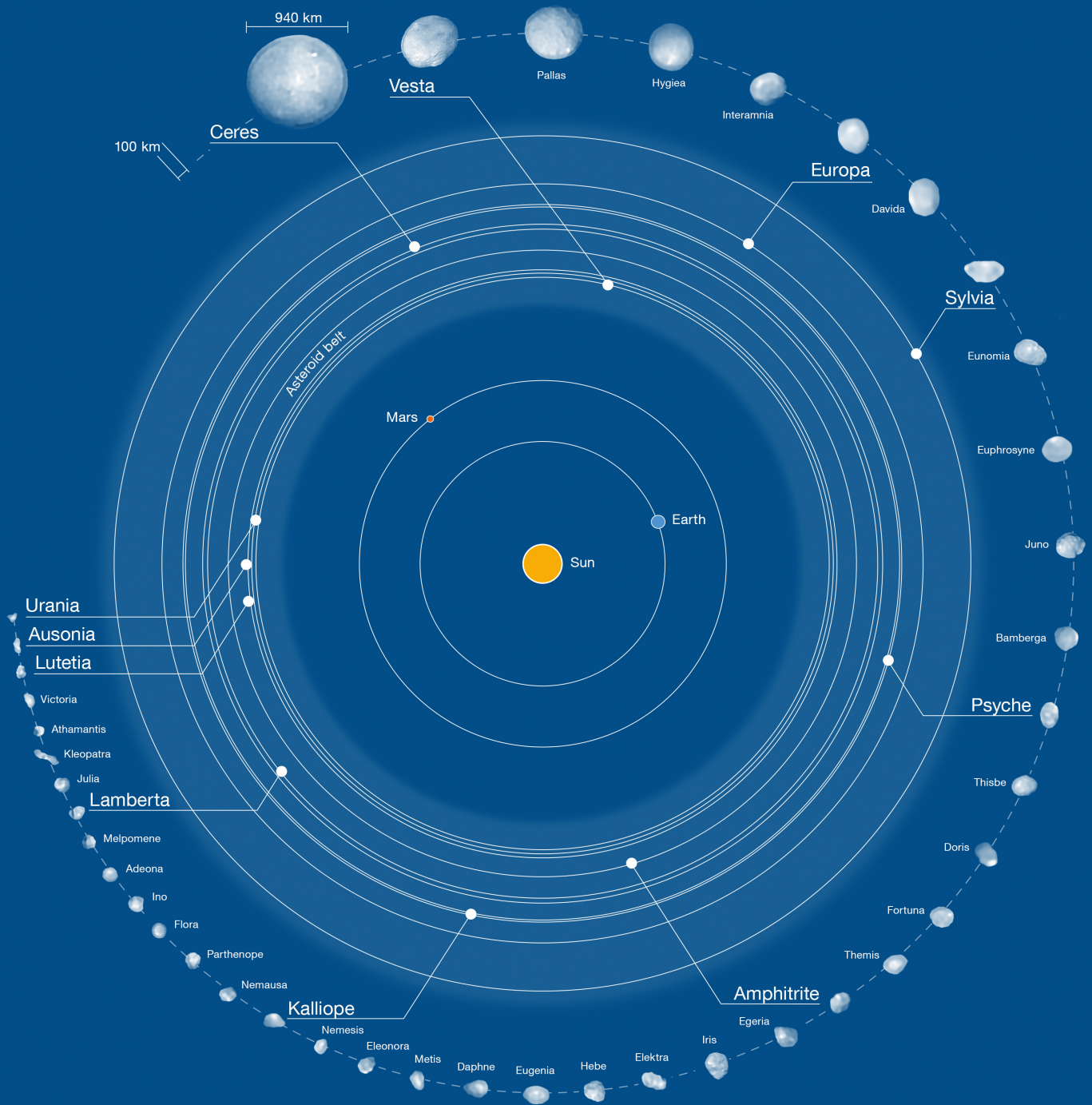
Peter Scicluna

moving to a new country, but turned out to be one of the best decisions I ever made. I learned a new language (well, a bit of it at least), experienced a vibrant research environment and made friends from a wide range of cultures. At the same time I learned the joys of studying dust, which is oddly satisfying because it seems so insignificant in the vastness of the Universe, yet is involved in so many important processes and is everywhere we look. As much as half the light we observe from the distant universe may have interacted with dust on its way to get here!

Initially, my thesis was supposed to be about star formation and developing software for dust radiative-transfer modelling (simulating how light interacts with dust before it is observed at a telescope). Part-way through my PhD I shifted my focus (not entirely endorsed by my supervisor!) from studying the births of stars to their deaths, and have retained a somewhat eclectic approach ever since. This led me to a postdoc in Taiwan where I worked in a fantastic research group under Francisca Kemper, where people studied any aspect of astrophysical dust they found interesting, from debris discs

around nearby stars to the most distant galaxies. This suited my eclectic tendencies, giving me a chance to branch out and try other things while continuing to focus my main efforts on dusty evolved stars. These are particularly interesting since they are in the process of ejecting their outer layers — enriched with the products of nuclear fusion — into interstellar space, where they may eventually become the building blocks of life.

After spending four years in beautiful Taiwan, I got the chance to return to ESO as a fellow, but this time on the "other side" — in Chile. I had previous experience working with observations across a wide wavelength range, but little to none with interferometry. Nevertheless, for my duties I support observations with the VLT Interferometer and haven't stopped learning new things about it since I arrived. Finally getting to travel to Paranal and see the VLT was awe inspiring, from the desolate scenery to the marvels of engineering that are the telescopes. Nevertheless, the real wonder is the sky; I am always forced to stop and stare for at least a few moments at night, reminding myself of why I do this as I try to drag my attention back to the task at hand.

MEET **42 ASTEROIDS** IN OUR SOLAR SYSTEM

940 km

100 km

Ceres

Vesta

Pallas

Hygiea

Interamnia

Europa

Davida

Sylvia

Eunomia

Euphrosyne

Juno

Bamberga

Psyche

Thisbe

Doris

Fortuna

Themis

Egeria

Iris

Amphitrite

Elektra

Hebe

Eugenia

Daphne

Metis

Eleonora

Nemesis

Kalliope

Nemausa

Parthenope

Flora

Ino

Adeona

Melpomene

Lamberta

Julia

Kleopatra

Athamantis

Victoria

Lutetia

Ausonia

Urania

Asteroid belt

Mars

Earth

Sun

The asteroids presented here, 42 of the largest in our
Solar System, were imaged with the European Southern
Observatory's Very Large Telescope. The orbits are not to scale.

ESO